Università di Firenze

Dottorato di Ricerca in Chimica e Tecnologia del Farmaco

Scuola di Dottorato in Scienze

Ciclo XXII (2007-2009)

Synthetic Receptors for Molecular Recognition of Carbohydrates

Tesi di dottorato di

Dott. Oscar Francesconi

Supervisori

Prof. Vittorio Dal Piaz

Dott. Stefano Roelens

Coordinatore del Dottorato

Prof.ssa Elisabetta Teodori

S.S.D. CHIM/08

Table of Contents.

Table of Contents…… **3**

Introduction……..... **5**

Section 1. Modification of the receptor binding side-arms. **15**

Design and Synthesis……... 15
Binding studies and structure elucidation…….. 18

Section 2. Modification of the receptor scaffold. **27**

Design and Synthesis……... 27
Binding studies and structure elucidation…….. 30

Section 3. Modifications of the pyrrolic binding groups. **37**

Design and Synthesis……... 37
Binding studies and structure elucidation…….. 39

Section 4. Modifications of the aminic binding groups. **49**

Design and Synthesis……... 49
Binding studies and structure elucidation…….. 54

Conclusions and general remarks…… **67**

Experimental Section. **69**

General…… 69
Conformational Analysis – NMR methods…… 70
Conformational Analysis – Molecular Modeling……... 70
Materials…….. 71
Abbreviations…….. 72
Synthesis……. 73
Titrations and Data Analysis…… 101

Bibliography…… **151**

Introduction

Oligosaccharides have intrigued scientist for decades because of the several key functions they elicit in biological systems. With respect to structure diversity, they exceed by far proteins and nucleic acids. This structural diversity allows the encoding of an enormous amount of information for specific molecular recognition processes, which makes carbohydrates critically involved in several biological processes, like protein folding and activity modulation.[1] In particular, carbohydrates are critically involved biological processes that concern communication between cells. Carbohydrates assembled in oligo- or polisaccharides within protein and lipidic glycoconjugates form the cell glycocalix. Exposed on the glycocalix of the cell surface, carbohydrates are involved in cellular adhesion and cell-bacteria and cell-virus interactions,[2] all of which are governed by a selective molecular recognition of specific carbohydrates.

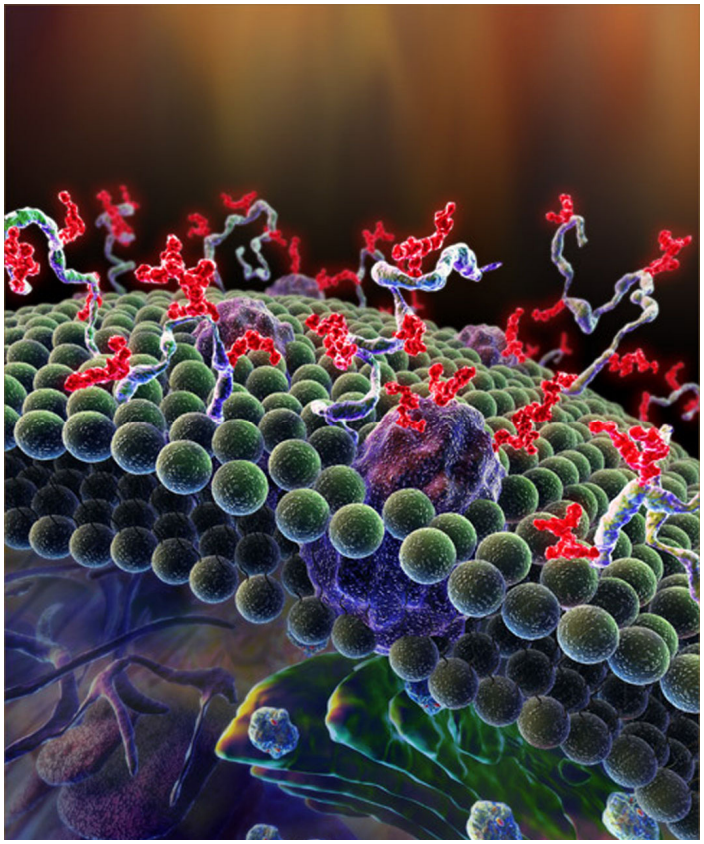

Figure 1. Representation of the glycocalix of a cell.

An increasing number of studies are highlighting the importance of carbohydrates in pathogen recognition, in the modulation of the immune system,[3] in the control of homeostasis and inflammation.[4] Like mammalian cells, many different pathogens, including viruses, bacteria, fungi and parasites, extensively use glycoproteins for diverse functions, in part similar to those of eukaryotic cells. However, as glycans on the pathogen (in particular, viral-derived glycoproteins) are produced by the cellular machinery, they are often recognized as “self” by the immune system. Therefore, the glycans of pathogen glycoproteins in the viral envelope or bacterial cell wall help to escape recognition by the immune system and subsequent destruction or neutralization of pathogen.

Within the immune system there are several classes of proteins dedicated to molecular recognition of glycans, commonly known as lectins. Examples include mannose-binding lectins (MBL),[5] DC-SIGN,[6] defensins[7] and macrophage mannose receptors[8] that recognize specific glycoconjugates, that is, specific glycosidic structures on proteins and lipids. Glycans on the viral envelope often have a crucial role in enabling an efficient transmission of the pathogen and/or entry into its susceptible target cells. Moreover, it has been shown that the presence of glycans on the envelope of viruses, such as HIV

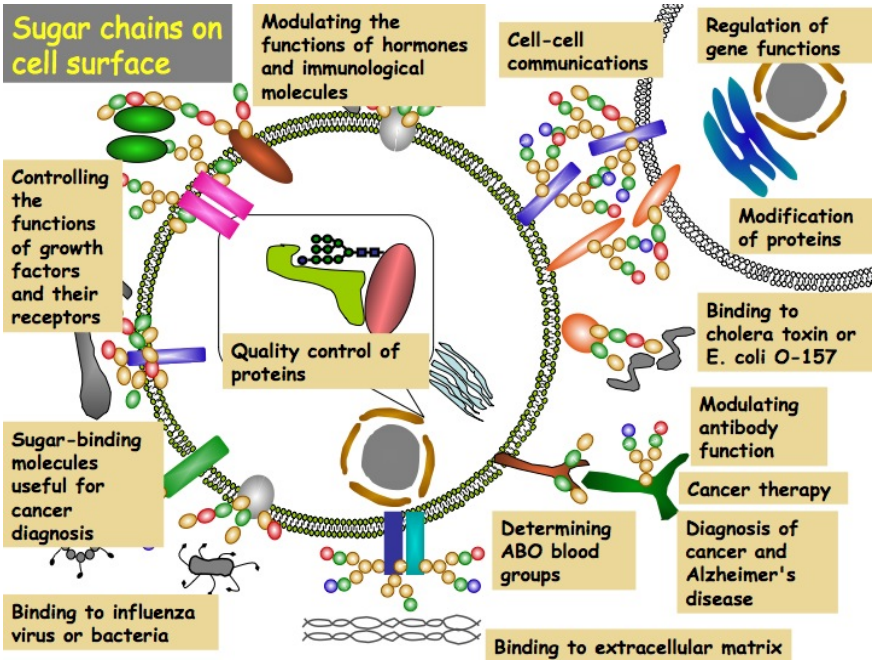

Figure 2. Schematic representation of glycoconiugate functions

and HCV, is also of crucial importance for evasion of the immunological surveillance of the host. Agents that interact with the viral-envelope glycans may, therefore, compromise the efficient entry of the virus into its susceptible target cells. These agents do not interfere with the glycosilation enzymes from the cell, but rather act by directly binding to the intact glycans on the viral envelope.[9;10] Perhaps more importantly, such carbohydrate-binding agents (CBAs) may force the virus to delete at least part of its glycan shield to escape drug pressure;[11] this might result in the initiation of an immune response against uncovered immunogenic envelope epitopes. CBAs may become the first chemotherapeutics with a dual mechanism of antiviral action: first, through direct antiviral activity, by binding the glycans of the viral envelope and subsequently blocking virus entry, and second, through indirect (additional) antiviral action resulting from the progressive creation of deletions in the envelope glycan shield, thereby triggering the immune system to act against previously hidden immunogenic epitopes of the viral envelope. In the broader perspective, apart from viruses, other pathogens such *Mycobacterium Tuberculosis*, *Helicobacter Pylori* and some parasites may also be susceptible to this novel therapeutic approach.

The surface unit of the HIV envelope glycoprotein gp120 is heavily glycosylated with N-linked mannose glycans,[9] which presumably shield the neutralizing epitopes.[12;13] Despite the large variation in the amino acid sequence of gp120 due to the immune selective pressure, the overall degree of glycosylation is preserved.[14] The C-type lectin DC-SIGN (dendritic cell-specific intracellular-grabbing non-integrin) expressed on the surface of dermal dendritic cells (DCs) has been implicated in HIV vaginal transmission.[15-17] DC-SIGN binds specifically to the oligomannosides on gp120 through protein–carbohydrate interactions in a multivalent and Ca^{2+}-dependent manner.[18;19] Carbohydrate structures on gp120 are targets for candidate antiviral agents and vaccines.[20;21] CBAs that could bind mannose glycans of gp120 may hinder or prevent the conformational changes and flexibility of gp120 that are required to properly interact with cell-membrane receptors, before or during the fusion process, during infection. Moreover CBAs drug pressure may reflect in a deletion of high-mannose type glycans and exposure of gp120 epitope inducing

immune system reaction. Therefore achieving CBAs selective for specific carbohydrates as mannose becomes a crucial issue.

In the study of those processes in which carbohydrates are implicated, chemical tools have proven indispensable. Synthetic oligosaccharides and glycoconjugates have been shown to be very useful for correlating molecular structure with biological function. Developments in this field of chemistry have lead to the identification of glycan functions, of the structural requirements essential for the function, to the elucidation of biosynthetic pathways, and to the generation of saccharide-based synthetic vaccines.[22] An important chemical tool is constitued by small synthetic molecules, which inhibit the biosynthesis of oligosaccharides and process enzymes by blocking the assembly of specific oligosaccharidic structures. Another strategy for understanding the importance of specific carbohydrates in complex saccharidic structures is based on metabolic interference with non-natural metabolic substrates, which may intercept a biosynthetic pathway and get incorporated into cell surface glycoconjugates.

A different approach for the study of functions connected to the glycoconjugate recognition consists in the inhibition of the process itself.[23] However, the identification of compounds blocking the glycan recognition remains the greatest challenge. There are two complementary approaches to inhibit the interaction between carbohydrates and receptors. The first approach is based on synthetic antagonists of the receptors that are involved in the recognition of carbohydrates in biological systems. The second approach is based on artificial synthetic receptors that work as carbohydrate-binding agents (CBAs), selectively recognizing the saccharide and preventing it from interacting with the natural receptor.[24] This second strategy falls within the competence of supramolecular chemistry.[25]

The development of effective and selective synthetic receptors for carbohydrates, especially in competitive solvents, is still an open challenge. The reason for this can be found in the difficulty of envisaging a receptor capable of determining preferential interactions with the hydroxylic groups of a carbohydrate in the presence of a strong competitive solvent like water. Furthermore, the selective recognition of carbohydrates is a highly difficult task, since many saccharides differ only in the spatial disposition of a single hydroxyl

group. Even lectins, the natural receptors of many carbohydrates, are well known for the notably low selectivity *vs.* their ligands. Indeed, the binding constant range for lectin-carbohydrate complexes is in the order of 10^3-10^4 M^{-1}, which are remarkably low values for biological interactions.

Despite these difficulties, considerable advances have been made in the field of molecular recognition of carbohydrates, especially in the last few years. There are two different strategies for the design of synthetic receptors for carbohydrates. The first strategy exploits non-covalent forces, while the second is based on the formation of a reversible covalent boron-oxygen bond between the diolic moiety of saccharides and boronic acids. While the second strategy is more effective in aqueous solvent, the first is based on a biomimetic approach more compatible with saccharide recognition in nature.

The recognition of carbohydrates through non covalent interactions has recently featured the development of synthetic receptors capable of interacting with mono- and disaccharides in water with affinities comparable to those of lectins for their biological targets.[26] It must be emphasized, however, that the achievement of effective synthetic receptors usually starts from developing systems capable of binding carbohydrates in organic solvents. This strategy, employing poorly competitive media to enhance hydrogen bonding interactions, allows to elucidate the essential requirements for molecular recognition of carbohydrates and to identify the appropriate geometry necessary for establishing an effective complexation through hydrogen bonding. Syntethic receptors effective in organic solvent have indeed lead to extend the design of structures to systems capable of recognition in progressively more competitive solvents, to improve affinity and selectivity, and finally to develop receptors capable of binding in water with unexpected affinity. An extensive literature has recently appeared, in which synthetic receptors of great interest are emerging, which can be anticipated to be useful in the near future for the recognition of glycoconjugates in biological systems.[24]

This PhD thesis focuses on the realization of new synthetic receptors as potential CBAs, with the aim of obtaining biological active tools to be used in pathological processes where molecular recognition of carbohydrates is critically implicated. In the last few years, we have developed a research program concerning the molecular recognition of monosaccharides, selected

among the most important in biological systems as epitopes of glycoconjugates, including the α and β anomers of the gluco, galacto, manno and N-acetilglucosamine series (Figure 3).

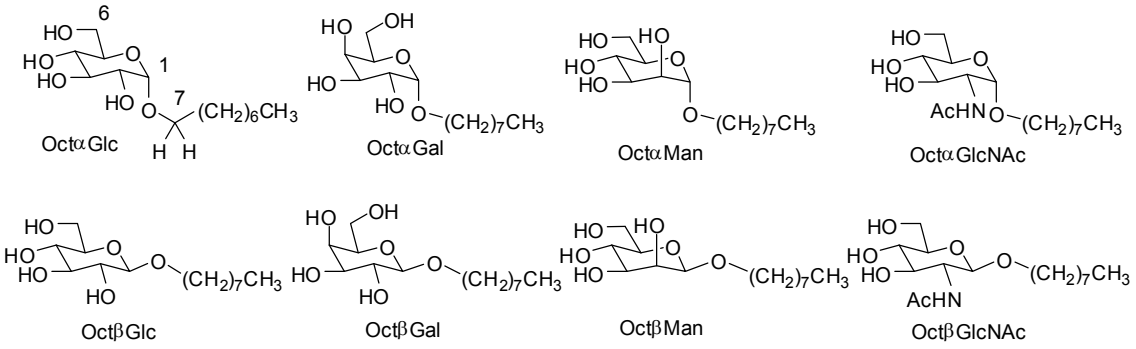

Figure 3. α and β anomer of the gluco, galacto, manno and N-acetilglucosamine series.

Recognition processes were studied in organic media, to enhance H-bonding interactions, and affinities were measured employing nuclear magnetic resonance spectroscopic techniques. A fundamental issue for the assessment of binding properties was the evaluation of affinities on a common scale, because the investigated receptor-glycoside systems fitted different binding models depending on the glycoside. To address this issue, we have developed the BC_{50}^{0} parameter,[27-29] a generalized affinity descriptor univocally defining the binding ability of a receptor in chemical systems involving multiple equilibria. The BC_{50}^{0} descriptor is defined as the total concentration of receptor necessary for binding 50% of the ligand when the fraction of bound receptor is zero that is, when forming the first complex molecule; thus, the lower BC_{50}^{0}, the higher the affinity. BC_{50}^{0} values are calculated from cumulative binding constants obtained by NMR data through the "BC_{50} calculator"[27] program.

X = Hydrogen bonding group

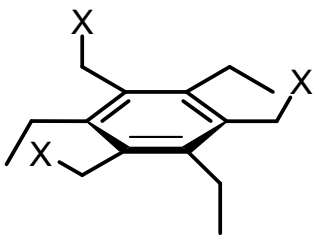

Figure 4. Tripodal benzene scaffold

Among the numerous artificial receptors reported to date, benzene-based tripodal structures, both macrocyclic and acyclic, have been successfully explored for the recognition of saccharides.[30-35] In our laboratory, a number of synthetic trpodal receptors have been designed and

prepared, which are able to bind monosaccharides with high affinity and selectivity, relying on hydrogen bonding and CH-π interactions. This family of synthetic receptors is characterized by an aromatic tripodal scaffold (Figure 4), alternately functionalized with three alkyl groups and three chains containing functional groups endowed with hydrogen bond donors and acceptors. It is well documented[36] that steric gearing in hexasubstituted benzene scaffolds organizes alternate substituents toward opposite sides of the plane containing the aromatic ring, therefore allowing binding groups to assume a convergent geometry capable of establishing binding interactions with the saccharides. Since the optimal disposition of the binding groups for an effective recognition was *a priori* unknown, a flexible receptor architecture has been chosen, in the belief that adaptivity would be advantageous. Indeed, in contrast to a preorganized structure that could match the structural guest requirements only if the binding groups were disposed exactly in the correct way, an adaptive receptor may achieve the most suitable geometry for the interaction by adapting to the guest, provided that the energy cost for this conformational change would be compensated by the binding energy gain. In order to investigate binding groups suitable for establishing effective interactions with the hydroxyl groups of the glycosides, in the last few years we explored several differently functionalized receptors. In a pioneering stage, ureidic functions have been anchored onto the tripodal scaffold, giving a receptor exhibiting significant affinity for monosaccharides, in particular for glucosides, and showing affinities in the millimolar range in chloroform (Figure 5).[28]

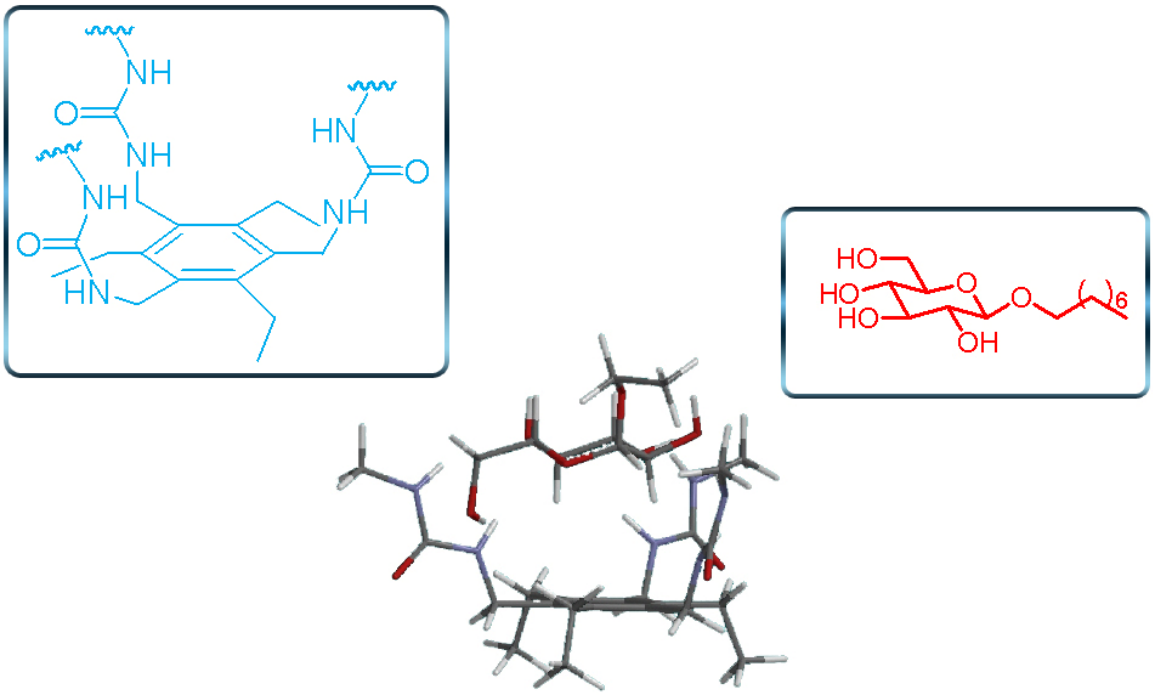

Figure 5. Molecular mechanics minimized structure of the ureidic receptor binding a glucoside

In order to improve the molecular recognition properties of the receptor, other binding groups were investigated. While amidic functions, which are well known H-bonding groups in biological systems, did not give encouraging results when assembled in the tripodal structure,[27] aminic and pyrrolic functions turned out to be very effective tools for biomimetic recognition of carbohydrates. Indeed, amino and hydroxy groups have been shown to be complementary H-bonding partners, both geometrically and coordinatively, giving rise to molecular recognition and self-assembly.[37;38] On the other hand, pyrroles, which are well established H-bonding donors largely employed for anion binding,[39] appear to be yet essentially unexplored for the recognition of carbohydrates. Amino and pyrrolic binding groups conveniently assembled on the 1,3,5-triethylbenzene scaffold afforded an adaptive receptor of significantly improved recognition properties toward monosaccharides (Figure 6).

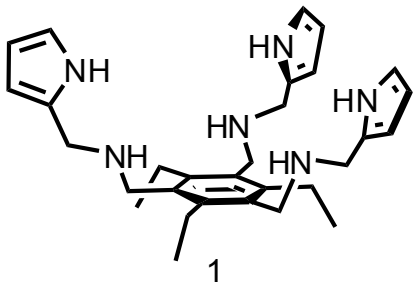

1

Figure 6. Adaptive tripodal receptor **1** exploiting amino-pyrrolic binding groups

These results have laid the foundation of a new generation of receptors based on the tripodal scaffold and featuring aminic and pyrrolic H-bonding groups.

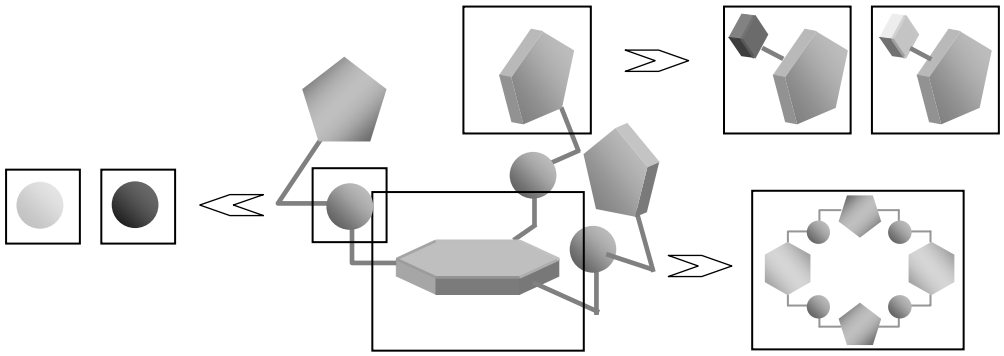

Figure 7. Schematic rappresentation of main modifications on parent pyrrolic receptor **1**.

In an effort to further improve on recognition properties, we investigated the effect of structural modifications of the parent pyrrolic tripodal receptor by implementing various substituents on the pyrrole ring, by replacing the aminic function with different binding groups, and by exploring new cyclic architectures of the basic tripodal scaffold (Figure 7). In this PhD thesis the design, synthesis, analysis and structure elucidation and evaluation of the binding properties of new carbohydrate receptors belonging to the amino-pyrrolic family are investigated, with the purpose of achieving high affinities and selectivities towards biologically relevant monosaccharides.

1 – Modification of the receptor binding side-arms.

Design and Synthesis.

In the work previously developed during a laurea thesis, the synthesis of receptor **1** and preliminary binding studies with monosaccharidic glycosides were investigated, evidencing a substantially improved affinity compared to parent ureidic receptor and a specific selectivity towards the β anomer of the glucose (OctβGlc).

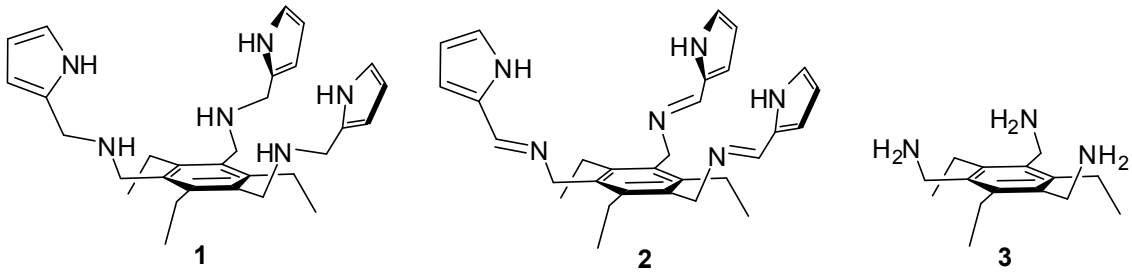

Figure 8. Parent pyrrolic receptor **1**, iminic receptor **2** and aminic receptor **3**

The synthetic precursor of the amino receptor **1**, the tris-imino analogue **2**, which was obtained from condensation of the pyrrole-2-aldehyde **4** with the aminic receptor **3**, may provide valuable structural and functional information, due to the particular characteristics introduced by iminic groups. Although strictly analogous to **1**, receptor **2** may exhibit significantly different binding properties, because of the H-bonding acceptor nature of the iminic groups, compared to the dual acceptor/donor character of amines, and because of the conformational constraint imposed by the iminic double bond. Indeed the imino group is coplanar with the pyrrolic ring due to conjugation, and locks the conformation into a chelating arrangement of the two nitrogen atoms. For these reasons, the imino-pyrrolic receptor **2** was tested toward glycosides in recognition studies.

To evaluate the contribution to binding brought by the amino groups, an isostructural replacement was planned with an alternative H-bonding group. To this end, the new receptor **5** was designed in which the amino groups were replaced by ether oxygens, in the belief of that such a modification would not

affect the receptor geometry while modifying the H-bonding properties of the etheroatom from a dual acceptor/donor character to an acceptor behaviour.

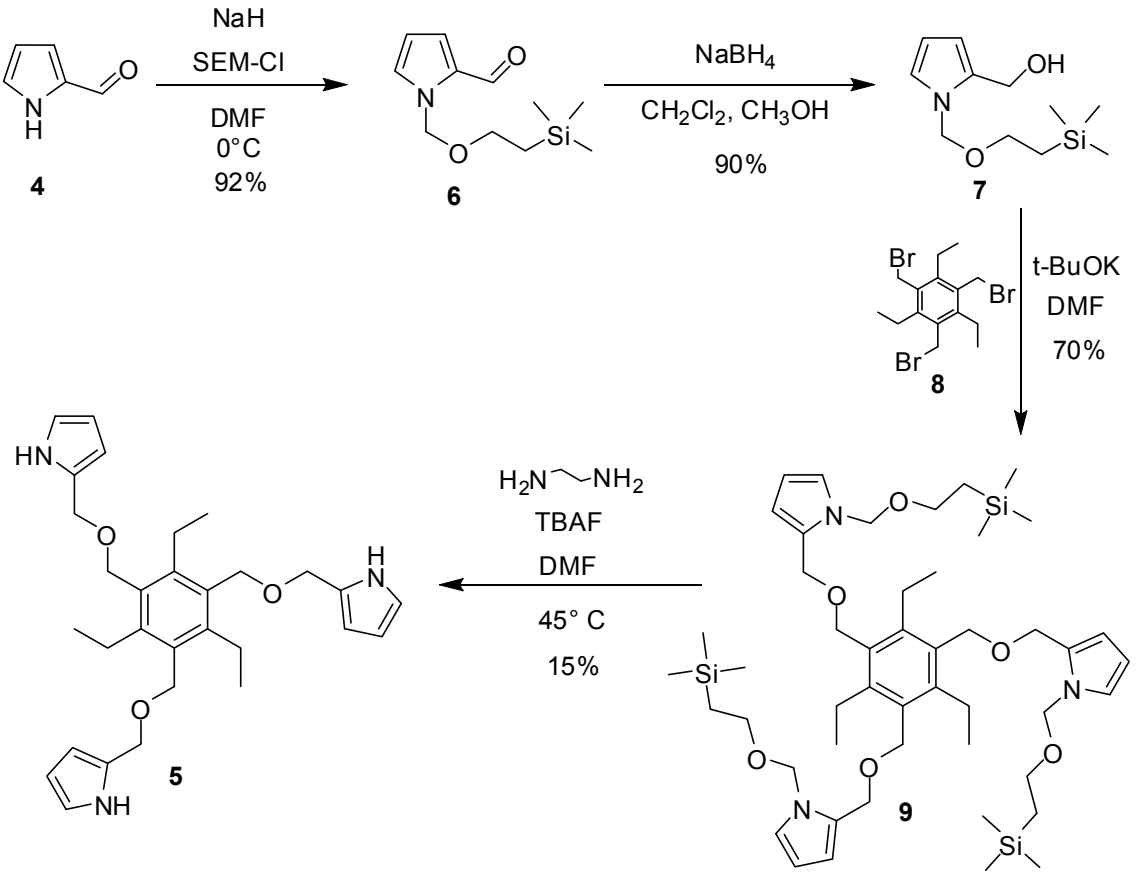

Scheme 1. Synthesis of receptor **3**.

The triether receptor **5** was prepared starting from the pyrrole-2-carboxaldehyde **4** through a synthetic pathway involving the classical Williamson synthesis of ethers groups. The acid NH group of the pyrrole ring was first protected as 2-(trimethylsilyl)ethoxy)methyl to give **6**, and then reduced to give the hydroxy compound **7**. The latter was reacted with the *tris*-bromomethylbenzene scaffold **8** to give the protected receptor **9**, from which receptor **5** was obtained after pyrrole deprotection. The binding properties of receptor **5** were measured toward the monosaccharidic glycosides of Figure 3 and compared to those observed with the plain triether **10** lacking pyrrole rings. Receptor **10** was in turn easily prepared by metoxylation of the tribromomethyl substrate **8** (Scheme 2).

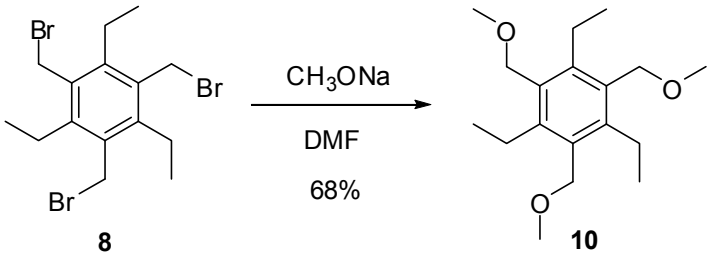

8 **10**

Scheme 2.

Fulfilling the geometrical requirements for an effective recognition is a crucial issue. Molecular mechanics calculations and binding results for receptor **1** have indicated that the correct geometry for binding is achieved by combining the amine and the pyrrole groups through a one methylene unit spacer, connected to the 2-position of the pirrole ring. The homologous receptors **11** and **12**, in which the binding arms have been elongates by one methylene unit with respect to **1** and **2**, were designed in order to gain information on the relevance of the spacer between the aromatic scaffold and the amino-pyrrole binding function. The synthesis of the two receptors has been accomplished by reacting **8** with potassium cyanide to obtain the trinitrile **13**. Cyanide groups were reduced to amines and condensed with the aldehyde **4** to give the tris-imino receptor **11**. Reduction of the Schiff base finally afforded receptor **12**.

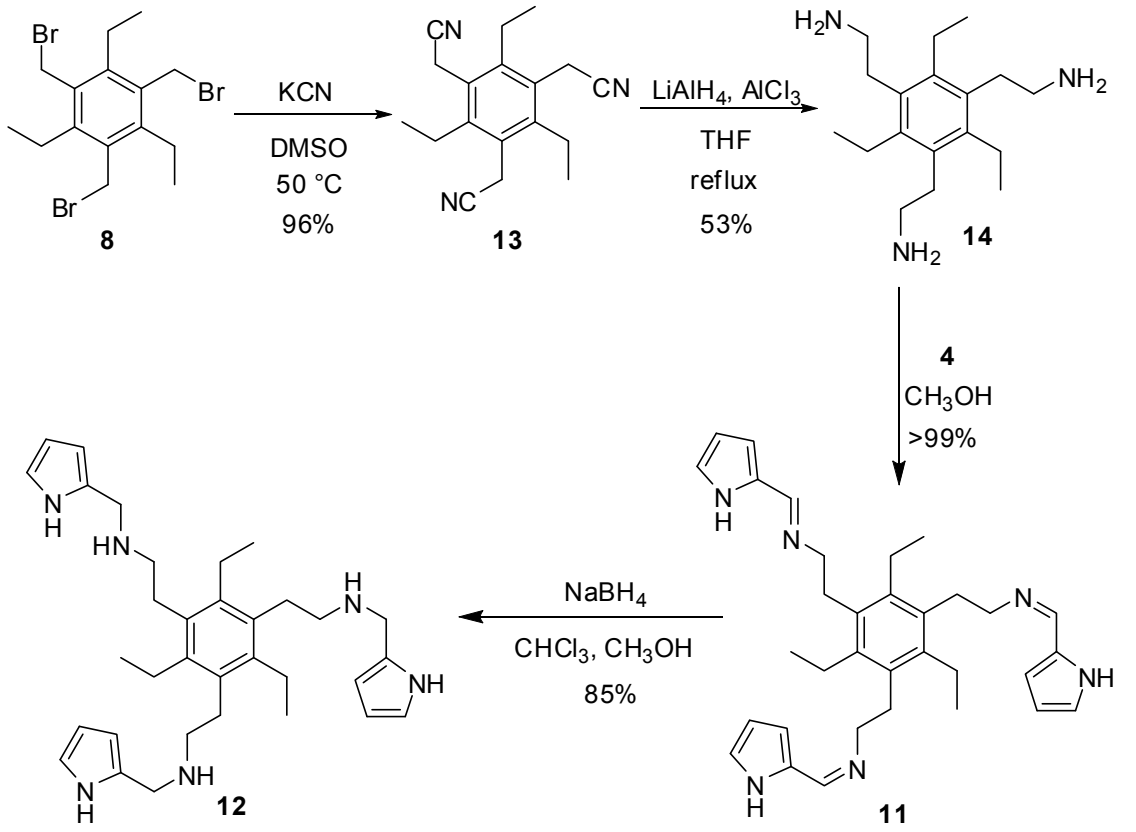

Scheme 3. Synthesis of receptors **12** and **13**.

Binding studies and structure elucidation.

The recognition properties of **2** were tested *vs* the set of octyl glycosides of the monosaccharides depicted in Figure 3. Association constants were measured by ^{1}H NMR titrations in $CDCl_3$ at T = 298 K, following a previously established protocol[28] and the results are reported in Table 1 as cumulative formation constants. Since, in addition to the 1:1 adducts, formation constants for complex species of higher stoichiometry were measured, affinities were assessed using the BC_{50}^{0} parameter (see Introduction). The BC_{50}^{0} values calculated from cumulative binding constants are reported in Table 1, together with those previously obtained for the parent receptor **1**[27] for direct comparison.

Table 1. Cumulative Association Constants (log β_n) for 1:1 and 2:1 Complexes of Receptors **2** with Octyl Glycosides and Corresponding BC_{50}^0 (μM) values for **1** and **2** in $CDCl_3$ at 298 K.[a]

glycoside	log β_{11}	log β_{21}	BC_{50}^0 (**2**)	BC_{50}^0 (**1**)
OctαGlc	3.573 ± 0.004		268 ± 2	570 ± 20
OctβGlc	5.30 ± 0.05	9.04 ± 0.09	4.8 ± 0.5 6780 ± 50[b] 7750 ± 90[c]	24 ± 2 19000 ± 1000[b] 11500 ± 300[c]
OctαGal	3.437 ± 0.002		368 ± 1	790 ± 20
OctβGal	3.921 ± 0.004		120 ± 1	70 ± 1
OctαMan	3.583 ± 0.006		262 ± 4	43 ± 1 12800 ± 300[b]
OctβMan	3.185 ± 0.009		660 ± 10	37 ± 1 13000 ± 400[b]
OctαGlcNAc	2.937 ± 0.001	n.d.[d]	1179 ± 3	72 ± 7
OctβGlcNAc	4.49 ± 0.04	7.95 ± 0.07	30 ± 2	18 ± 1

[a]The receptor's dimerization constant was measured independently under the same conditions and set invariant in the nonlinear regression analysis. For **2**, log β_{dim} = 0.92 ± 0.02. [b] Measured by NMR in CD_3CN. [c] Measured by ITC in CH_3CN. [d]Non detectable.

Since these values were obtained in a noncompetitive solvent, binding constants were also measured in CD_3CN, to ascertain whether recognition would still occur in a more competitive medium. A 1:1 association with OctβGlc could indeed be detected, and the results are reported in Table 1.

An independent support to the observed binding data was obtained by isothermal titration calorimetry (ITC), whose results are reported in Table 2. Besides the very good agreement between the association constants obtained by the ITC and NMR techniques (see Table 1), thermodynamic parameters

Table 2. Association Constants K_a (M^{-1}) and Thermodynamic Parameters (kcal mol^{-1}) for 1:1 Association of Receptors **1** and **2** with OctβGlc.[a]

Receptor	K_a	$-\Delta G°$	$-\Delta H°$	$-T\Delta S°$
1	129.0 ± 1.6	2.87 ± 0.01	11.3 ± 0.8	8.4
2	87.4 ± 1.7	2.65 ± 0.01	6.0 ± 0.8	3.4

[a]Measured by ITC from titration experiments at T = 298 K in CH_3CN on 1.0 mM solutions of receptor injecting 25-50 mM solutions of glycoside.

evidenced a strong enthalpic contribution to the association, which resulted in much smaller binding free energy values because of the large and adverse entropic contribution. Recognition of glycosides by the tripodal pyrrolic receptors can thus be ascribed to a strong enthalpic interaction, likely resulting from multiple H bonding. A peculiar feature emerging from Table 1 is that the aminic receptor **1** is generally more effective than the iminic receptor **2**, whereas the latter is distinctly more selective than the former. Indeed, both are selective for OctβGlc, but selectivity spans a range of over 30-fold for **1** and nearly 250-fold for **2**. Except for OctαGlc and OctαGal, for which lower affinities are observed, all glycosides are strongly bound to **1**; on the contrary, OctβGlc is preferred by **2** by orders of magnitude with respect to the other monosaccharides. The fact that OctβGlcNAc, which like OctβGlc possesses all equatorial substituents, is bound only 6-fold less effectively than OctβGlc indicates that the correct complementarity is achieved for equatorial H-bonding groups. Analogous conclusion can be drawn for **1**, for which OctβGlcNAc is bound even more strongly than OctβGlc. In contrast, axial hydroxyl groups seem to feature a mismatched binding geometry, affecting **2** distinctly more than **1** and showing that geometric and coordinative requirements are significantly more strict for the former than for the latter. It can be concluded that this pyrrolic tripodal architecture is well suited to preferentially bind to the all-equatorial conformation of glucose and glucosamine, while conformational restrictions imposed by the imine double bonds of **2** significantly improve selectivity with respect to the aminic receptor **1**, as a result of a reduced flexibility.

The X-ray structures of receptors **2** supported the above conclusions, providing an insight into the origin of the observed binding features. The ORTEP projections of the structure of **2** crystallized from $CHCl_3$/EtOH, depicted in

Figure 9, show the expected alternate arrangement of substituents, with the three pyrrolic arms on the same side of the aromatic ring forming a cleft, in the center of which an ethanol molecule has been captured. As anticipated, the iminic and the pyrrolic nitrogen atoms lie coplanar in all the three side chains, because of the conjugation of the iminic double-bond with the pyrrole ring; rotation about the CH_2-NH single-bond brings one of the three arms to converge toward the inside of the cleft and to chelate the alcoholic hydroxyl with the two nitrogen atoms. The H-bonding chelate arrangement is noteworthy not only for the nearly perfect planar geometry of the assembly, but also for the matched complementarity of the involved functional groups, with the hydroxyl accepting one H-bond from the pyrrole NH and donating one H-bond

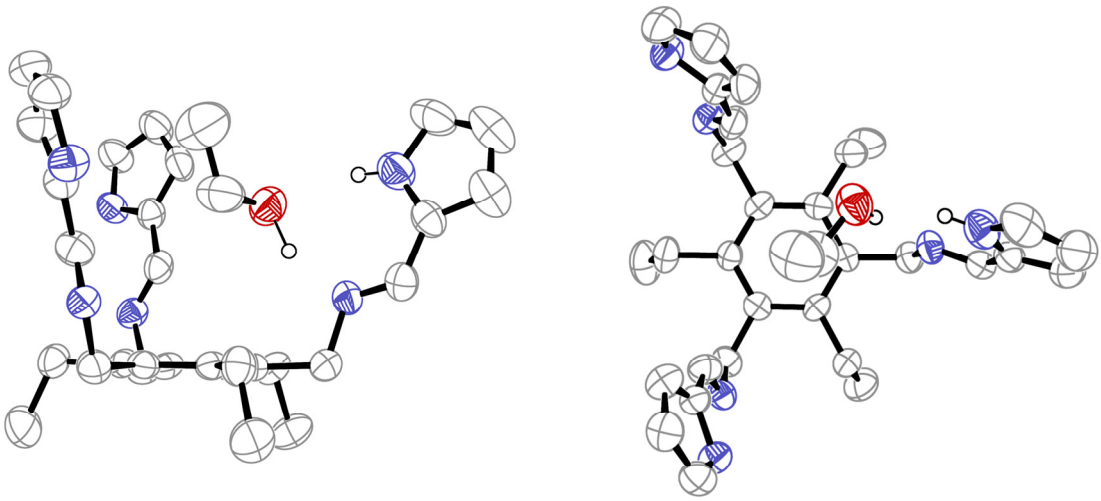

Figure 9. ORTEP projections of the X-ray structure of **2**·EtOH. Left: side view; right: top view. Ellipsoids are at 50% probability. Nitrogen and oxygen atoms are represented as shaded ellipsoids. Hydrogen atoms are omitted for clarity, except for those involved in H-bonding. Selected distances and angles: N–H ··· O, 2.10 Å (161.6°); N(H) ··· O, 2.93 Å; O–H ··· N, 1.76 Å (153.6°); O(H) ··· N, 2.80 Å.

to the imine nitrogen: this way, the chelating donor/acceptor motif of the receptor perfectly matches the dual donor/acceptor nature of the hydroxyl group.

Quite remarkably, a nearly identical structure was observed from crystals obtained from $CHCl_3$/MeOH, indicating that the H-bonded chelate with an hydroxylic species included in the cleft represents a structural preference for the pyrrolic tripodal receptor. Unfortunately, crystals suitable for X-ray structure

analysis could not be obtained for any of the adducts with the investigated glycosides; however, it is plausible that in the presence of glycosidic guests of the appropriate size and possessing appropriately located hydroxyl groups, all the three pyrrolic side chains may converge to cooperatively engage more than one H-bond, giving rise to a reinforced enthalpic interaction and enhanced selectivities.

Independent evidence of the recognition properties of the pyrrolic tripodal receptor **2**, in agreement with binding studies in solution, was obtained in the gas-phase from mass spectrometer experiments. In the positive ion mode ESI-MS spectrum of an equimolar mixture of **2** and OctβGlc, the [**2**·OctβGlc+H]$^+$ complex was present as the major peak, after the base peak of the free receptor, together with a peak of smaller intensity for dimeric **2** (Figure 10, bottom). An analogous spectrum was obtained by injecting an equimolar mixture of **2** and OctαGlc, showing the same set of peaks in comparable intensities, with the [**2**·OctαGlc+H]$^+$ complex present as the minor of the three peaks. The observed relative intensities suggested the formation of a more stable complex for OctβGlc than for OctαGlc. Experiments performed under the same conditions on receptor **1** with OctαGlc and OctβGlc gave very similar results, showing the corresponding peaks of the receptor, of its dimer, and of the complex present in comparable intensities for the two anomeric glycosides (Figure 10, top). The common features exhibited by this set of ESI-MS spectra, although just providing a qualitative picture, demonstrated the presence of the complex species as a major components for all the investigated mixtures.

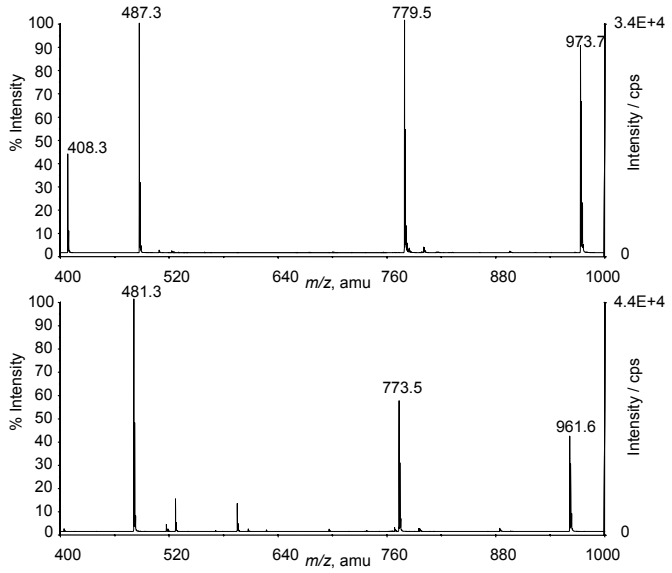

Figure 10. (+) ESI-MS spectra of: Bottom) **2** + OctβGlc, 0.2 mM each; *m/z* 481.3, [**2**+H]$^+$; *m/z* 773.5, [**2**·OctβGlc+H]$^+$; *m/z* 961.6, [**2**·**2**+H]$^+$. Top) **1** + OctβGlc, 0.2 mM each; *m/z* 487.3, [**1**+H]$^+$; *m/z* 779.5, [**1**·OctβGlc+H]$^+$; *m/z* 973.7, [**1**·**1**+H]$^+$. Solvent: $CHCl_3/CH_3CN$ 1:1; ESI voltage: 6 kV; sampling cone potential: 56 V.

A more quantitative description of the relative affinities of **2** and **1** for OctαGlc and OctβGlc could be obtained through collision induced dissociation (CID) experiments performed on a triple quadrupole mass spectrometer. A scan of the intensity of the [**2**·OctβGlc+H]$^+$ and [**2**+H]$^+$ ions originating from the ion of the complex selected at *m/z* 773.5 with increasing potential gave the profiles shown in Figure 11 (top), which crossed for a collision energy value of 8.1 eV, corresponding to the energy required to dissociate 50% of the complex under the specific experimental conditions. The corresponding CID profiles originating from the [**2**·OctαGlc+H]$^+$ ion under identical conditions (Figure 11, bottom) exhibited a crossing point for a collision energy value of 7.7 eV, showing that dissociation of the OctαGlc complex required a collision energy smaller by 1 eV

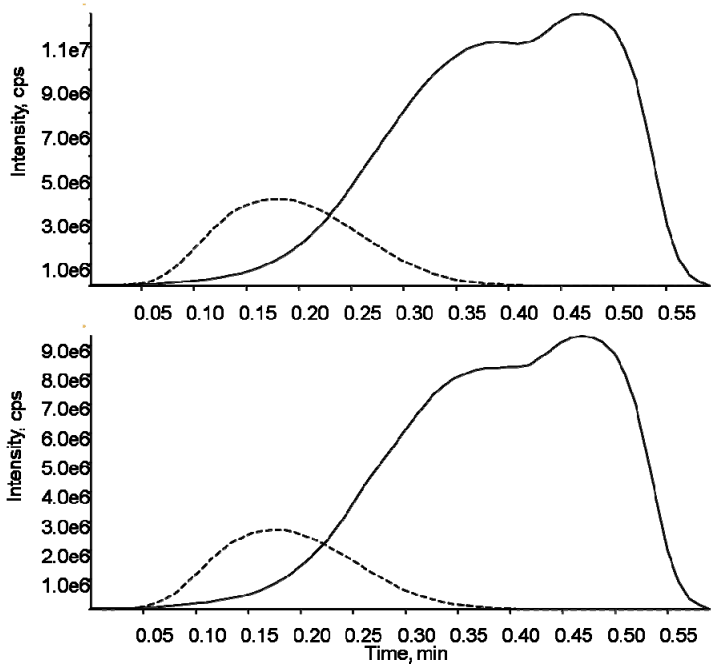

Figure 11. CID MS/MS Analysis of the complex detected as the $[M+H]^+$ ion at *m/z* 773.5. Products: 773.5 ($[M+H]^+$, dotted line), 481.3 ($[\mathbf{2}+H]^+$, solid line). Solvent: $CHCl_3/CH_3CN$ 1:1; ESI voltage: 6 kV; sampling cone potential: 56 V; signal acquisition: 0.60 min, 59 scans over collision energies from – 8.0 to – 37.0 eV in 0.5 eV steps (Q0 = -11 eV); collision-gas pressure: P = 2.64 10^{-5} torr. Top: **2** + OctβGlc, 0.2 mM each. Bottom: **2** + OctαGlc, 0.2 mM each.

than that required by the OctβGlc complex. CID profiles were analogously obtained for complexes of **1** with OctαGlc and OctβGlc, run under identical experimental conditions in order to obtain comparable results. The corresponding profiles, similar in all respect to those depicted in Figure 11, gave crossing points for collision energies of 7.4 and 6.4 eV for OctβGlc and OctαGlc, respectively. Quite gratifyingly, results in the gas-phase showed the same trend observed in solution: besides the same β/α selectivity order, both glycoside anomers were more strongly bound to **2** than to **1** in solution *and* in the gas-phase.

In contrast to the described results, NMR binding studies on the triether receptor **5**, reported in Table 3 as cumulative binding constants and BC_{50}^{0} values, showed a dramatic decrease of the affinity toward OctβGlc compared to the amino-pyrrolic receptor **1**, which spanned nearly two orders of magnitude. The results for the corresponding receptors **10** and **3** lacking the pyrrolic binding groups, are also reported in Table 3 for direct comparison. It can easily be appreciated that pyrrole groups bring a 150-fold increase in affinity for the

aminic receptor **1** with respect to **3** and 30-fold increase for the ethereal receptor **5** with respect to **10**, whereas replacement of ethereal oxygen for the

Table 3. Cumulative Association Constants (log β_n) for 1:1, 2:1 Complexes of Receptors **1**, **3**, **5** and **10** with OctβGlc and Corresponding BC_{50}^{0} (μM) values for in $CDCl_3$ at 298 K.[a]

	1	**3**	**5**	**10**
log β_{11}	4.61 ± 0.03	2.616 ± 0.003	2.612 ± 0.088	1.154 ± 0.007
log β_{21}	7.79 ± 0.06		4.242 ± 0.134	
BC_{50}^{0}	24 ± 2 19000 ± 1000[b]	3690 ± 50	2200 ± 400 108000 ± 7000[b]	70000 ± 1000

[a]The receptor's dimerization constant was measured independently under the same conditions and set invariant in the nonlinear regression analysis. For **1**, log β_{dim} = 1.07 ± 0.01. For **3**, log β_{dim} = 1.83 ± 0.02. [b]Measures by NMR in CD_3CN.

amino group induces a drop in affinity of nearly 100-fold in the pyrrolic receptors **1** and **5** and 20-fold in the plain receptors **3** and **10**. This evidence suggests a synergistic effect between the pyrrole and the amino groups, boosting the binding ability in a non-additive manner, and a preference for the aminic NH to behave as a H-bonding donating function in the investigated tripodal architecture. The main conclusion that can be drawn from the analysis of the above data is that both the amino and the pyrrolic groups contribute substantially to the binding ability of the receptor and cannot be effectively replaced by other H-bonding functionalities. Indeed, as previously observed for the amidic and ureidic functions, even the ethereal oxygen cannot behave as an effective H-bonding group. Apparently, the H-bonding donor ability of the aminic NH group is essential for the binding properties of the tripodal architecture for glycoside recognition.

Concerning the chain length, of the binding arms, locating the amino group one methylene further away from the scaffold induces a complete loss of affinity. Indeed, any attempts to evaluate the affinities of **11** and **12** toward OctβGlc failed to provide evidence of binding, giving a clear-cut answer to the question about the choice of the spacer length. Although the flexible arms of the adaptive tripodal receptor can assume a large number of different conformations, somewhat counter intuitively the geometry requirements for

binding are so strict that even a minor increase in the chain length can deplete the binding ability. This evidence highlights that the architecture of the amino pyrrolic receptor is well suited indeed for recognition of carbohydrates.

In conclusion, the amino-pyrrolic combination of H-bonding ligands appears to be too well matched to be effectively replaced by alternative binding groups, when appropriately located in the binding arms of the tripodal receptor, although fixing the conformation into a coplanar chelating arrangement, as in the iminic receptor **2**, seems to confer improved binding ability and distinct selectivity toward the glucose moiety.

2 – Modification of the receptor scaffold.

Design and Synthesis.

The results reported in the previous section indicate unambiguously that a correct H-bonding motif for carbohydrate recognition consist in amine and pyrrole groups spaced by a methylenic unit. Moreover a correct assemblage on a tripodal scaffold to achieve the suitable geometry for the interaction requires the amino-pyrrole function to be spaced from the aromatic platform by a methylenic unit as well.

Taking in account the above structural prerequisites, receptor **15** preseting four binding arms on the benzene scaffold was designed to increase the number of potential H-bonding interactions with glycosides. The conformational flexibility of the molecule may allow a convergent disposition of all four binding arms. Receptor **15** was prepared by reacting the tetrabromomethyl scaffold **16** with sodium azide to yield **17**, which was subsequently converted into the tetraamine **18** by Staudinger reduction and hydrolysis. Condensation with **4** followed by reduction of the Schiff base yielded receptor **15**, that was tested in binding studies with the glycosides of Figure 3.

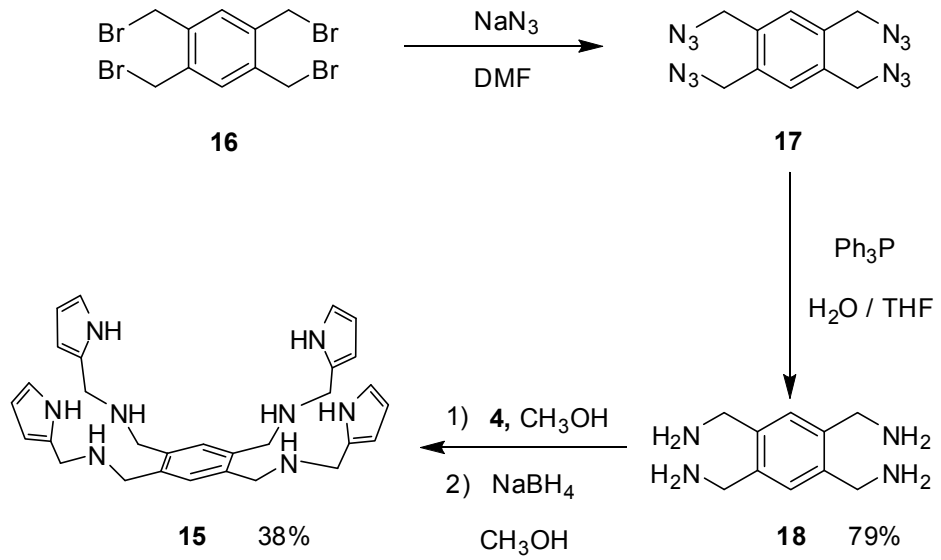

Scheme 4. Synthesis of receptor **15**.

A cyclic amino-pyrrole of appropriate size (**19**) was designed to evaluate the effect of the preorganization induced by the cyclic structure on binding

properties. The dialdehydic pyrrole **24**[40] required for the cyclization reaction with the diamine **25**, was prepared from the monoaldehyde **4**. Protection of the pyrrolic nitrogen as carbamate (**20**) and of the aldehydic group as acetal yielded compound **21**. Subsequent deprotection of the pyrrolic nitrogen afforded **22**, which was formylated in the α position through the Vilsmeier reaction to give **23**. Hydrolysis of the acetal group finally yielded **24**. Receptor **19** was synthesized via one-pot [2+2] cyclization reaction between diamine **25** and dialdehyde **24** in the presence of OctβGlc as a template. The resulting Schiff base was finally reduced to the macrocyclic tetraamine **19**. In presence of the template the reaction gave an overall yield of 71%, whereas in the absence of OctβGlc only 25% yield was obtained.

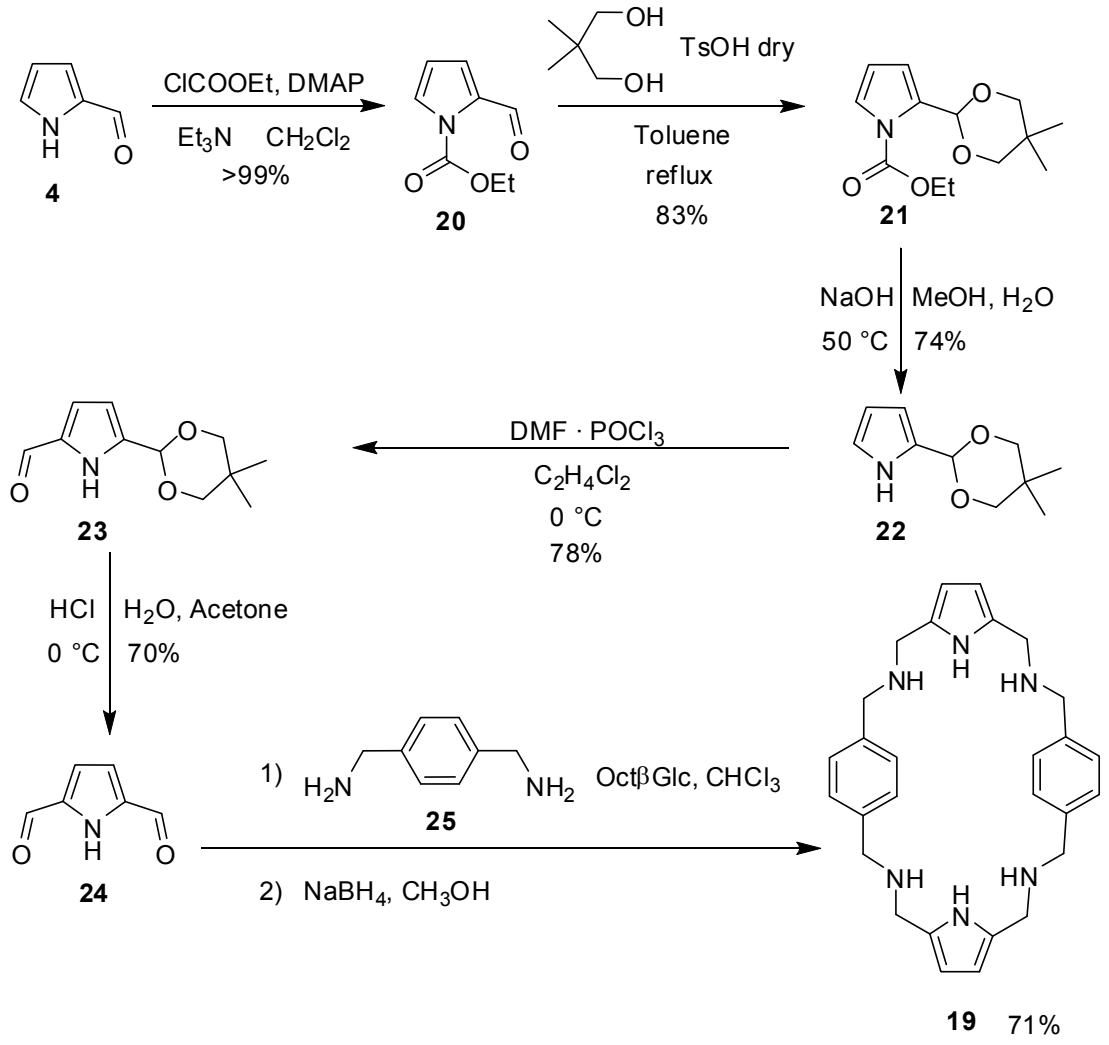

Scheme 5. Synthesis of cyclic receptor **19**.

In addition cyclic and acyclic amino-pyrrole receptors, cage receptors were also explored. Receptor **26**[41] was designed to lock the tripodal pyrrolic receptor **1** into a cage architecture. Receptor **26** spontaneously formed in quantitative yield by one-pot self-assembly of 5 components: when a 2:3 mixture of triamine **3** and dialdehyde **24** was stirred in methanol, a single compound was unexpectedly obtained in quantitative yield, unambiguously identified as the hexaimine macrobicyclic cage **27** by NMR, ESI-MS and HRMS (Scheme 6).[42-46] Since **27** is very poorly soluble in methanol, reversible imine condensation was driven toward the complete formation of a single product by precipitation. Solubility is not, however, the only driving factor, since the corresponding reaction of the triaminoethyl homologue **14** gave only an intractable polymeric material by precipitation. Clearly, **27** is the thermodynamically favoured product arising from condensation of 5 reacting molecules, which self-assemble through the concerted formation of 6 imine bonds.

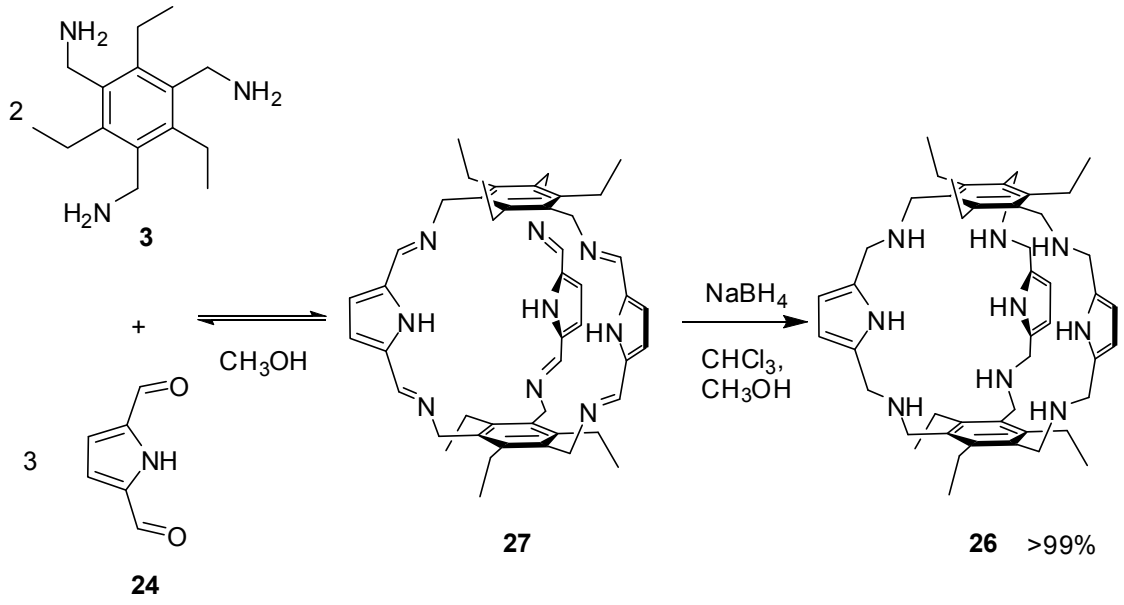

Scheme 6. Synthesis of cage receptor **26**.

One pot reduction of **27** with $NaBH_4$ gave the corresponding macrobicyclic hexaamine **26** in essentially quantitative yield. In contrast to **27**, **26** is freely soluble in lipophilic solvents. The ESI-MS and HRMS spectra of **26** confirmed the identity of the cage, while ^{1}H and ^{13}C NMR spectra displayed signals in agreement with a highly symmetrical structure.

Binding studies and structure elucidation.

X-ray structure of **26**, showes a nearly perfect C_3 symmetry of the cage,[47;48] apparently persistent in solution, with all the amine groups pointing inward, the ethyl groups pointing outward, and the pyrrole rings facing the cavity (Figure 12). Although pyrrole rings are somewhat tilted, a roughly spherical cavity is envisaged from the picture: the size of the cavity, whose diameter between the benzene rings is 8.4 Å, and the arrangement of the amino groups appear well suited for guest binding.

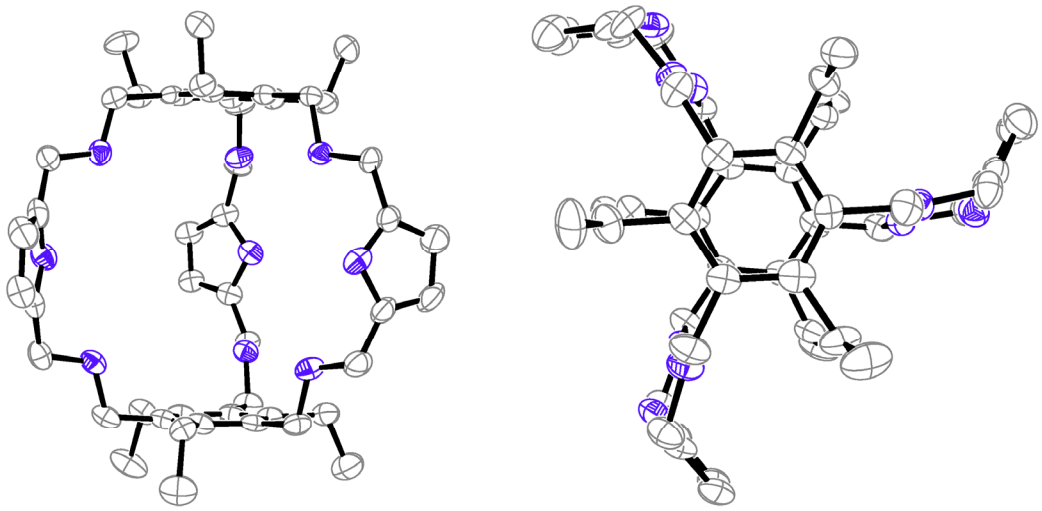

Figure 12. ORTEP projections of the X-ray structure of **26**. Left: side view; right: top view. Ellipsoids are at 50% probability. Nitrogen atoms are represented as shaded ellipsoids. Solvent molecules and hydrogen atoms are omitted for clarity.

Binding experiments were thus performed by ^{1}H NMR in $CDCl_3$ using OctβGlc. The spectra obtained by varying the **26**/OctβGlc mole ratio at constant total concentration of reactants are reported in Figure 13. Disappearance of signals of **26** and appearance of a new set of signals testified the formation of a host-guest complex in slow-exchange regime with the free species on the NMR time scale. It can be noted that the single signal for the 3 equivalent pyrrolic NH protons is split into 3 non-equivalent singlets, while the pyrrolic CH signal splits into 3 strongly coupled non-equivalent signals, showing that the C_3 symmetry is lost upon complexation. Both slow exchange and desymmetrization, together with the marked downfield shift of the NH signals, point to the formation of a hydrogen bonded complex with the glucoside at least partially included into the

cavity. Indeed, a separate set of signals is observed for the glucose moiety as well, upfield with respect to that of the free glucoside, consistent with the shielding effect of the benzene rings; the H-3, H-4, and H-5 protons experience the largest shifts, suggesting inclusion from the side opposite to the glycosidic chain.[13] A 1:1 stoichiometry was inferred from complete disappearance of the free host for just over a stoichiometric reactant ratio and from the maximum intensity of the complex's signals observed for 1:1 mole ratio; the corresponding association constant value K_a = 4.83(8) 10^4 M^{-1}, which stands for a 20.7 μM affinity of **26** for OctβGlc, was obtained with excellent agreement from 4

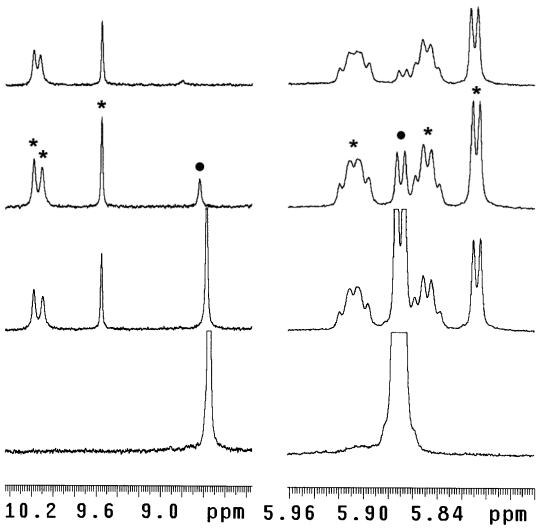

Figure 13. ^{1}H NMR spectra (400 MHz, 25 °C, $CDCl_3$) of mixtures of **26** and OctβGlc for varying mole ratio (bottom to top: 1:0; 2:1; 1:1; 1:2) at constant total concentration of reactants. Only the pyrrole NH (left) and CH (right) signals of **26** are shown. (∗) [**26**· βGlc]; (•) free **26**.

independent experiments at different reactant concentrations. Quite strikingly, the same experiment performed with the α anomer (OctαGlc) did not show any evidence of binding, indicating that **26** is able to bind the β anomer exclusively. We believe that improved performance results from both a precise size fit of the β-glucoside and a closer complementarity of the amino/pyrrole group in H-bonding to the glucose moiety.

Further evidence supported the binding ability of **26**. Methyl-β-D-glucopyranoside (MeβGlc) is insoluble in $CDCl_3$. When solid MeβGlc was shaken with a millimolar solution of **26** in $CDCl_3$, the solid partially dissolved and

the spectrum of the resulting solution unambiguously showed that over 40% of the cage was present in the complexed form. Bound **26** raised to 50% in CCl_4 and to 75% when the experiment was performed in C_6D_6, proving that the cage receptor is capable of bringing insoluble β- (but not α-) glucosides into lipophilic solvents of low polarity. Indeed, MeαGlc was not appreciably dissolved in any of the above solvents. Most remarkably, β-D-glucose (βGlc) itself could be dissolved into benzene up to nearly 20% of bound receptor, whereas αGlc could not. Thus, the possibility that the observed β/α selectivity may be steric in origin, caused by the bulky octyl group, can be ruled out.

The cage receptor was further tested in $CDCl_3$ toward α and β octyl glycosides of biologically relevant monosaccharides, namely, galactopyranosides (Gal) and mannopyranosides (Man). Although interaction between partners was evidenced by shift of some signals of both the host and the guest, the presence of a separate set of signals for the complex species was not detected in any case. Competitive experiments feeding **26** with equimolar mixtures of OctβGlc and each of the selected glycosides showed that for a 1:1:1 ratio of reactants the fraction of **26** bound to OctβGlc was decreased, with respect to that observed in the absence of competitors, by significantly less than 10% in the most adverse case. Experimental evidence demonstrated that none of the tested glycosides could effectively compete with OctβGlc for **26**.

Interestingly, the hexaimine cage **27** did not exhibit the same binding ability of **26**. Addition of OctβGlc to a solution of **26** in $CDCl_3$ did not show evidence of complexation, but rather induced slow re-equilibration of the cage to oligomeric products. Likewise, mixing **2** and **24** in the presence of OctβGlc as a template gave substantial amounts of oligomeric iminic products, together with lower yields of **27**. Apparently, the iminic cage does not bind to OctβGlc and therefore using the latter as a template hampers, rather than assisting, the formation of the cage. This contrasting behavior is most likely related to the geometrical restrictions imposed by the iminic double bond, which must lie coplanar to the conjugated pyrrole ring, rather than to the basicity/coordinative properties of the imine nitrogen, considering that the cage size is essentially identical.

An independent experimental support was desirable to validate the binding affinity results. Unfortunately, crystals suitable for X-ray analysis could not be obtained for any of the complexes of **26** with glucosides. However, ESI-MS provided a clear-cut evidence in full agreement with the NMR binding studies. Two equimolar solutions of **26** with OctβGlc and OctαGlc, respectively, of the same concentration, were submitted to positive ion mode ESI-MS analysis under the same conditions. While in the spectrum of the former a peak for the [**26**·OctβGlc+H]$^+$ complex was present with comparable abundance with respect to the [**26**+H]$^+$ peak, in the spectrum of the latter the peak of the complex could only be detected at the noise level (Figure 3). The latter spectrum appeared unaffected by three subsequent 2-fold increase of the concentration of the OctαGlc injected. In addition, the spectrum of an equimolar

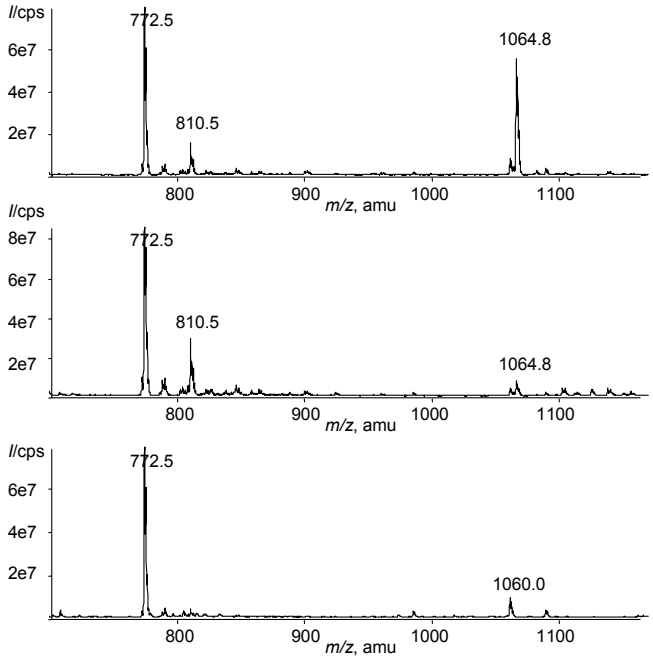

Figure 14. (+) ESI-MS spectra of: top) **26** + OctβGlc, 0.2 mM each; medium) **26** + OctαGlc, 0.2 mM each; bottom) **26** + βGlc pentaacetate, 0.2 mM each. Solvent: $CHCl_3/CH_3CN$ 1:1; ESI voltage: 6 kV; sampling cone potential: 56 V. *m/z* 772.5, [**26**+H]$^+$; *m/z* 794.6, [**26**+Na]$^+$; *m/z* 810.5, [**26**+K]$^+$; *m/z* 1064.8, [**26**·β(α)Glc+H]$^+$.

mixture of **26** and βGlc pentaacetate, run for comparison under the same conditions, revealed a complete lack of the peak of the complex, showing that in the absence of free hydroxyl groups, binding to the glucose moiety in the gas-

phase does not occur. Clearly, OctαGlc, which differs from OctβGlc just for the stereochemistry at C-1, was not bound to **26** to a significantly larger extent than βGlc pentaacetate.

A conclusive evidence was obtained by collision induced dissociation (CID) experiments run on a triple quadrupole mass spectrometer. A scan of the intensity of the [**26**·OctβGlc+H]$^+$ and [**26**+H]$^+$ ions originating from the ion of the complex selected at *m/z* 1065 with increasing potential gave the profiles shown in Figure 15 (bottom), which crossed for an energy value of 13.9 eV, corresponding to the energy required to dissociate 50% of the complex under the specific experimental conditions. The CID profiles originating from the [**26**·OctαGlc+H]$^+$ ion under identical conditions (Figure 15, top) did not exhibit any crossing point in the whole range of potential, proving that spontaneous dissociation of the complex is prevalent for [**26**·OctαGlc] and that dissociation due to collisions is negligible at all concentrations, since identical

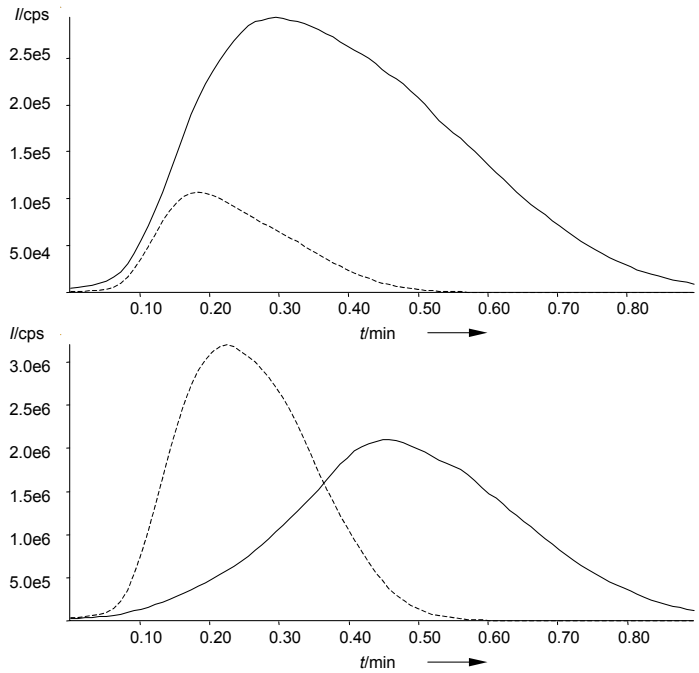

Figure 15. CID MS/MS Analysis of the complex detected as the [M+H]$^+$ ion at *m/z* 1065. Products: 1065 ([M+H]$^+$, dotted line), 772 ([**26**+H]$^+$, solid line). Solvent: $CHCl_3/CH_3CN$ 1:1; ESI voltage: 6 kV; sampling cone potential: 56 V; signal acquisition: 0.90 min, 89 scans over collision energies from 6 to 50 eV in 0.5 eV steps; collision-gas pressure: P = 2.64 10^{-5} torr. Bottom: **26** + OctβGlc, 0.2 mM each. Top: **26** + OctαGlc, 0.2 mM each.

results were obtained for 4 different concentrations of the OctαGlc injected. Exclusive recognition of the β anomer, observed in solution, was thus confirmed in the gas-phase.

Concerning the monocyclic receptor **19**, affinities versus OctβGlc and OctβMan were measured through binding experiments performed by ^{1}H NMR in $CDCl_3$, the resulting are reported in Table 4 in comparison with those of the open-chain receptor **1**.

Table 4. Intrinsic Median Binding Concentration (BC_{50}^0, μM) and Cumulative Association Constants (log β_n) for Receptor to Glycoside (R:G) Complexes of **1** and **19** with Octyl Glycosides in $CDCl_3$ at 298 K.[a]

	OctβGlc		OctβMan	
	log β (R:G)	BC_{50}^0	log β (R:G)	BC_{50}^0
1	5.30 ± 0.05 (1:1) 9.04 ± 0.09 (2:1)	24 ± 2	3.185 ± 0.009 (1:1)	37 ± 1
19	3.242 ± 0.032 (1:1) 5.31 ± 0.15 (2:1)	540 ± 40	3.379 ± 0.002 (1:1)	421 ± 2

[a] The receptor's dimerization constant was measured independently under the same conditions and set invariant in the nonlinear regression analysis. For **1**, log β_{dim} = 1.07 ± 0.01. For **19**, log β_{dim} = 0.823 ± 0.034.

As can be seen, for both glycosides, a drop of over one order of magnitude is observed for the cyclic with respect to the open-chain receptor, indicating that the cyclic structure is not beneficial to the binding properties. Furthermore, no significant selectivity is observed between Glc and Man. This is somewhat surprising in view of the template effect observed in the synthesis of **19**. Indeed, in contrast to the iminic cage receptor **27**, the monocyclic tetraimine progenitor of **19** showed unambiguous template effect with OctβGlc, suggesting that the para-substitution of the aromatic rings provides the correct size for binding the glucoside, whereas the meta-substitution results too tight for a correct binding geometry. On the other hand, the opposite is true for the aminic receptors **19** and **26**, for which high affinity is observed for the meta-substituted cage receptor, whereas poor binding toward OctβGlc was observed for the

para-substituted monocyclic receptor. Clearly, conformational restrictions imposed by the iminic double bond and/or the absence of H-bonding donor capabilities, in addition to the slight difference in size induced by the meta/para substitution, play a crucial role in these structures, these evidences confirm the notion that adaptivity is advantageous if a preorganized structure in not perfectly fit to the ligand.

To better evidence improved binding-properties, binding experiments on the four-armed receptor **15** were performed by ^{1}H NMR in CD_3CN, a more competitive medium compared to $CDCl_3$. Receptor **15** was tested towards OctβMan, a glycoside of particular interest for which binding affinities were also measured in CD_3CN for receptor **1**.

Table 5. Cumulative Association Constants (log β_n) for 1:1, 1:2 Complexes of Receptors **1** and **15** with OctβMan and Corresponding BC_{50}^0 (μM) values in CD_3CN at 298 K.[a]

	1	**15**
log β_{11}	2.097 ± 0.004	2.138 ± 0.047
log β_{12}		3.46 ± 0.32
BC_{50}^0	13000 ± 400	6000 ± 800

[a] Receptor **1** dimerization constant log β_{dim} = 1.59 ± 0.03.

An increase in affinity of a factor of 2 was observed with respect to the 3-armed receptor **1**. However, to a closer inspection of data, the increase in affinity is clearly due to the presence of a 1:2 complex, since the 1:1 association showed a closely similar binding constant. This can be easily explained by considering that the four binding arms may be disposed pair-wise on opposite sides of the benzene ring, making **15** a ditopic receptor for glycosides. Based on these considerations, the intrinsic binding ability of **15** would not be enhanced compared to **1**, suggesting the three arms of the latter may not all be involved in binding. In conclusion, a significant binding enhancement could not be achieved neither by increasing the number of binding arms, nor by constraining the tripodal receptor into a cyclic or bicyclic cage structure, whereas an inhibition of binding was even observed for the monocyclic receptor.

3 – Modification of the pyrrolic binding groups.

Design and Synthesis.

Although cyclic and cage structures are appealing for specific recognition properties, their synthesis is often complicated by unpredictable amount of polymeric side products. Moreover, the highest affinities in glycoside recognition were obtained by acyclic tripodal pyrrolic receptors. Therefore new modifications aimed at improving binding affinities by implementing new H-bonding groups, were focused on the functionalization of the α position of the pyrrolic moieties of receptor **1**.

Molecular models suggested, although only qualitatively, that acetalic substituents located in the α position of pyrroles as H-bonding acceptors may assume a convergent geometry, which may be appropriate for binding. Receptor **28** was easily prepared by condensation of the triamino scaffold **3** with the appropriate pyrrolaldehyde **23** and subsequently reduction of the iminic intermediate.

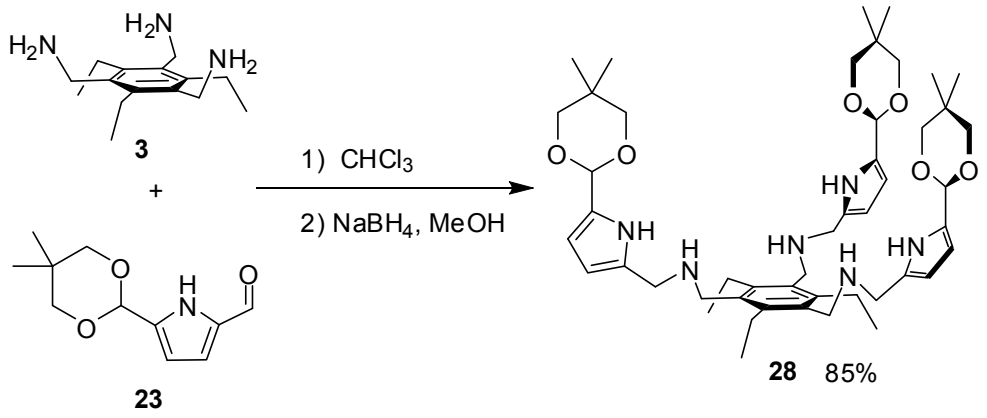

Scheme 7. Synthesis of receptor **28**.

Receptors **29**, **30** and **31** were designed in order to investigate how differences in the H-bonding nature of substituents in the α position of pyrroles could tune the receptor binding ability. While both receptors **29** and **30** presented a conformationally restricted H-bonding acceptor group, due to the conjugation of the aldeidic and ester double bonds with the pyrrolic ring, such restrictions were not present in the structure of the aminic receptor **31**. Receptor

29 was prepared from the pyrrole ester **32** that was formylated in the α position by the Vilsmeier reaction to give **33**. Reaction with the triaminic scaffold **3** and reduction of the resulting Schiff base afforded receptor **29** in good yields.

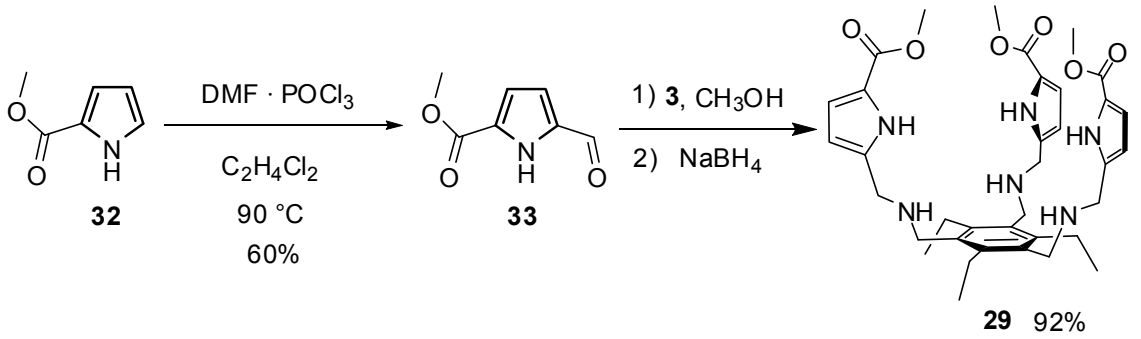

Scheme 8. Synthesis of receptor **29**.

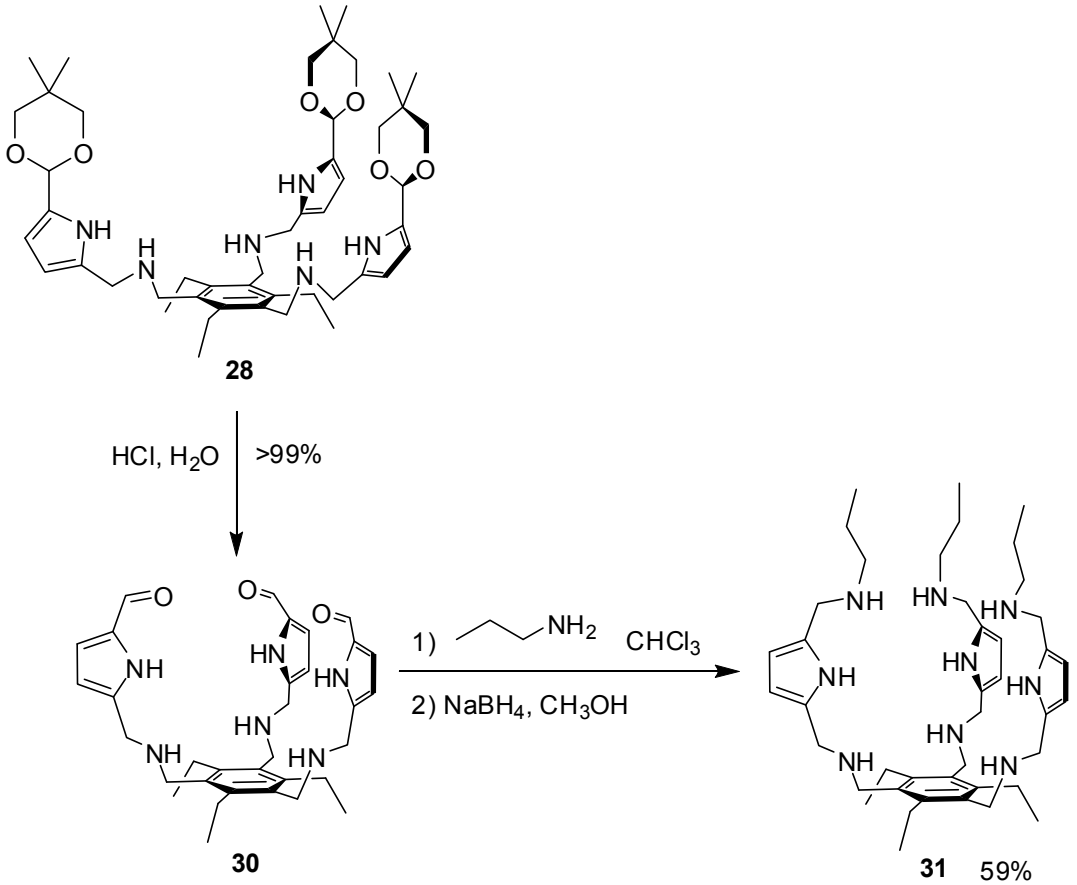

Scheme 9. Synthesis of receptors **30** and **31**.

Receptor **30** and **31** were prepared from the triacetal **28**. Hydrolysis of acetal functions gave the aldeidic receptor **30**, which was reacted with *n*-propylamine; subsequently reduction of the Schiff base yielded receptor **31**.

Binding studies and structure elucidation.

The recognition properties of **28** were tested *vs* the set of octyl glycosides of the monosaccharides. Association constants were measured by ^{1}H NMR titrations in $CDCl_3$ and the results are reported in Table 6.

Table 6. Cumulative Association Constants (log β_n) for 1:1 and 2:1 Complexes of Receptor **28** and Octyl Glycosides and Corresponding BC_{50}^0 (μM) values for **28** and **1** in $CDCl_3$ at 298 K.[a]

glycoside	log β_{11}	log β_{21}	BC_{50}^0 (**28**)	BC_{50}^0 (**1**)
OctαGlc	3.23 ± 0.01	4.98 ± 0.16	570 ± 20	570 ± 20
OctβGlc	4.40 ± 0.04	7.30 ± 0.09	39 ± 3	24 ± 2
OctαGal	2.651 ± 0.005	n.d.[b]	2250 ± 20	790 ± 20
OctβGal	3.730 ± 0.002	5.04 ± 0.05	185 ± 1	70 ± 1
OctαMan	5.54 ± 0.12	9.71 ± 0.18	2.8 ± 0.7	43 ± 1
OctβMan	[c]	[c]	< 1	37 ± 1
OctαGlcNAc	5.18 ± 0.02	8.94 ± 0.04	6.4 ± 0.3	72 ± 7
OctβGlcNAc	5.14 ± 0.03	9.08 ± 0.04	6.9 ± 0.5	18 ± 1

The receptor's dimerization constant was measured independently under the same conditions and set invariant in the nonlinear regression analysis. For **28**, log β_{dim} = 0.075 ± 0.017.
[b]Nondetectable. [c]Too large to be measured.

It is clearly apparent that, compared to **1**, affinities are lower for Gal but higher for GlcNAc and even more for Man, spanning a selectivity range exceeding 3 orders of magnitude. However, the most striking result is the affinity exhibited for OctβMan, which is estimated in the nanomolar range. Indeed, binding constants were too large to be measured by ^{1}H NMR, but an upper limit of 1 μM for BC_{50}^0 could be inferred by comparison with the titration data of OctαMan. As far as we are aware of, this is one of the largest affinity ever reported for a synthetic receptor for mannose. Selectivity *vs* other glycosides is also noteworthy, with an outstanding factor of more than 800 between OctαMan and OctαGal, and expectedly much larger between OctβMan and OctαGal. In contrast, poorer discrimination is observed between OctαMan and α- and OctβGlcNAc, although selectivity may be anticipated to be significant for OctβMan.

To assess the affinity of **28** for OctβMan, rather than evaluating binding constants by a different technique, we thought it would be more informative and significant to measure affinities in a more competitive solvent. Association constants measured in CD_3CN are reported in Table 7, together with the corresponding BC_{50}^0 values.

Table 7. Cumulative Association Constants (log β_n) for 1:1 and 2:1 Complexes of **28** with Octyl Glycosides in CD_3CN, Corresponding BC_{50}^0 (μM) values, and Affinity Ratios (AR) between BC_{50}^0 values in CD_3CN and $CDCl_3$.[a]

glycoside	log β_{11}	log β_{21}	BC_{50}^0 (**28**)	AR
OctαGlc	1.592 ± 0.008	n.d.[b]	25,600 ± 500	45
OctβGlc	2.100 ± 0.003	n.d.[b]	7,940 ± 50	204
OctαGal	1.55 ± 0.01	n.d.[b]	28,300 ± 800	13
OctβGal	1.988 ± 0.002	n.d.[b]	10,290 ± 50	56
OctαMan	2.233 ± 0.003	n.d.[b]	5,850 ± 40	2090
OctβMan	3.12 ± 0.02	5.40 ± 0.08	680 ± 30	>680
OctαGlcNAc	2.231 ± 0.002	n.d.[b]	5,880 ± 20	919
OctβGlcNAc	2.155 ± 0.003	n.d.[b]	6,990 ± 50	1013

[a] β_{dim} nondetectable. [b]Nondetectable.

It is easily appreciated that, even in a competitive solvent, affinities still lie in the low millimolar range, with the notable exception of OctβMan, which is bound to **28** with an affinity in the micromolar range and with a β/α selectivity factor of nearly an order of magnitude. On the assumption that in acetonitrile affinities of both anomers of mannose are damped to the same extent with respect to chloroform, we can estimate the affinity of **28** for OctβMan to be 330 nM in $CDCl_3$, a figure that confirms its unprecedented recognition properties. As a general evidence, affinities are attenuated with respect to $CDCl_3$ to a much greater extent for Man and GlcNAc than for the other glycosides. Gratifyingly, results were confirmed by ITC measurements in CH_3CN, which gave affinities for OctαMan and OctβMan in good agreement with NMR data and evidenced a substantial enthalpic contribution, compensated by an adverse entropic contribution.

Binding results were independently confirmed in the gas phase by ESI–MS experiments. In the positive ion mode ESI–MS spectra of equimolar mixtures of **28** and OctβMan, OctαMan, and OctαGal, respectively (Figure 16), the peak of the 1:1 complex was observed as the base peak for βMan, with intensity comparable to the peak of the free receptor, but reduced to 30% for OctαMan, whereas it could only be detected at the noise level for OctαGal. Instead, βGlc pentaacetate gave no evidence of complexation, showing that, in the absence of H-bonding hydroxyl groups, recognition of a strongly bound glucoside is depleted.

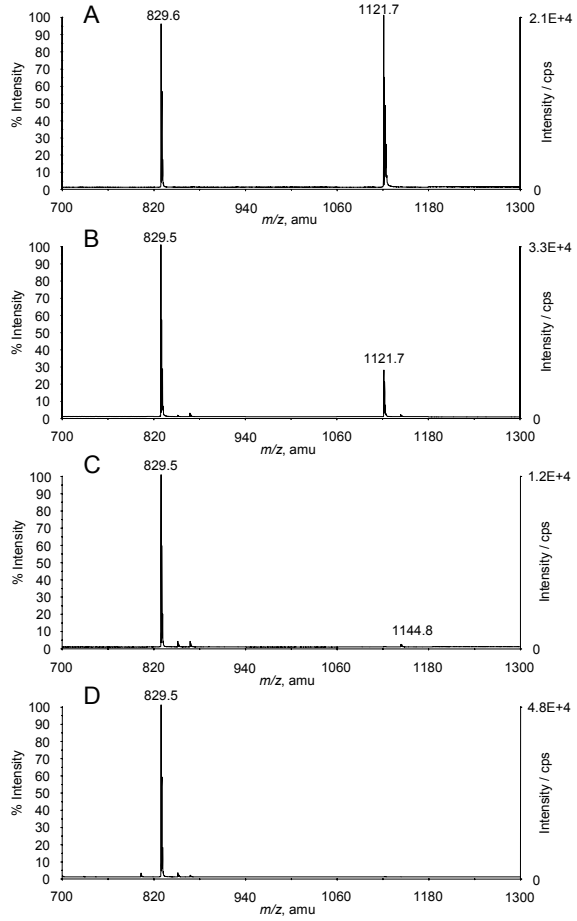

Figure 16. (+) ESI-MS spectra of: **A**) **28** + OctβMan, 0.2 mM each; **B**) **28** + OctαMan, 0.2 mM each; **C**) **28** + OctαGal, 0.2 mM each; **D**) **28** + βGlc pentaacetate, 0.2 mM each. *m/z* 829.5, [**28**+H]$^+$; *m/z* 1121.7, [**28**·glycoside+H]$^+$; *m/z* 1144.8, (impurity). Solvent: CH_3CN; ESI voltage: 6 kV; orifice: 46 V.

A definitive evidence of complex stability was obtained from the above mixtures by ESI–MS/MS collision induced dissociation (CID) experiments

(Figure 17). CID profiles gave 50% of complex dissociation for collision energies of 19.0 eV and 14.5 eV for OctβMan and OctαMan, respectively, showing a significantly higher stability of the OctβMan complex, whereas spontaneous dissociation of the adduct was observed for OctαGal.

Some structural evidence of the receptor-glycoside complexes was highly desirable but, unfortunately, all attempts to obtain X-ray quality crystals failed, giving oils or glassy solids from various solvents. However a combination of molecular modeling calculations and of NMR data, including the variation of chemical shifts upon complexation, as well as intermolecular NOEs, have been

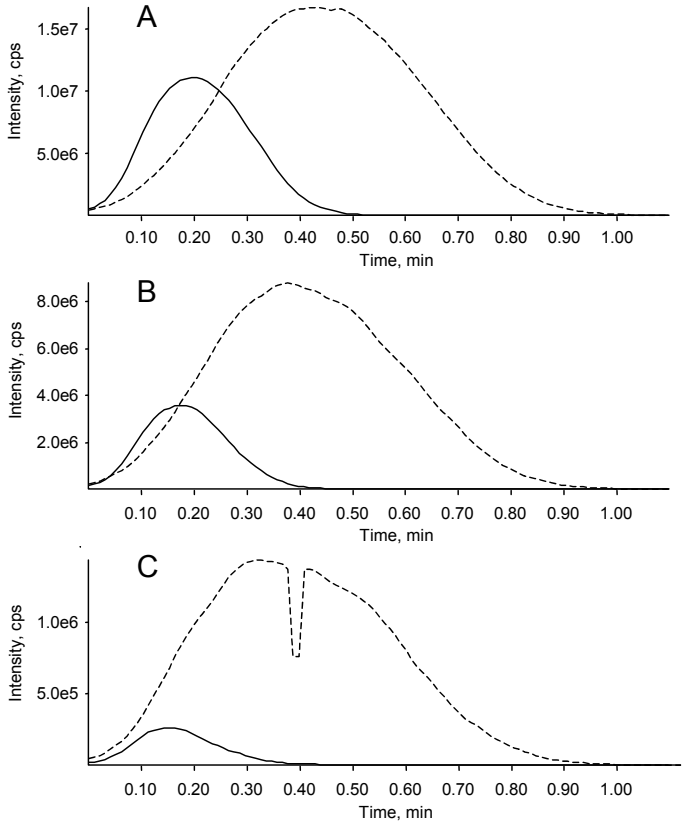

Figure 17. CID MS/MS Analysis of the complex detected as the $[M+H]^+$ ion at *m/z* 1121.7. Products: 1121.7 ($[M+H]^+$, solid line), 829.5 ($[\mathbf{28}+H]^+$, dotted line). Solvent: CH_3CN; ESI voltage: 6 kV; sampling cone potential: 46 V; signal acquisition: 1.11 min, 109 scans over collision energies from 6 to 60 eV in 0.5 eV steps; collision-gas pressure: P = 3.0 10^{-5} torr. **A)**: **28** + OctβMan, 0.2 mM each; Crossing point: 19.0 eV. **B)**: **28** + OctαMan, 0.2 mM each; Crossing point: 14.5 eV. **C**): **28** + OctαGal, 0.2 mM each.

employed to assess the structure of the receptor-glycoside complex in solution. It should be pointed out that the structure in solution provides information on the "biologically active" geometry, which may not be provided by the solid state structure analysis. The structure of the complex between OctβMan and receptor **28** was fully characterized in collaboration with the group of Prof. Jesús Jiménez-Barbero of the Centro de Investigaciones Biológicas (CSIC) in Madrid and compared to the structure of the complex between OctβMan and receptor **1**.[49]

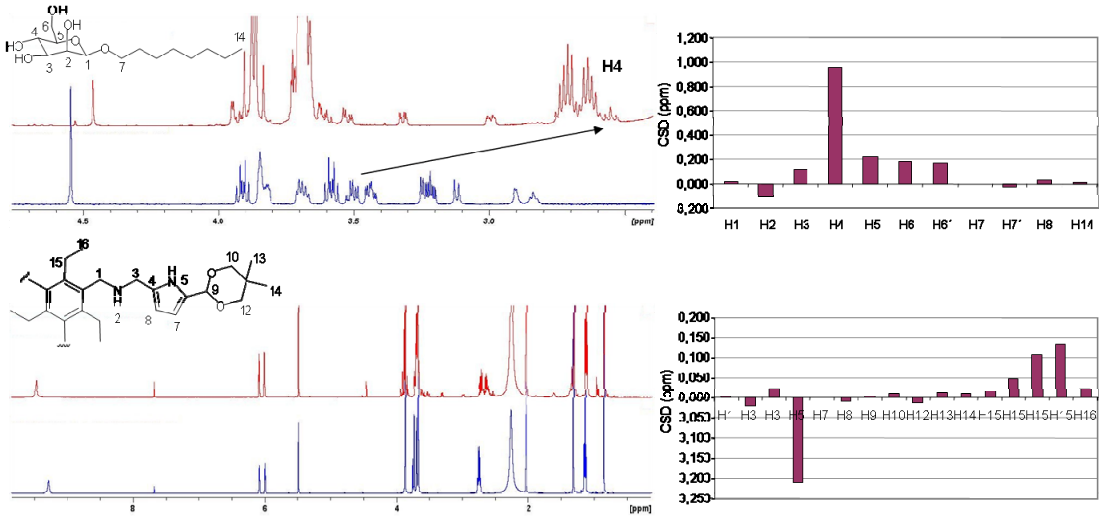

Figure 18. Left panel: 500 MHz ^{1}H NMR spectra in CD_3CN at 298 K of: top) OctβMan, neat (in blue) and in the presence of 3 equiv of **28** (in red); bottom) **28** neat (in blue) and in the presence of OctβMan as above (in red). Right panel: top) plot of the observed chemical shift differences (CSDs) of OctβMan in the presence of **28**; bottom) plot of the observed CSDs of **28** in the presence of OctβMan. The schemes of OctβMan and of receptor **28** showing the atomic numbering is depicted. The variation of the chemical shift of Man H-4 is indicated. The change in multiplicity of this signal is due to the lost of the coupling to the hydroxyl proton upon binding.

Comparison between the NMR spectra recorded for the free and bound species, showed clear and significant changes in the signals of both receptor **28** and OctβMan, when combined in acetonitrile solution (Figure 18). For instance, the two H-3 protons of the receptor, which resonate as one single signal in the free state, become two AB systems in the presence of the mannoside. Furthermore, the two H-10 and H-12 protons appear as complex multiplets in the presence of the sugar. The largest chemical shift differences between the free and the bound state are observed for NH-5 and for H-15, which also

becomes two different multiplets upon binding. Regarding the sugar moiety, a drastic upfield shift of nearly 1 ppm is observed for H-4 in the presence of receptor **28**, with important shieldings for H-5 and both H-6 protons. The observed high-field shift of H-3 is also noteworthy.

Conclusive evidence of the occurrence of a stable complex in solution was provided by the observation of intermolecular ligand/receptor NOEs. Indeed, the following intermolecular contacts were clearly evident as cross peaks in the NOESY map: NH-5/H2, NH-5/H-7´, NH-5/H-6', NH-5/H-8, NH-5/H-3, CH_3-13/H-1, CH_3-13/H-2, CH_3-13/H-3, and CH_3-13/H-5 (Figure 19).

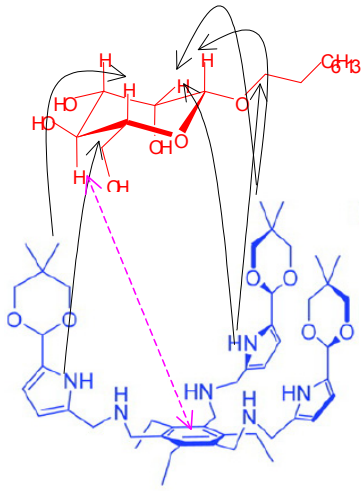

Figure 19. Schematic representation of NOE contacts is depicted

Altogether, these data seem to indicate the existence of some specific binding modes characterizing the complex of the receptor with OctβMan. It should be pointed out that, although from binding measurements multiple complex species were revealed in solution, under the concentration condition employed in this investigation the dominant species is the 1:1 complex, which accounts for over 60% of the species present in solution, with higher stoichiometry complexes amounting to less than 20%, thus substantially determining the NMR phenomenology.

Molecular modelling calculations providing three families of structures within 9.3 kJ mol^{-1}. The lowest energy family corresponded to the structure depicted in Figure 20 A, which included seven geometries featuring slightly different orientations of the sugar and of the "arms" of the tripodal receptor, as shown in Figure 20 B and C. These geometries were considered to correspond to the most likely NMR-based experimental solution and were further explored. Indeed, the dramatic shielding

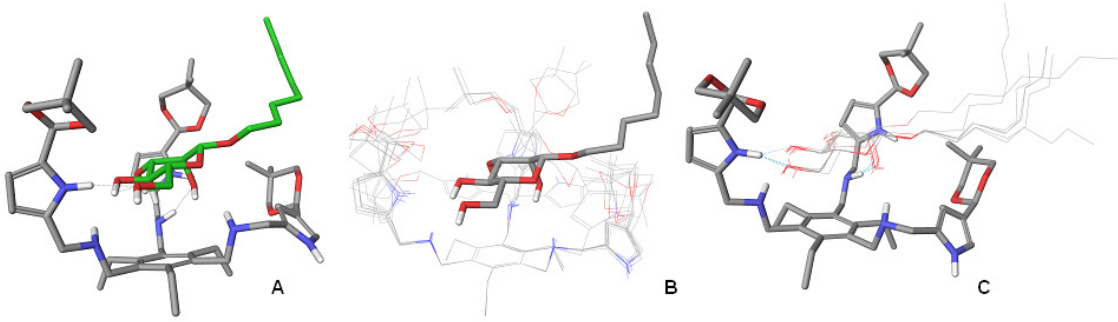

Figure 20. A: Structure of the global minimum of the 1:1 complex between **28** and OctβMan. B: Perspective from the sugar showing the orientations of the pyrrolic binding arms. C: Perspective from the receptor showing the orientations of the sugar. Hydrogen bonds are depicted in dashed lines.

of the H-4 proton of OctβMan, experimentally observed in the presence of the receptor, strongly supports the proximity of this nucleus to the centre of the benzene ring of the receptor, a feature shared only by the lowest energy family of conformations. The observed receptor-ligand intermolecular NOEs were thus compared to the corresponding distance values estimated for the structures of this family and, for most geometries the estimated AMBER* intermolecular distances, the observed NOE cross peaks were in good agreement.

The preference observed for the β with respect to the α anomer is easily accounted for by the lack of steric hindrance offered by the β Octyl chain toward the acetalic ring, with the *gem*-dimethyl substituent lying just above the α face of the mannose ring. For the α-anomer, the aliphatic side chain would point towards the acetal moiety. The structure of the complex is further reinforced by additional intermolecular hydrogen bonds (six structures involving O-6, two involving O-3 and O-4, and one involving O-5), although less conserved than the OH-2/NH bond.

Comparison between the structures of complexes of receptors **28** and **1**, would shed light on the binding properties exerted toward the monosaccharidic ligands. Indeed, **1** has been shown to exhibit good binding affinities but a rather shallow selectivity profile toward a set of monosaccharidic octyl glycosidees. A corresponding investigation was therefore undertaken, following the same methodology, on the complex between **1** and OctβMan, and the results are reported in Figure 21.

It can easily be appreciated that the observed chemical shift differences follow the same trend as those of receptor **28**, although with smaller values. For example, although the strongest shift of the mannosyl residue is consistently observed for the H-4 proton, the CSD value is only approximately 1/3 of the value observed for receptor **28** (Figure 21). Furthermore, very weak intermolecular NOEs were observed just above the noise level under the same experimental conditions. Following the same molecular modeling protocol, a proposed structure of the most likely interaction mode could be drawn for the corresponding complex (Figure 22). Although the relative arrangement of the partners in the complex appears to be analogous to that described for **28**, the

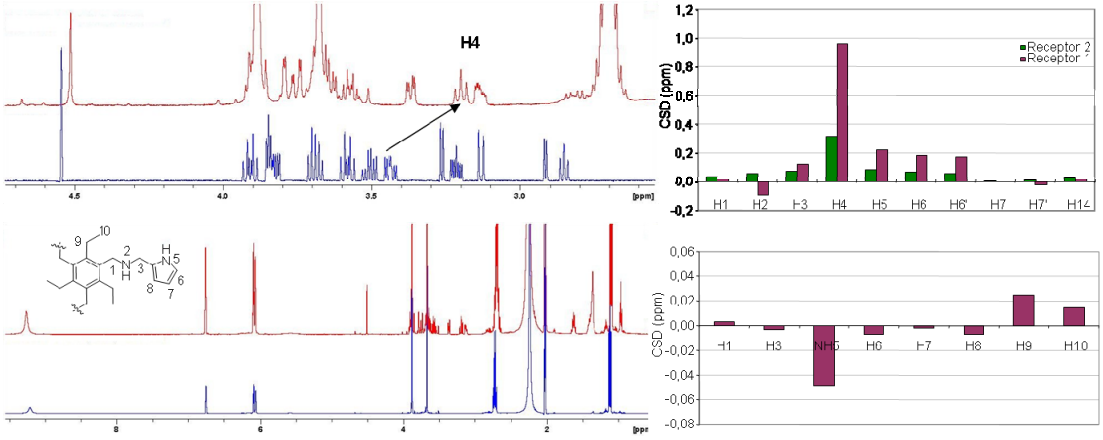

Figure 21. Left panel: 500 MHz ^{1}H NMR spectra in CD_3CN at 298 K of: top) OctβMan, neat (in blue) and in the presence of 3 equiv of **1** (in red); bottom) **1** neat (in blue) and in the presence of OctβMan as above (in red). Right panel: top) plot of the observed CSDs of OctβMan in the presence of **28** and **1**; bottom) plot of the observed CSDs of **1** in the presence of OctβMan. The scheme of receptor **1** showing the atomic numbering is depicted. The variation of the chemical shift of Man H-4 is indicated. The change in multiplicity of this signal is due to the lost of the coupling to the hydroxyl proton upon binding.

two entities lie further apart, as can be inferred from the distance between the H-4 proton of OctβMan and the centroid of the phenyl ring. The average distances between the protons of the sugar and the receptor are also larger than those observed in the complex of **28**, in agreement with the lack of clearly observable NOEs, and detectable intermolecular hydrogen bonds are less frequent than those revealed for **28**. Thus, as a general feature, the lack of

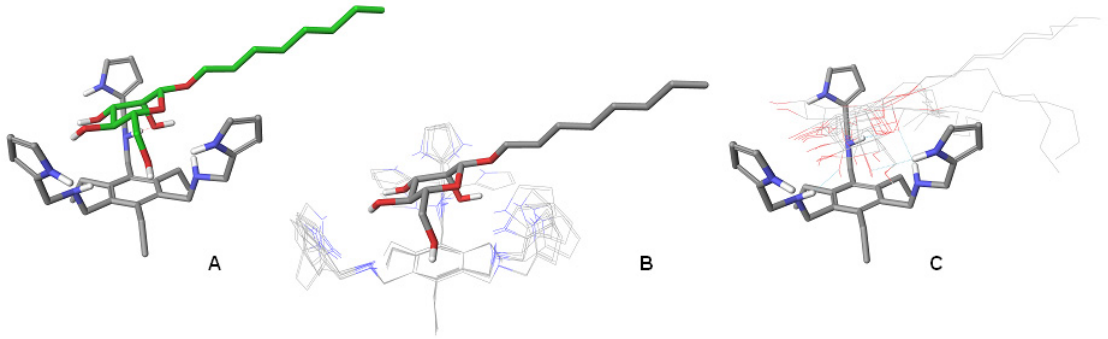

Figure 22. A: Structure of the global minimum of the 1:1 complex between **1** and OctβMan. B: Perspective from the sugar showing the orientations of the pyrrolic binding arms. C: Perspective from the receptor showing the orientations of the sugar.

the acetal groups makes the cleft of the receptor more "wide-open" compared to **28** and, consequently, the glycosidic ligand enjoys a larger degree of motion, resulting in looser contacts with the receptor. Furthermore, the inward orientation of the pyrrolic NH involved in the conserved H-bonding is lost in the unsubstituted receptor. In agreement with this picture, the affinity values measured for **1** toward OctαMan and OctβMan[8] indicate a weaker interaction compared to that of receptor **28**.

The structural analysis described shows that the origin of the enhanced binding ability of **28** rests, rather, on the conformational features brought about by the acetalic substituents, which impose a narrower size and a restricted mobility of the receptor's cleft in the bound state, thus favouring the formation of stronger hydrogen bonding to the saccharidic ligand, and which appear to be particularly well suited for binding the beta mannoside.

In the light of the results described for the acetalic receptor, the effect of replacing the latter group with alternative H-bonding groups was investigated with the related aldehydic, aminic and esteric receptors. The recognition properties of **29**, **30** and **31** were tested *vs* OctβMan. Association constants were measured by ^{1}H NMR titrations in CD_3CN and affinities were assessed by the BC_{50}^{0} parameter (Table 8).

Table 8. Cumulative Association Constants (log β_n) for 1:1, 2:1 Complexes of Receptors **28**, **29**, **30** and **31** with OctβMan and Corresponding BC_{50}^{0} (μM) values in CD_3CN at 298 K.[a]

	28	**29**	**30**	**31**
log β_{11}	3.12 ± 0.02	2.428 ± 0.073	2.444 ± 0.027	3.427 ± 0.035
log β_{21}	5.40 ± 0.08	3.92 ± 0.27	3.84 ± 0.19	5.97 ± 0.11
BC_{50}^{0}	680 ± 30	3400 ± 500	3300 ± 200	430 ± 40

[a]Receptor **31** dimerization constant log β_{dim} = 2.630 ± 0.072. β_{dim} for **28**, **29**, **30** nondetectable.

From the analysis of Table 8 it can be seen that, while for the ester **29** and the aldehyde **30** a decrease in affinity was measured compared to **28**, the aminic receptor **31** showed a slightly enhanced binding ability. Substituents coplanar with pyrrole aromatic ring presumably force the receptor to assume a conformation unsuitable for binding OctβMan, whereas receptor **31**, featuring a more flexible structure could better adapt to the ligand. In addition, the dual H-bonding nature of the amino group could also establish a donating interaction with the accepting glycoside hydroxyls confirming that the amino group is a powerful tool for the design of effective receptors for the recognition of carbohydrates.

4 – Modification of the aminic binding groups.

Design and Synthesis.

Structural modifications of receptor **1** have brought significant improvements in the recognition of monosaccharides in particular toward glucose with the iminic receptor **2** and the cage receptor **26** and toward mannose with the acetalic receptor **28** and the aminic **31**. Recognition of mannose in competitive solvents, is a subject of high interest, because mannose is involved in pathological processes and because effective synthetic receptors for mannose are still lacking. On the basis of the results obtained with our tripodal receptors, to further improve on binding ability some new structural modifications on the amino binding groups of receptor **1** have been explored.

Among the plethora of synthetic receptors for carbohydrates reported in the literature, only a limited number are chiral. In addition, of the several papers dealing with recognition of carbohydrates by chiral synthetic receptors, only a few are concerned with the effect of receptor's chirality on the enantioselective recognition of sugars.[50-64] This is somewhat surprising because selective recognition can be expected when enantiomerically pure natural saccharides bind to opposite enantiomers of a chiral receptor. Indeed, apart from the extensive work of Diederich and coworkers on dendritic clefts and cyclophanic and macropolycyclic receptors,[50-58] following the first report by Davis and coworkers,[59] very few investigations were specifically focused on the enantioselective recognition of monosaccharides by chiral receptors.[60-64] In particular, to our knowledge, the enantioselective recognition of mannosides has only been reported in two cases, in which 1-octyl-α-D-mannopyranoside binds to the enantiomers of the receptor with little or no discrimination.[51;62]

The chiral tripodal receptor **34** was designed with the idea to obtain a chiral receptor exploiting the aminic and the pyrrolic function and fulfilling the geometric requirements for binding. Replacement of *trans*-1,2-diaminocyclohexane **35** for the amino groups in the structure of **1**, leading to the corresponding hexaamino receptor **34**, appeared to be the appropriate

35

Figure 23. *trans*-1,2-diaminocyclohexane

modification: since **35** has been shown to recognize the *trans*-1,2 arrangement of a number of diols through a well-matched H-bonding network,[37;65;66] it could be anticipated to recognize the *trans*-1,2 diol arrangement in monosaccharides and, in addition, both the enantiomerically pure (*R*,*R*) and (*S*,*S*) diamines were readily available to investigate the enantioselective recognition of monosaccarides.

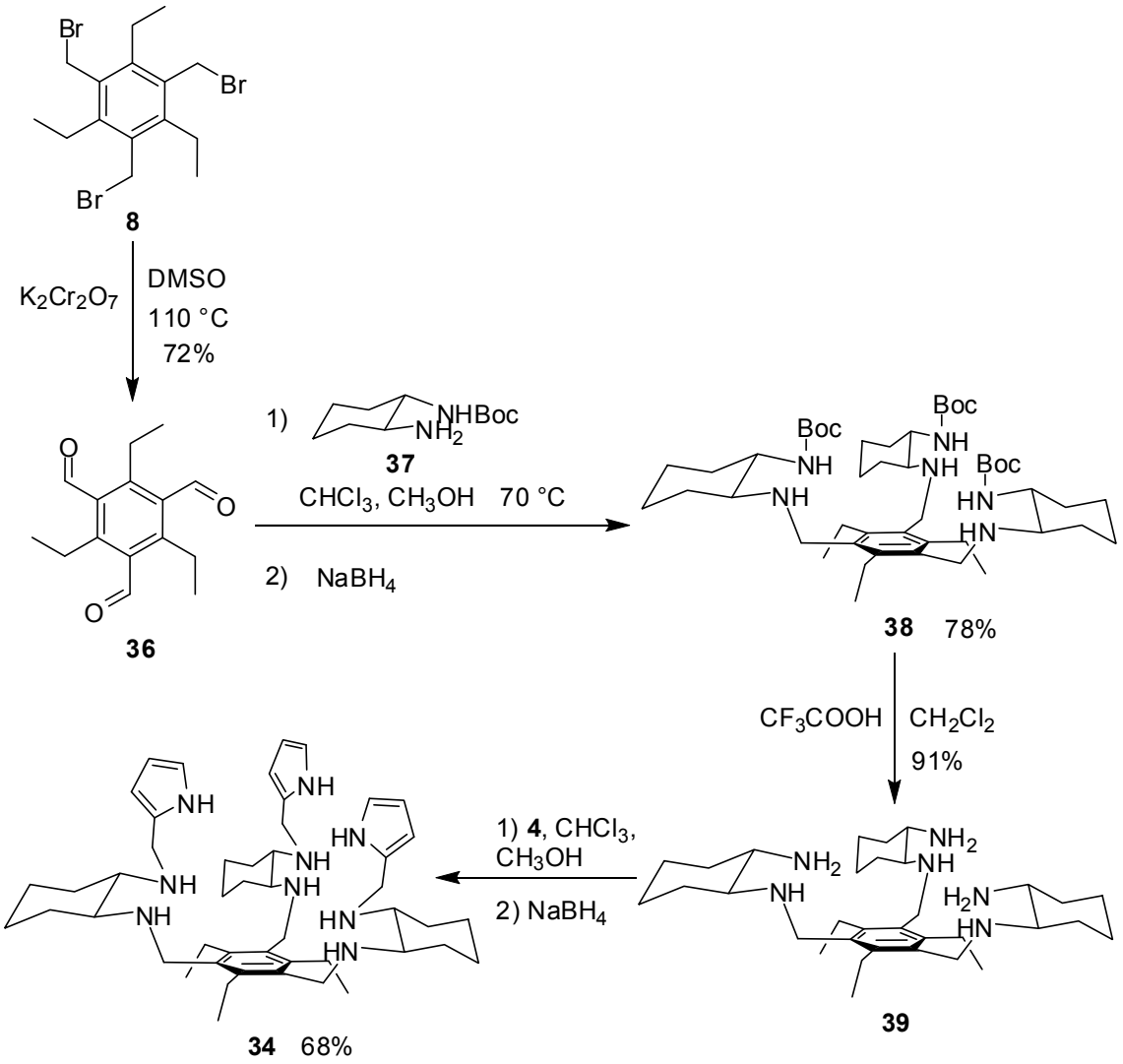

Scheme 10. Synthesis of receptor **34**.

The synthesis of **34** was accomplished from the tribromomethyl scaffold **8**, which was oxidized to the trialdehyde **36**. The aldehydic scaffold was reacted with the monoprotected diamino compound **37** to yield **38**. Acidic removal of the Boc protecting groups gave the hexamino compound **39**, that was utilized as a reference receptor to ascertain the contribution from the pyrrolic groups to the

recognition of monosaccharides of receptor **34**, which was obtained by condensation with pyrrole aldehyde **4** and subsequent reduction. Receptor **34** was thus prepared in both enantiomerically pure forms, the (*R,R,R,R,R,R)* enantiomer (***R*-34**) and the (*S,S,S,S,S,S*) enantiomer (***S*-34**), which were submitted to binding tests.

To ascertain the contribution of *trans*-1,2-diaminocyclohexane functions on these new generation of receptors, the achiral hexamino receptors **40** and **41** were designed, featuring different level of sbstitution. The results obtained with these two receptors may give valuable information about the significance of chirality in the recognition process. Receptor **40** was prepared from the trialdehydic scaffold **36** that was reacted with the monoprotected diaminic **43** to yield the triiminic compound **44**. The Boc protecting groups were removed under acidic conditions and the obtained compound **45** was condensed with the aldehyde **4** and reduced to give receptor **40**.

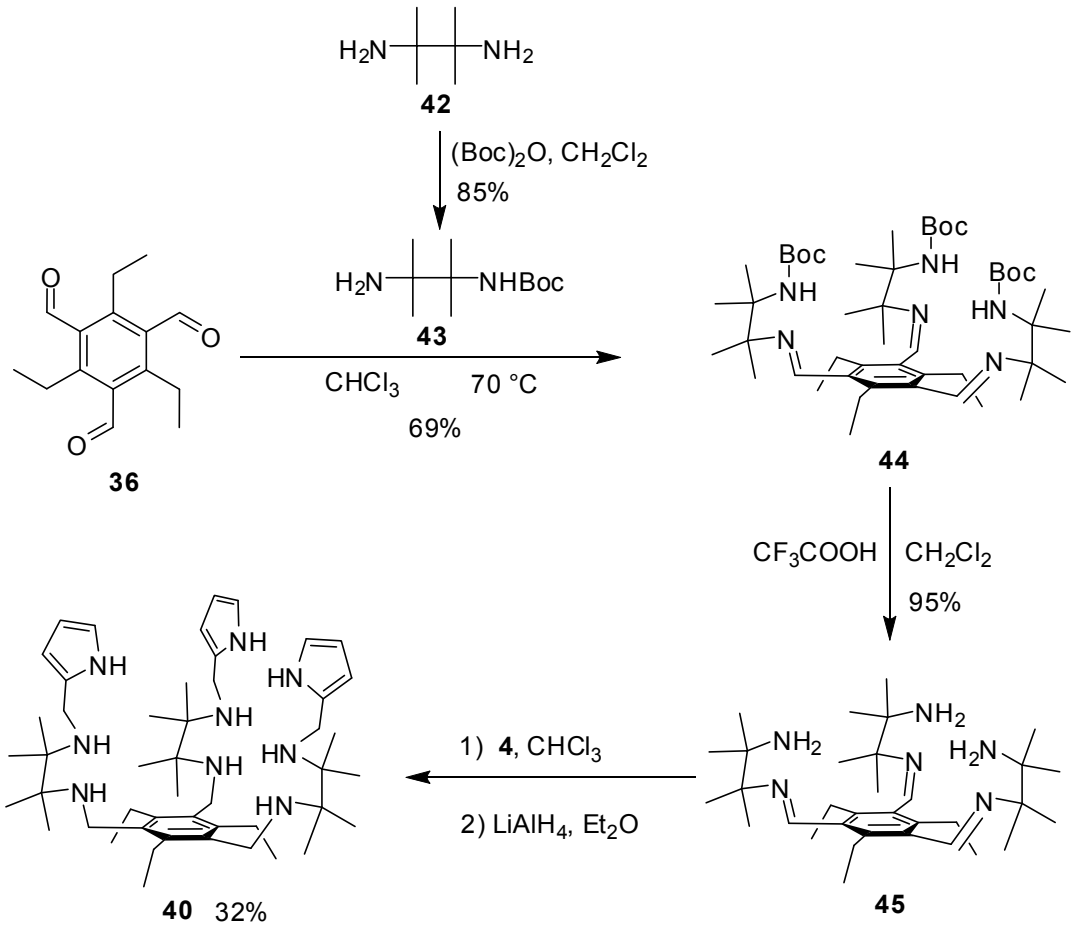

Scheme 11. Synthesis of receptor **40**.

Receptor **41** was prepared by condensation of the trialdehydic scaffold **36** with the protected diamine **47** and subsequent reduction. Compound **48** was deprotected, condensed with **4** and reduced to yield receptor **41**.

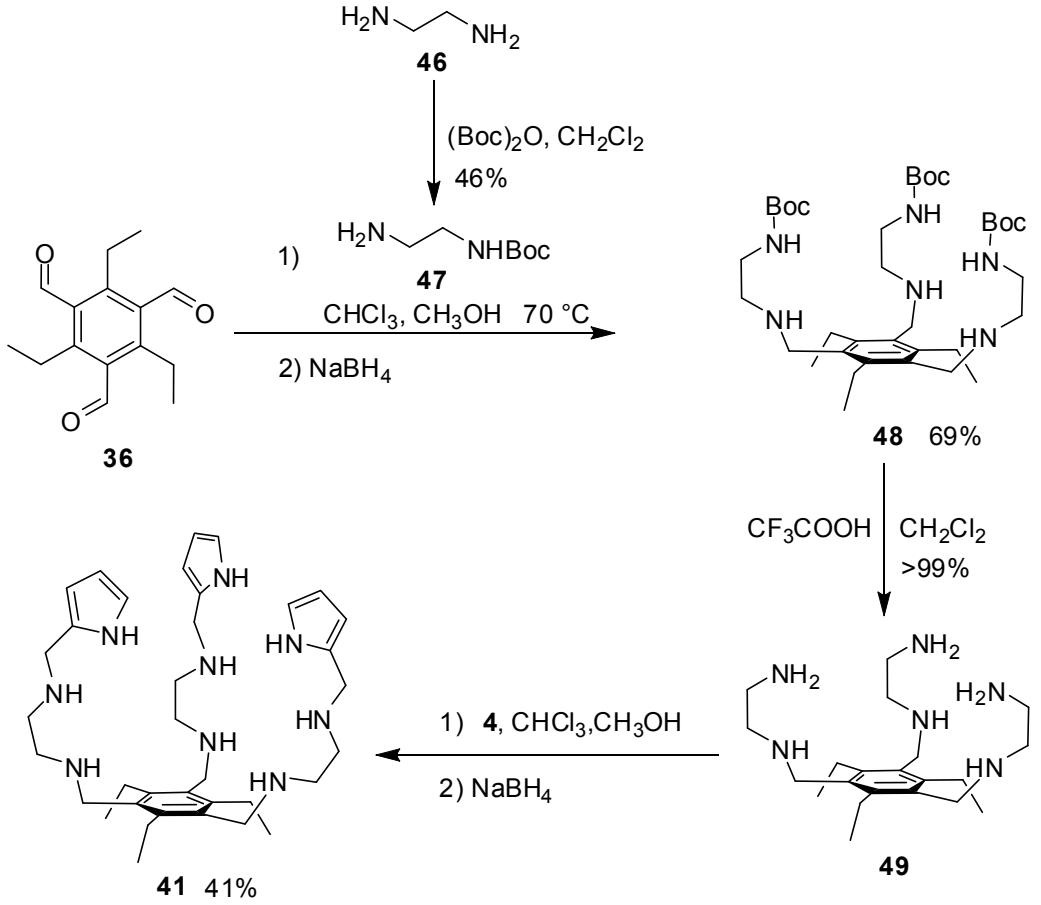

Scheme 12. Synthesis of receptor **41**.

The synthesis of a new receptor **50** with a cage tripodal architecture was also attempted. In analogy to the hexamino/pyrrolic cage **26**, receptor **50** would present the same bicyclic structure but would differ for the replacement of *trans*-1,2-diaminocyclohexane for the amino group. Although receptor **26** specifically recognizes the β-glucosyl residue, the measured affinity for OctβGlc in $CDCl_3$ was no larger than 20 μM. We attributed the cause of this relatively modest affinity to the size of the cavity, which appeared to be slightly too tight for the glucosyl residue. Receptor **50** would also present a slightly enlarged cavity compared to receptor **26**, hopefully endowed with an improved affinity even in competitive media. The preparation of **50** was thus attempted according to

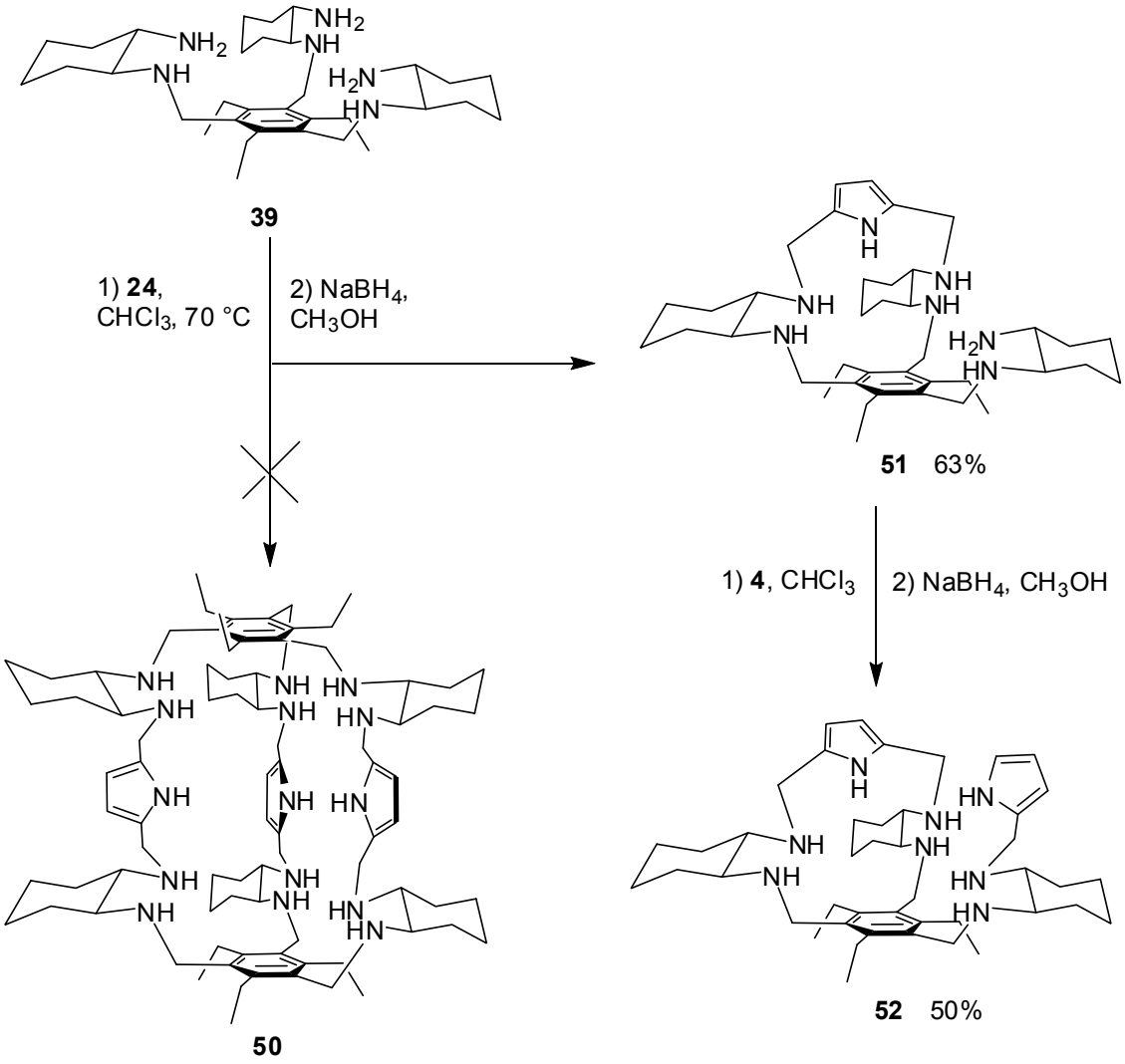

Scheme 13. Synthesis of receptor **52**.

Scheme 13. Tripodal hexaamine **39** was condensed with pyrrole-2,5-dicarbaldehyde **24** under the conditions used for preparing the bicyclic receptor **26**. Contrary to the expectations, the monocyclic compound **51** was obtained instead of the bicyclic cage **50**. Although the best yield was obtained for a 1:1 ratio of reactants, **51** always constituted the major product isolated from the oligomeric reaction mixture, whereas **50** could not be isolated in any case. Apparently, the described structure modification biased the Schiff base equilibrium toward the formation of a pyrrole-bridged ring regardless of the reactants ratio. While all attempts to prepare the desired cage receptor **50** failed, the monocyclic **51** turned out to be a valuable alternative intermediate. Indeed, condensation of **51** with **4** readily afforded the hexaamino dipyrrolic tripodal compound **52**, which from preliminary testing appeared to be a

promising receptor for monosaccharides. Receptor **52** was thus prepared in both enantiomerically pure forms, the (*R,R,R,R,R,R)* enantiomer (***R*-52**) and the (*S,S,S,S,S,S*) enantiomer (***S*-52**), which were submitted to binding tests.

Binding studies and structure elucidation.

To investigate how the replacement of the aminic binding groups with the chiral *trans*-1,2-diaminocyclohexane functions could affect the binding ability of the new generation of receptors, recognition properties of hexaminic ***R*-39** and ***S*-39** were compared to those relative to the plain triaminic receptor **3** towards OctβGlc. Association constants were measured by ^{1}H NMR titrations in $CDCl_3$ and affinity results are reported in Table 9.

Table 9. Cumulative Association Constants (log β_n) for 1:1, 2:1 Complexes of Receptors ***R*-39**, ***S*-39** and **3** with OctβGlc and Corresponding BC_{50}^{0} (μM) values for in $CDCl_3$ at 298 K.[a]

	***R*-39**	***S*-39**	**3**
log β_{11}	3.704 ± 0.005	3.133 ± 0.002	2.616 ± 0.003
log β_{21}		4.272 ± 0.060	
BC_{50}^{0}	249 ± 2	729 ± 3	3690 ± 50

[a]The receptor's dimerization constant was measured independently under the same conditions and set invariant in the nonlinear regression analysis. For **3**, log β_{dim} = 1.83 ± 0.02. For ***R*-39** and ***S*-39** β_{dim} nondetectable.

While the triaminic receptor **3** could recognize OctβGlc with an affinity in the millimolar range, both ***R*-39** and ***S*-39** can establish a more effective interaction with the glucoside, with an affinity increased up to the micromolar range. For ***R*-39** an improvement of 1-order of magnitude compared to **3** was observed, supporting the hypothesis of a good match between the *trans*-1,2 diamine and *trans*-1,2 diol arrangement. Moreover a modest selectivity *versus* OctβGlc was observed, probably caused by a better fit of the all-*R* enantiomer with the chiral glucosidic structure. A deeper insight on the relevance of chirality in carbohydrate recognition by the new generation of receptors may be gained from the affinity results obtained with the amino-pyrrolic derivatives ***R*-34** and ***S*-34**.

The recognition properties of pyrrolic hexaminic receptors ***R*-34** and ***S*-34** were tested *vs* the set of octyl glycosides of the monosaccharides. Association constants were measured by ^{1}H NMR titrations in CD_3CN and affinities results are reported in Table 10.

Although measurements were performed in acetonitrile, a competitive H-bonding media, interesting results were obtained toward all the investigated monosaccharides, with affinities among the highest observed for amino-pyrrolic receptors. Among the results obtained, the affinity of receptor ***R*-34** towards OctαMan is outstanding. As far as we are aware of, this is the largest affinity ever reported for a synthetic receptor for the α anomer of mannose. Moreover ***R*-34** showed an α/β selectivity of nearly an order of magnitude. The results demonstrated that the substitution of the aminic with the *trans*-1,2 diaminic group significantly enhanced the binding ability of the tripodal receptors towards saccharides.

To understand the contribution of chirality in the recognition process, the results were compared to the binding affinities obtained with the enantiomeric receptor ***S*-34**. The most significant differences are the affinity for OctβMan in the micromolar range, and an appreciable β/α selectivity within the mannose serie. It is worth noting that the *R* enantiomer is selective for the α anomer, whereas the *S* enantiomer is selective for the β anomer of mannose, underlining the role of chirality of the receptor in the recognition of natural saccharides. Enantioselective recognition is also observed with OctβGlc, OctαGal, OctαGlcNAc, although with much smaller selectivity.

Table 10. Intrinsic Median Binding Concentration (BC_{50}^{0}, μM) and Cumulative Association Constants (log β_n) for Receptor to Glycoside (R:G) Complexes of ***R*-34** and ***S*-34** with Octyl Glycosides in CD_3CN at 298 K.[a]

	***R*-34**		***S*-34**	
glycoside	log β (R:G)	BC_{50}^{0}	log β (R:G)	BC_{50}^{0}
OctαGlc	2.847 ± 0.048 (1:1) 4.890 ± 0.084 (2:1)	1300 ± 100	3.000 ± 0.009 (1:1)	1000 ± 200
OctβGlc	3.002 ± 0.027 (1:1) 4.89 ± 0.11 (2:1)	930 ± 50	2.667 ± 0.016 (1:1) 4.691 ± 0.022 (2:1)	1820 ± 50
OctαGal	2.878 ± 0.014 (1:1) 4.582 ± 0.095 (2:1)	1250 ± 40	2.497 ± 0.002 (1:1)	3190 ± 10
OctβGal	2.611 ± 0.002 (1:1)	2450 ± 9	2.551 ± 0.031 (1:1) 4.18 ± 0.13 (2:1)	2500 ± 200
OctαMan	3.866 ± 0.011 (1:1) 6.295 ± 0.052 (2:1) 6.116 ± 0.053 (1:2)	127 ± 3	3.346 ± 0.018 (1:1) 5.20 ± 0.16 (2:1)	4400 ± 200
OctβMan	3.010 ± 0.040 (1:1) 5.14 ± 0.10 (2:1)	870 ± 70	3.230 ± 0.012 (1:1) 5.093 ± 0.089 (2:1)	570 ± 20
OctαGlcNAc	2.919 ± 0.048 (1:1) 4.99 ± 0.11 (2:1)	1100 ± 100	3.116 ± 0.018 (1:1) 4.905 ± 0.084 (2:1)	730 ± 30
OctβGlcNAc	2.995 ± 0.078 (1:1) 5.11 ± 0.13 (2:1)	900 ± 100	3.030 ± 0.003 (1:1)	933 ± 7

[a] β_{dim} nondetectable.

Achiral receptors **40** and **41** shed further light on the role of the chirality of receptor. Recognition properties of **40** and **41** compared with those relative to ***R*-34** and ***S*-34** towards α and β mannosides, measured by ^{1}H NMR titrations in CD_3CN, are reported in Table 11. It can easily be appreciated that, while both chiral receptors ***R*-34** and ***S*-34** recognize the mannosides with an appreciable anomeric selectivity, the ethylenediaminic receptor **41** binds the two anomers almost with the same affinity. This behaviour is most likely due to the conformational constraint imposed by the cyclohexane rings in ***R*-34** and ***S*-34**, fixing the structure into a geometry that induces a well differentiated recognition for the two anomers. While millimolar affinities were observed for receptor **41**, quite surprisingly receptor **40** did not exhibit any recognition ability toward mannosides. This unpredictable result was probably due to the steric hindrance introduced by the four methyl groups located very close to the binding amines, which could hamper the binding interaction. As a consequence receptor **40**, although presenting the same diamino-pyrrolic moiety as receptors **41** and **34**, is totally unable to recognize the mannose glycosides.

Table 11. Intrinsic Median Binding Concentration (BC_{50}^0, μM) for Complexes of Receptors **41**, **40**, ***R*-34** and ***S*-34** with Octyl Mannosides in CD_3CN at 298 K.[a]

Receptors	OctαMan	OctβMan
41	3120 $\pm$ 30	2750 $\pm$ 40
40	n.d.[b]	n.d.[b]
***R*-34**	127 $\pm$ 3	870 $\pm$ 70
***S*-34**	4400 $\pm$ 200	570 $\pm$ 20

[a] β_{dim} nondetectable. [b] Nondetectable.

The most interesting binding properties were observed with the monocyclic receptors ***R*-52** and ***S*-52**.

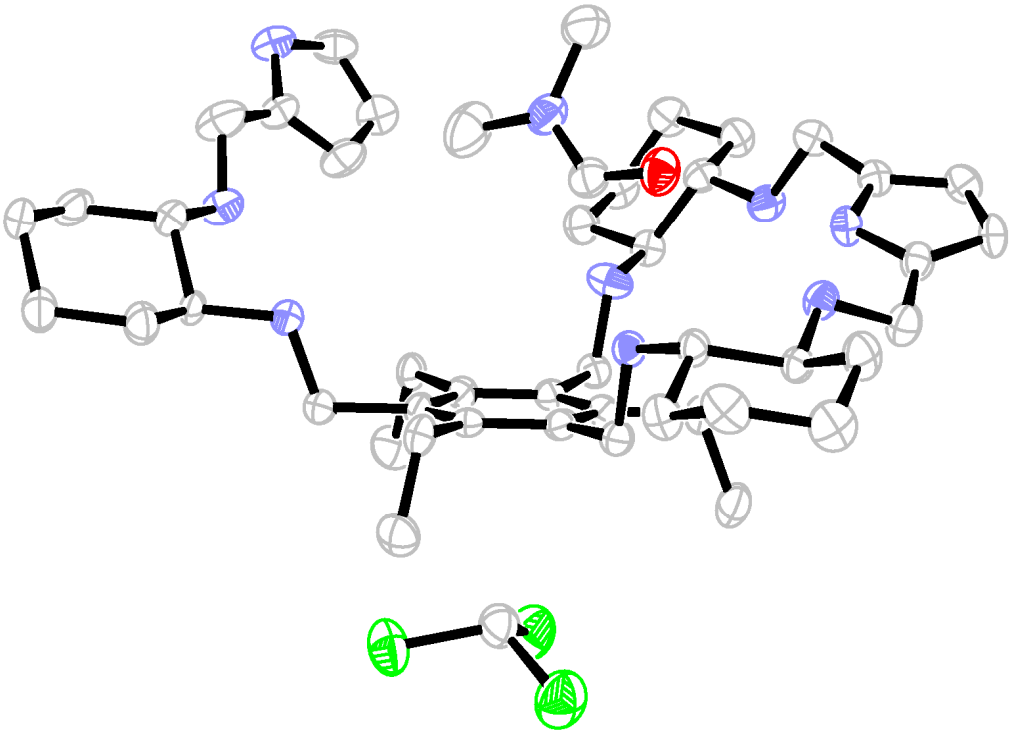

Figure 24. ORTEP projections of the X-ray structure of ***S*-52**·DMF·$CHCl_3$. Ellipsoids are at 50% probability. Nitrogen and oxygen atoms are represented as shaded ellipsoids. Hydrogen atoms are omitted for clarity. Selected distances: (endocyclic pyrrole) N–H ··· O (DMF), 2.21 Å; (DMF) C-H ··· π (benzene scaffold), 2.68 Å; ($CHCl_3$) C-H ··· π (benzene scaffold), 2.53 Å.

The ORTEP projection of the X-ray structure of ***S*-52**, crystallized from $CHCl_3$/DMF, is depicted in Figure 24 and shows that the cyclic portion and the acyclic pyrrolic binding arm are disposed on the same side of the aromatic ring to form a cleft, in the center of which a DMF molecule has been captured. The macrocycle presents a noteworthy convergent disposition of H-bonding donor and acceptor groups of both *trans*-1,2-diaminocyclohexanes and of the pyrrolic ring to which the carbonyl oxygen of DMF is bound from the endocyclic pyrrole NH group. DMF is also stabilized by an additional CH-π interaction of carbonyl CH with the aromatic ring of the benzene scaffold. In addition one molecule of $CHCl_3$ co-crystallized is bound through another CH-π interaction to the other side of the benzene ring. In can be expected that while H-bonding group may match hydroxyl moieties of glycosides, the glycoside backbone could interact through CH-π interaction with the aromatic ring, stabilizing the complex.

Furthermore, an additional interaction may be established with the acyclic pyrrolic arm, that could hook to the monosaccharide in a well organized arrangement.

A preliminary screening by extraction experiments on the binding properties of **52**, using the methyl glycosides of the set of monosaccharides, indicated that, while Glc, Gal, and GlcNAc were moderately bound and extracted from the solid, a strong recognition occurred with mannosides (Table 12),

Table 12. Concentration ([G], mM) and equivalent (equiv) of glycoside extracted into $CDCl_3$ from solid methyl glycosides by a solution of ***R*-52** (2.9 mM) and of ***S*-52** (3.1 mM) at T = 298 K.[a]

	***R*-52**		***S*-52**	
Glycoside	[G]	equiv	[G]	equiv
MeαGlc	1.81	0.62	1.82	0.59
MeβGlc	2.85	0.98	2.64	0.85
MeαGal	2.10	0.72	2.09	0.67
MeβGal	1.47	0.51	1.41	0.46
MeαMan	2.41	0.83	2.62	0.85
MeβMan	6.45	2.21	7.88	2.54
MeαGlcNAc	1.80	0.62	1.99	0.64
MeβGlcNAc	1.53	0.52	1.06	0.34

[a]Calculated by integration from the NMR spectra.

where ***S*-52** appeared more effective than ***R*-52** toward the β anomer. Moreover, when an equilibrated mixture of solid mannose, fully insoluble in chloroform and showing a 2:1 α/β anomeric ratio, was stirred with an equimolar solution of ***S*-52** in $CDCl_3$, 35% of the solid was dissolved by the receptor in a reversed 1:2 α/β anomeric ratio, showing that βMan was preferentially extracted into solution. βMan was also extracted in benzene, though to a smaller extent (10%), where αMan could not be detected. Even stronger evidence of binding was obtained using the methyl glycosides of mannose (MeαMan and MeβMan), which are likewise fully insoluble in chloroform. Indeed, when a 3.1 mM solution of ***S*-52** in $CDCl_3$ was independently treated with an excess of solid MeαMan and MeβMan, a markedly larger amount of the latter (7.9 mM, 2.5 equiv) than the

former (2.6 mM, 0.85 equiv) was found in solution, confirming a strong preference of the receptor for βMan. It is noteworthy that more than the stoichiometric amount of MeβMan is extracted by ***S*-52** from the solid, suggesting the occurrence of complexes of stoichiometry higher than 1:1. This evidence was confirmed by treating a solid mixture of MeαMan and MeβMan with a 2.9 mM solution of ***S*-52** in $CDCl_3$, in a competitive experiment featuring a 1:1:1 mole ratio of reactants, which extracted 0.17 equiv of MeαMan and 0.90 equiv of MeβMan from the glycoside mixture, showing a nearly 2-fold enhancement of selectivity with respect to the independent extraction of the glycosides. Altogether, extraction experiments demonstrated that receptor ***S*-52** is able to effectively dissolve βMan and its methyl glycosides in lipophylic organic solvents with a significant selectivity over the corresponding α anomers. Eventually, a direct evidence of complexation was obtained by mass spectrometry. The positive mode ESI-MS spectra of mixtures of either MeαMan or MeβMan with ***S*-52**, extracted into acetonitrile, unambiguously showed in both cases the peak of the 1:1 complex. The presence of higher stoichiometry species could not be demonstrated because of the very dilute conditions in a polar solvent used for the MS experiments.

A quantitative assessment of binding affinities was obtained by ^{1}H NMR titrations of both the ***R*-52** and ***S*-52** receptors with OctαMan and OctβMan in which the octyl chain ensured the necessary solubility for the binding measurements. Because the interaction of the receptors with the glycosides

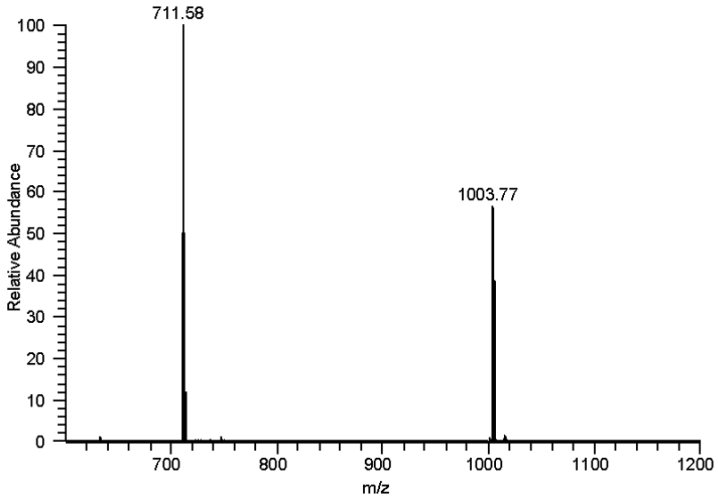

Figure 25. Positive mode ESI-MS spectrum of a mixture of ***S*-52** (0.18 mM) and OctβMan (0.90 mM) in CH_3CN. *m/z*: 711.58, [***S*-52** + H]$^+$;1003.77, [***S*-52**·OctβMan + H]$^+$.

was too strong to be measured in $CDCl_3$ by NMR, showing a complex pattern of species in solution, association constants were measured in CD_3CN at T = 298 K, where the occurrence of complex formation was proven by MS spectroscopy. The ESI-MS spectrum of a mixture of ***S*-52** and OctβMan in acetonitrile is reported in Figure 25 showing the presence of the 1:1 adduct. Thus, binding interactions were still evident in the markedly more polar medium. Association constants were measured by ^{1}H NMR titrations in CD_3CN and affinities results are reported in Table 13. From data of Table 13 it is clearly apparent that, while no enantiodiscrimination is observed in the binding of OctαMan, a 15:1 enantioselectivity is apparent in the binding of OctβMan which, to our knowledge, is the highest value reported in the literature; the 83 μM value for the affinity observed in acetonitrile is also noteworthy, testifying strong binding even in a markedly polar medium. While the previously described tripodal achiral receptor **28** gave a selective recognition of OctβMan showing an affinity of 680 μM in acetonitrile, the new generation chiral receptor ***S*-52** exhibits a nearly 10-fold enhancement in affinity, together with outstanding enantioselectivity, which make it the most effective mannoside receptor up to date. Compared to the chiral acyclic receptors ***R*-34** and ***S*-34**, the binding abilities of both ***R*-52** and ***S*-52** receptors, except for mannose, are slightly smaller. It is reasonable to believe that conformational constrains imposed

Table 13. Intrinsic Median Binding Concentration (BC_{50}^{0}, μM) and Cumulative Association Constants (log β_n) for Receptor to Glycoside (R:G) Complexes of ***R*-52** and ***S*-52** with Octyl Glycosides in CD_3CN at 298 K.[a]

	***R*-52**		***S*-52**	
glycoside	log β (R:G)	BC_{50}^{0}	log β (R:G)	BC_{50}^{0}
OctαGlc	2.506 ± 0.005 (1:1)	3120 ± 40	2.165 ± 0.020 (1:1) 5.010 ± 0.010 (2:1)	2490 ± 30
OctβGlc	2.493 ± 0.004 (1:1)	3220 ± 30	2.852 ± 0.012 (1:1) 4.600 ± 0.027 (1:2)	1250 ± 30
OctαGal	2.527 ± 0.004 (1:1)	2970 ± 30	2.497 ± 0.002 (1:1)	3180 ± 10
OctβGal	2.937 ± 0.002	1157 ± 6	2.745 ± 0.011 (1:1) 4.802 ± 0.046 (2:1)	1530 ± 30
OctαMan	3.488 ± 0.010 (1:1) 5.944 ± 0.025 (2:1)	299 ± 6 5570 ± 20[b]	3.516 ± 0.010 (1:1) 5.866 ± 0.034 (2:1)	286 ± 6 3500 ± 20[b]
OctβMan	2.877 ± 0.016 (1:1) 4.30 ± 0.19 (2:1) 7.438 ± 0.079 (3:1)	1220 ± 40 10900 ± 100[b]	4.000 ± 0.052 (1:1) 7.04 ± 0.14 (1:2) 10.05 ± 0.15 (1:3)	83 ± 7 2120 ± 20[b]
OctαGlcNAc	2.314 ± 0.003 (1:1)	4850 ± 40	2.787 ± 0.003 (1:1) 4.163 ± 0.078 (2:1)	1570 ± 10
OctβGlcNAc	2.869 ± 0.012 (1:1) 5.615 ± 0.046 (1:2)	760 ± 30	2.723 ± 0.008 (1:1) 5.270 ± 0.028 (2:1)	1300 ± 20

[a] β_{dim} nondetectable. [b]Measures by NMR in CD_3CN/DMSOd6 90:10.

by the cyclic structure impose strict binding requirements, resulting in mismatching in the recognition

processes with the majority of glycosides, whereas OctβMan apparently satisfies such requirements, being strongly recognized by the receptor ***S*-52**.

Finally to elucidate the role of the hexocyclic pyrrolic binding groups in the recognition process, the binding properties towards mannosides of receptors ***R*-51** and ***S*-51** were investigated and compared those of receptors ***R*-52** and ***S*-52**. The results are reported in Table 14. Although monopyrrolic receptors still recognize mannosides with quite high affinities, an enhanced binding ability is observed in most cases when the acyclic pyrrole group is present in the receptor structure. Indeed, except for ***S*-52**, for which an increase in affinity toward OctαMan is lacking, increased binding is observed in all other cases, with a peak for the recognition of OctβMan by ***S*-52**, which exhibits a 5-fold increase.

Table 14. Intrinsic Median Binding Concentration (BC_{50}^{0}, μM) and Cumulative Association Constants (log β_n) for Complexes of Receptors ***R*-51**, ***S*-51** and ***R*-52**, ***S*-52** with Octyl Mannosides in CD_3CN at 298 K.[a]

		OctαMan	OctβMan
	log $\beta_{1:1}$	2.937 ± 0.005	3.163 ± 0.019
***R*-51**	log $\beta_{2:1}$		5.087 ± 0.099
	BC_{50}^{0}	1160 ± 10	650 ± 30
***R*-52**	BC_{50}^{0}	299 ± 6	286 ± 6
	log $\beta_{1:1}$	2.875 ± 0.004	3.363 ± 0.019
***S*-51**	log $\beta_{2:1}$		5.12 ± 0.16
	BC_{50}^{0}	1340 ± 10	420 ± 20
***S*-52**	BC_{50}^{0}	1220 ± 40	83 ± 7

[a] β_{dim} nondetectable

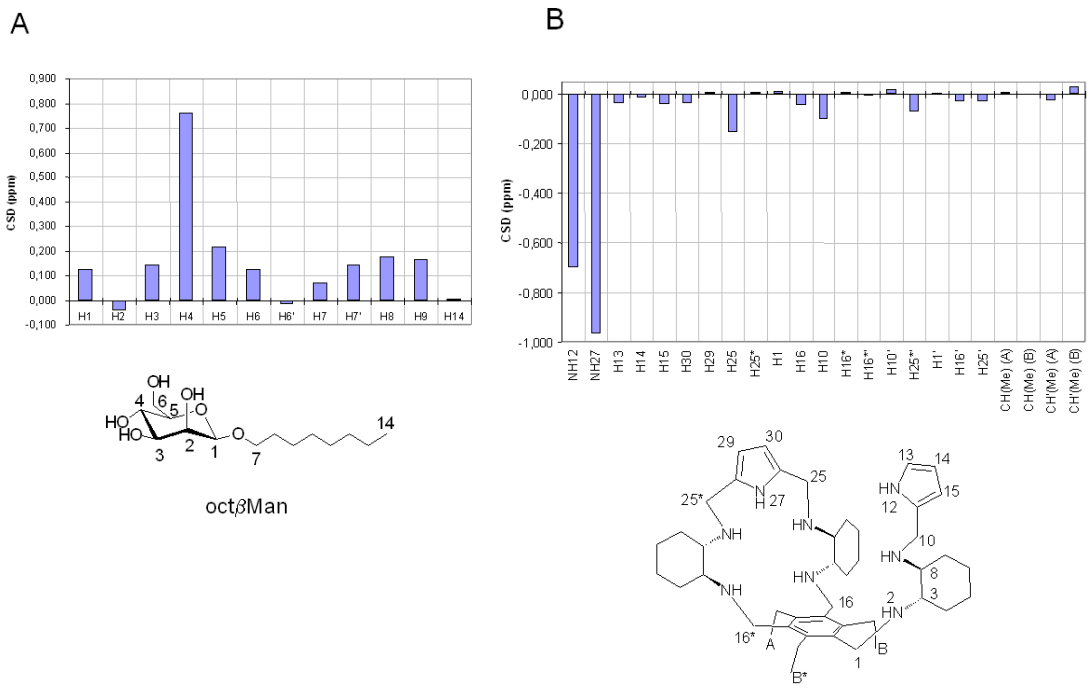

Figure 26. Chemical shift differences between (A) free and bound OctβMan and (B) free and bound **S-52** in CD_3CN at 298 K. Atom numbering is given in the chemical structures.

A conclusive evidence of binding was provided by several intermolecular NOE contacts, together with clear and significant changes in both the signals of receptor ***S*-52** and of the glycoside, when both entities were combined in acetonitrile (Figures 26, Table 15), which not only demonstrated the occurrence of receptor ligand interactions, but also allowed a definition of the structure of the complex in solution. Indeed, while all attempts to obtain X-ray quality crystals of receptor-mannose complex failed, the structure of the complex of ***S*-52** with OctβMan in solution could be solved by a combination of experimental NMR data and molecular modeling calculations. Interestingly, although NMR experiments were acquired at such a concentration that the 1:1 complex accounted for nearly 50% of the species in solution, whereas the 1:2 complex

Table 15. NOE intensities (600 MHz, 300 ms mixing time, 298 K) for the complex between ***S*-52** and OctβMan in CD_3CN (OctβMan 0.95 mM, ***S*-52** 1.2 mM).

***S*-52**	OctβMan	Intensity
NH-27	H-2	medium
NH-27	H-6	strong
NH-12	H-2	weak
NH-12	H-6	medium
H-13	H-8	weak
H-8	H-6	very weak
H-25*´	H-2	medium-strong

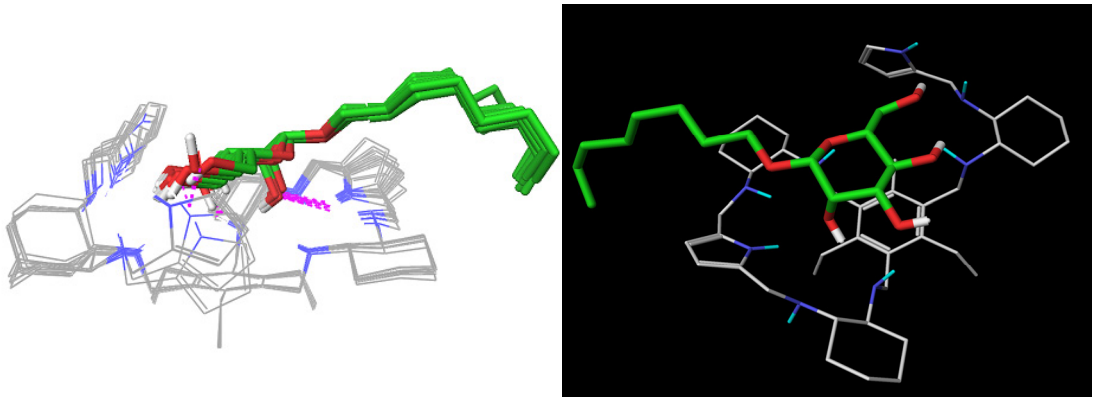

Figure 27. Left. Superimposition of the 12 energy minima structures as obtained from the molecular modelling protocol. The relative orientation (type-A arrangement) of the sugar versus the receptor is depicted. The flexible arm may adopt different orientations (see supporting information). Right. Structure of the global minimum geometry of the type-A family.

was only 5%, a single structure did not satisfy all the experimental data, suggesting the occurrence of two different arrangements of the partners in the dominant 1:1 complex. The molecular modeling protocol applied gave two families of low-energy conformers for the complex between ***S*-52** and OctβMan: (1) type-A, with 12 structures within 4.3 kJ mol^{-1} from the global minimum , and (2) type-B, with 3 structures within 9.0 kJ mol^{-1} from the global minimum, both of which were required to fit with good agreement all the experimental NMR evidence simultaneously, including the dramatic upfield shift of the H-4 proton of the mannose moiety, which in all conformations is located at 2.7-2.8 Å from the

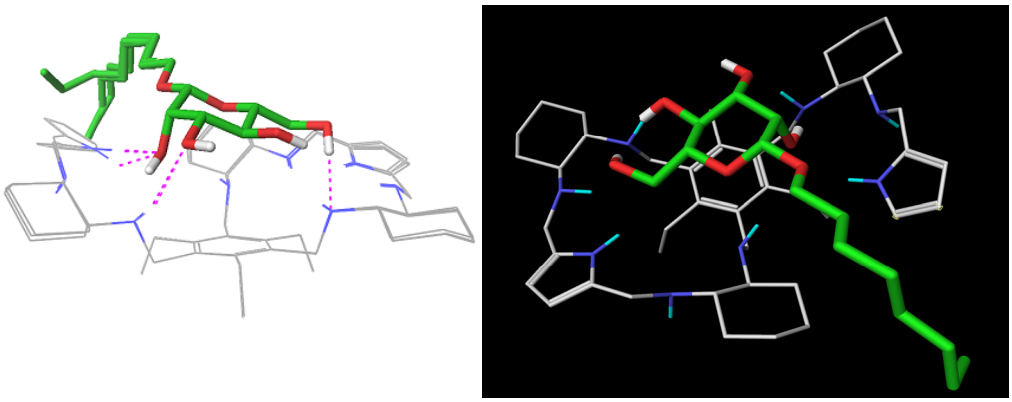

Figure 28. Left. Superimposition of the 3 energy minima structures as obtained from the molecular modelling protocol. The relative orientation (type-B arrangement) of the sugar versus the receptor is depicted. The flexible arm may adopt different orientations (see supporting information). Right. Structure of the global minimum geometry of the type-B family

centroid of the benzene ring of the receptor. The two families of conformers and the corresponding minimum energy structures for each family are depicted in Figures 27 and 28. Remarkably, the H-bond between a pyrrolic NH and the axial mannosyl OH is the most conserved interaction among the whole set of structures; likewise, in both families the glycosidic chain lies above a pyrrolic ring, in agreement with the unexpected upfield shift experienced by the H-7, H-8, and H-9 protons of the octyl chain. Moreover, in all conformers the β-face of mannose lies on top of the benzene ring of the receptor, in a roughly face-to-face disposition. Such an arrangement suggests that strong H-bonding, particularly to the axial hydroxyl, and additional CH-π interactions may be responsible for the observed affinity for the β anomer of mannosides.

Conclusions.

In this PhD thesis the molecular recognition properties of synthetic amino-pyrrolic receptors were studied towards biologically relevant carbohydrates. Starting from the encouraging results obtained in last few years with pyrrolic receptor **1**, new receptors were synthesized. Receptors with different architectures and H-bonding properties were designed with the aim of obtaining the information to understand the requirements necessary for effective recognition. Moreover, chiral receptors were developed to investigate the enantioselective recognition of monosaccharides. Amino and pyrrolic groups spaced by a methylenic unit and appropriately disposed on a tripodal scaffold have proved to be a successful pattern in the recognition of monosaccharides. Binding properties of the receptors prepared have been investigated with different and complementary techniques, like nuclear magnetic resonance, mass spectrometry and calorimetry. These studies have provided an evaluation of the binding abilities of the receptors explored toward a set of monosaccharides selected among the most frequently encountered as epitopes in biological systems. Through a scrupulous analysis of the measured binding constant, a whole set of affinity data were obtained, among which some interesting receptors clearly emerged, showing affinities and selectivities among the best ever published in the chemical literature.

In particular, the hexamine macrobicyclic cage **26** demonstrated to specifically recognize the β anomer of D-glucose and its alkyl glucosides with complete β/α selectivity, and to effectively discriminate β monosaccharides of the *gluco* series from both α and β anomers of the *galacto* and *manno* series. This discovery is bound to have an impact on the understanding of the structural features and the rational design of synthetic receptors for the molecular recognition of carbohydrates.

Apart from glucose-selective receptors, the acetalic pyrrolic tripodal receptor **28** exhibited remarkable recognition properties toward mannosides. Indeed, results demonstrated that implementation of additional H-bonding substituents, strategically located into the architecture of the pyrrolic tripodal

scaffold, could dramatically enhance both the affinity for a specific glycoside and selectivity with respect to other monosaccharides.

Concerning the family of chiral receptors, while the hexamino tripyrrolic receptor ***R*-34** demonstrated the best recognition properties toward the α anomer of mannoside ever reported for a H-bonding synthetic receptors, the hexamino dipyrrolic receptor ***S*-52** enantioselectively recognized β-mannose and β-mannosides with remarkable affinity in a competitive medium (acetonitrile), distinct selectivity with respect to the α-anomer, and the highest enantioselectivity of the *all-S* with respect to the *all-R* receptor reported to date.

Structures of the most significant receptor-glycoside complexes in solution were fully characterized in collaboration with Prof. Jesús Jiménez-Barbero of the Centro de Investigaciones Biológicas, CSIC, of Madrid. The structure of the complexes was elucidated through NMR binding studies associated with molecular modelling calculations, and afforded valuable information for future design of new receptors.

These results reported in this PhD thesis, even though were obtained in organic media, represent an encouraging step ahead in the achievement of new synthetic receptors as potential CBAs, particulary toward mannose recognition, which has a key role in several pathological processes, like infection by HIV, HCV and by other bacteria and parasites. On the whole, the results obtained with the developed receptors represent a significant progress in molecular recognition of carbohydrates and open the way to new future advances.

Experimental Section

General.

Mass spectra were recorded on a Shimadzu GCMS-QP5050A in direct injection. ESI mass spectra were recorded on an API 365 PE-Sciex triple quadrupole equipped with a standard Ionspray interface from Applied Biosystems and on a LCQ-Fleet Ion Trap equipped with a standard Ionspray interface from Thermo Scientific. ESI-MS analysis was performed in positive ion mode. HRMS were performed on a LTQ-IT-Orbitrap with a spray voltage of 2.10 kV and a resolution of 100000 (FWHM). NMR spectra for characterization of products and binding experiments were recorded on Varian Gemini 200 and Mercury Plus 400 instruments. High field NMR experiments were performed on a Bruker Avance 900 spectrometer equipped with a reverse detection z-gradient TXI cryo-probe. Chemical shifts are reported in part per million (δ) relative to TMS, using the residual solvent line as secondary internal reference (7.26 ppm for spectra run in $CDCl_3$, 1.96 ppm for spectra run in CD_3CN, 4.65 for spectra run in D_2O, 3.34 ppm for spectra run in CD_3OD and 2.54 ppm for spectra run in DMSO-d6). ^{13}C NMR spectra were obtained at 50 MHz and 100 MHz. Chemical shifts are reported in δ relative to TMS, using the central solvent line as secondary internal reference at 77.0 ppm for spectra run in $CDCl_3$, 49.86 ppm for spectra run in CD_3OD and 40.45 ppm for spectra run in $DMSOd_6$. Isothermal Titration Microcalorimetry experiments were performed at 298 K with a VP-ITC microcalorimeter (MicroCal, Inc., Northampton, MA). After an initial injection of 1 μL, aliquots of the glycoside solution were stepwise injected into the sample cell containing a solution of the receptor. All experiments were performed in acetonitrile. Heats of dilution were measured by injecting the glycoside solution into neat acetonitrile and then subtracted from the binding heats. The thermodynamic parameters and K_a values were calculated by fitting experimental data to a single binding site model using the ORIGIN 7.0 sofware package.

Conformational Analysis – NMR methods.

NMR experiments were performed at 500 MHz on a Bruker AVANCE spectrometer, at 298 K, unless otherwise stated. The experiments were performed in CD_3CN, stored on basic Al_2O_3. Experiments on the free species were recorded at 2.1 mM concentration for the glycoside (Octyl β-D-mannopyranoside, OctβMan) and 3.96 mM for receptor **28**. According to the titration data, for a 3:1 receptor/ligand ratio, the 1:1 complex is present in ca. 60% amount; the 2:1 complex in 20% amount, and the free glycoside is present in 20% amount. Thus, for the detailed studies on the complexes formed in solution, 1.05 mM for the glycoside and 3.17 mM for the receptor were the concentrations employed. Analogous experiments were carried out for receptor **1**. For receptor **52** Experiments on free reagents were recorded at 2.1 mM for the glycoside (OctβMan) and 1.88 mM for receptor **52**, whereas for their combination the concentrations were 0.95 mM and 1.2 mM, respectively. Under these concentration conditions, the 1:1 complex accounts for nearly 50% of the species in solution, whereas the 1:2 complex is only 5%. the NMR experiments were thus expected to provide information on the dominant 1:1 complex. In addition to standard 1D ^1H NMR spectra, COSY, TOCSY (35 ms mixing time) and NOESY (500 ms mixing time) experiments were also acquired, using standard BRUKER sequences, to assign the resonances of all the molecular entities, free and bound, as well as to detect the relevant intramolecular and intermolecular distances.

Conformational Analysis – Molecular Modeling.

Initial structures of OctβMan and receptors were built using the Maestro software package[67] and minimized using conjugate gradients with the AMBER* force field[68], and a dielectric constant of 37.5 Debyes (acetonitrile) with extended cutoff to treat remote interactions. A maximum number of 5000 iterations were employed with the PRCG scheme, until the convergence energy threshold was 0.05. Once the optimum geometries had been achieved, a conformational search protocol was adopted, using a Monte Carlo torsional sampling method (MCMM) with automatic setup during the calculation, energy window of 50 kJ mol^{-1}, 1000 maximum number of steps, and 100 steps per

torsion of the bond to be rotated. The best structures obtained from this calculation in terms of energy were chosen and then, the mannoside was manually docked within the cavity and further minimized. The complexes were found to be stable, since the sugar remained inside the receptor cleft by energy minimization. Thus, this local minimum was taken as starting geometry for an additional conformational search process, with no constraints, with the same settings as before. The obtained structures were classified according to clusters, which differ in the orientation of the saccharide with respect to the receptor. The lowest energy structure cluster geometries were considered to correspond to the most likely NMR-based experimental solution and were further explored.

Material.

Reagents were purchased from commercial suppliers and used without purification. OctαGlc, OctβGlc and OctβGal were commercial samples. The other octyl glycosides were known compounds[69-71] and were prepared according to a literature method.[72] Spectral assignments, confirmed through 2D-NMR spectra, were in agreement with literature data.[69-71] Methyl glycosides were commercial samples. 1,3,5-*tris*(Aminomethyl)-2,4,6-triethylbenzene **3**, 1,3,5-triethyl-2,4,6-*tris*(bromomethyl)benzene **8**,[28] 5-(5,5-Dimethyl-1,3-dioxan-2-yl)-pyrrole-2-carbaldehyde **23**[40] and pyrrole-2,5-dicarbaldehyde **24**,[40] 2,3-dimethylbutane-2,3-diamine **42**[73] were prepared according to known method. Unless otherwise stated, all air and moisture sensitive reactions were performed under inert atmosphere.

Abbreviations.

DMF	N,N-dimethylformamide
SEM-Cl	2-(trimethylsilyl)ethoxymethyl chloride
TBAF	tetrabutylammonium fluoride
DMSO	dimethylsulfoxide
THF	tetrahydrofuran
$(Boc)_2O$	di-tert-butyl dicarbonate
TFA	trifluoroacetic acid
$PrNH_2$	n-propylamine
RT	room temperature

1-((2-(trimethylsilyl)ethoxy)methyl)-pyrrole-2-carbaldehyde (6).

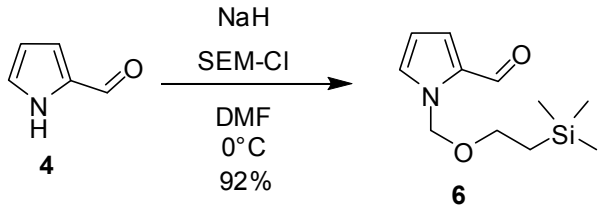

To a suspension of sodium hydride (1.13g, 47.1 mmol) in anhydrous DMF (7 mL), **4** (2.68 g, 28.2 mmol) was added and evolution of hydrogen was observed. The mixture was stirred at room temperature for 30 minutes since dissolution of the suspension. The solution was cooled at 0 °C and 2-(trimethylsilyl)ethoxymethyl chloride (4.71 g, 28.3 mmol) was slowly added. The reaction mixture was stirred for 1 h at 0 °C, then poured into 550 mL of icy $NaHCO_3$ 10% and extracted with CH_2Cl_2 (3 x 200 mL). The organic layers were washed with water (3 x 200 mL), dried over Na_2SO_4, filtered and concentrated to give crude **6** (5.86 g, 26.0 mmol, 92%) as a pale yellow oil. Product was used without further purification for the next reaction. ^{1}H-NMR (200 MHz, $CDCl_3$): δ 9.59 (s, 1H); 7.15-7.14 (m, 1H); 6.99-6.97 (m, 1H); 6.31-6.29 (m, 1H); 5.71 (s, 2H); 3.58-3.50 (m, 2H); 0.94-0.86 (m, 2H); -0.02-(-0.05) (m, 9H).

1(1-((2-(trimethylsilyl)ethoxy)methyl)-2-hydroxymethyl-pyrrole (7).

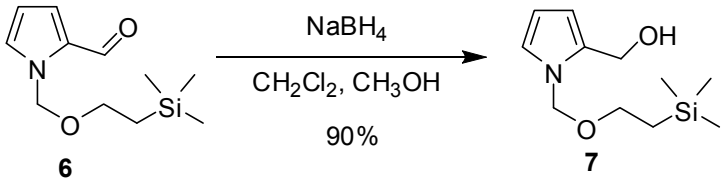

To a solution of **6** (5.86 g, 26.0 mmol) in CH_2Cl_2 (260 mL), freshly prepared suspension of $NaBH_4$ (1.97 g, 52.1 mmol) in CH_3OH (75 mL) was added. The reaction was stirred for 1 h at r.t., poured into water (500 mL) and extracted with CH_2Cl_2 (3 x 200 mL). The organic layers were washed with water (3 x 200 mL), dried over Na_2SO_4, filtered and concentrated. The crude mixture was purified by flash chromatography (CH_3OH/CH_2Cl_2 = 4/96, silica gel) to give **7** (5.32 g, 23.4 mmol, 90%) as yellow solid. M.p.: 36-38 °C. ^{1}H-NMR (200 MHz,

$CHCl_3$): δ 6.78-6.73 (m, 1H), 6.23-6.18 (m, 1H), 6.11-6.05 (m, 1H), 5.29 (s, 2H), 4.62 (d, *J* = 6 Hz, 2H), 3.55-3.44 (m, 2H), 2.49 (t, *J* = 6 Hz, 1H), 0.95-0.84 (m, 2H), 0.05- (-0.05) (m, 9H). ^{13}C-NMR (50 MHz, $CDCl_3$): δ 132.30, 123.00, 110.52, 107.42, 76.30, 65.89, 56.48, 17.98, 1.26.

1,3,5-*tris*[methyl-(2-(1-trimethyl-silyl-ethoxy-methyl)-pirrolylmethyl)-ether]-2,4,6-triethylbenzene (9).

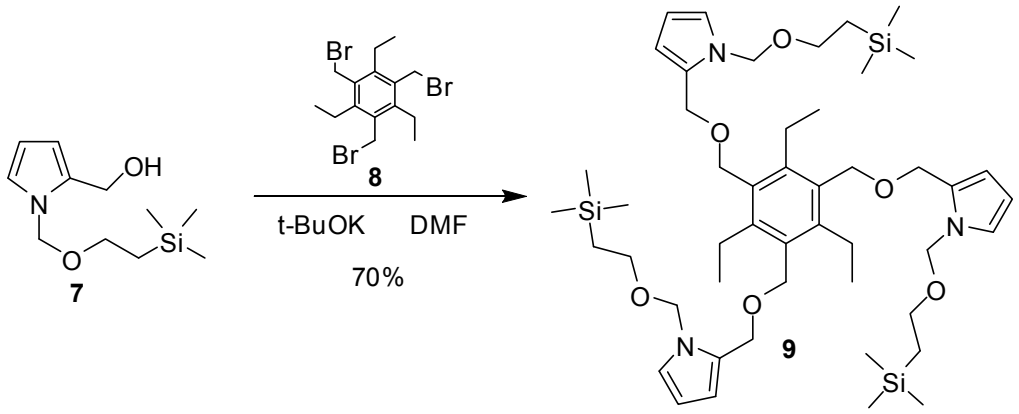

To a solution of **7** (594 mg, 2.62 mmol) in anhydrous DMF (5.2 mL), potassium *tert*-butoxide (253 mg, 2.25 mmol) was slowly added. To the reaction mixture, **8** (195 mg, 0.442 mmol) was added under stirring in 10 min. The mixture was stirred at r.t. for 1 h, poured into water (70 mL), neutralized with phosphates buffer and extracted with CH_2Cl_2 (3 x 25 mL). The organic layers were washed with water (3 x 50 mL), dried over Na_2SO_4, filtered and concentrated. The crude mixture was purified by flash chromatography (acetone/CH_2Cl_2 = 3/97, silica gel) to give **9** (272 mg, 0.309 mmol, 70%) as a pale yellow glassy solid. ^{1}H-NMR (200 MHz, $CHCl_3$): δ 6.77-6.70 (m, 3H), 6.24-6.17 (m, 3H), 6.11-6.05 (m, 3H), 5.25 (s, 6H), 4.59 (s, 6H), 4.40 (s, 6H), 3.51-3.39 (m, 6H), 2.61 (q, *J* = 7.3 Hz, 6H), 1.04 (t, *J* = 7.3 Hz, 9H), 0.94-0.80 (m, 6H), 0.03- (-0.14) (m, 27H). ^{13}C-NMR (50 MHz, $CDCl_3$): δ 144.84, 131.75, 128.96, 123.05, 111.57, 107.29, 76.19, 65.50, 65.44, 63.96, 22.66, 17.89, 16.56, 1.18.

1,3,5-*tris*[methyl-(pirrolylmethyl)-ether]-2,4,6-triethylbenzene (5).

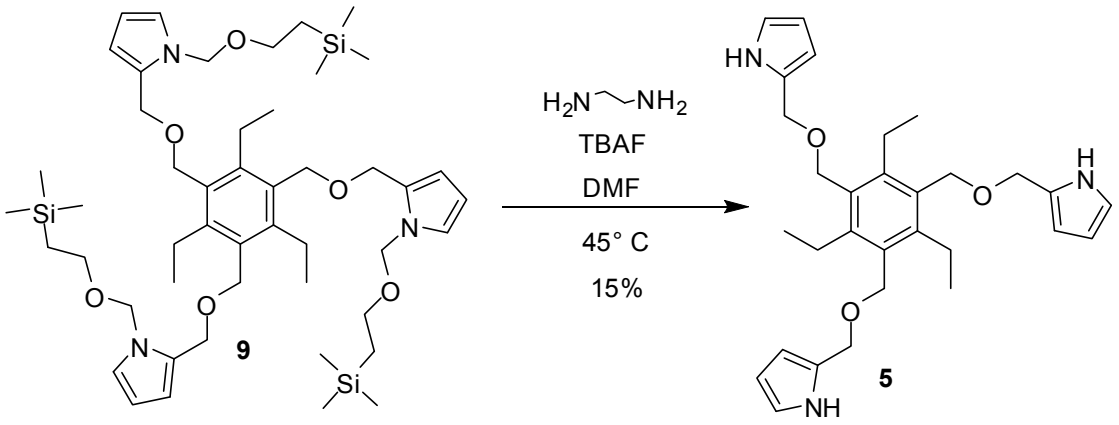

To a solution of **9** (676 mg, 0.768 mmol) in DMF (2.5 mL), ethylenediamine (1.03 g, 17.1 mmol) and TBAF (2.18 g, 6.91 mmol) were added. The solution was stirred for 60 h at 45 °C, then poured into water (70 mL) and extracted with CH_2Cl_2 (3 x 25 mL). The organic layers were washed with water (3 x 50 mL), dried over Na_2SO_4, filtered and concentrated. The crude mixture was purified by flash chromatography on silica gel (acetone/CH_2Cl_2 = 10/90, then acetone/CH_2Cl_2 = 20/80) to give **5** (55 mg, 0.112 mmol, 15%) as a yellow solid. M.p.: 113-114 °C. ^{1}H-NMR (200 MHz, $CDCl_3$): δ 48.52 (s, 3H), 6.57-6.50 (m, 3H), 6.21-6.14 (m, 3H), 6.14-6.07 (m, 3H), 4.54 (s, 6H), 4.46 (s, 6H), 2.61 (q, *J* = 7.3 Hz, 6H), 1.03 (t, *J* =7.3 Hz, 9H). ^{13}C-NMR (50 MHz, $CDCl_3$): δ 144.95, 131.50, 127.75, 118.17, 107.90, 107.59, 64.99, 64.93, 22.22, 16.23. ESI-MS *m/z* (%): 512.4 (100) $[M+Na]^+$.

1,3,5-triethyl-2,4,6-tris(methoxymethyl)benzene (10).

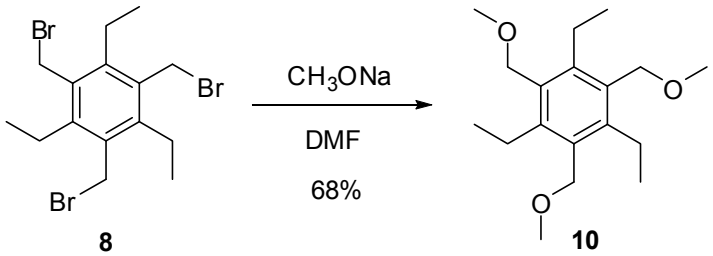

To a suspension of **8** (197 mg, 0.447 mmol) in anhydrous DMF (2.7 mL), sodium methoxyde (82 mg, 8.52 mmol) was added at r.t. and stirred for 2 h. The

mixture was poured into water (30 mL) and extracted with CH_2Cl_2 (3x10 mL). The organic layers were washed with water (3x20 mL), dried over Na_2SO_4, filtered and concentrated. The crude mixture was purified by flash chromatography (ethyl acetate/petroleum ether = 20/80, silica gel) to give **10** (90 mg, 0.306 mmol, 68%) as a white solid. M.p.: 84-85 °C. Anal. Calcd for $C_{18}H_{30}O_3$: C, 73.43; H, 10.27; O, 16.30. Found C, 73.33; H, 10.27. ^{1}H-NMR (200 MHz, $CDCl_3$): δ 4.45 (s, 6H), 3.42 (s, 9H), 2.83 (q, *J* = 1.75 Hz, 6H), 1.19 (t, *J* = 1.75 Hz, 9H). ^{13}C-NMR (50 MHz, $CDCl_3$): δ 144.52, 131.57, 68.37, 57.96, 22.54, 16.26. ESI-MS *m/z* (%): 317.3 (100) $[M+Na]^+$.

1,3,5-*tris*((2-pyrrolylmethylen)-aminomethyl)-2,4,6-triethylbenzene (2).

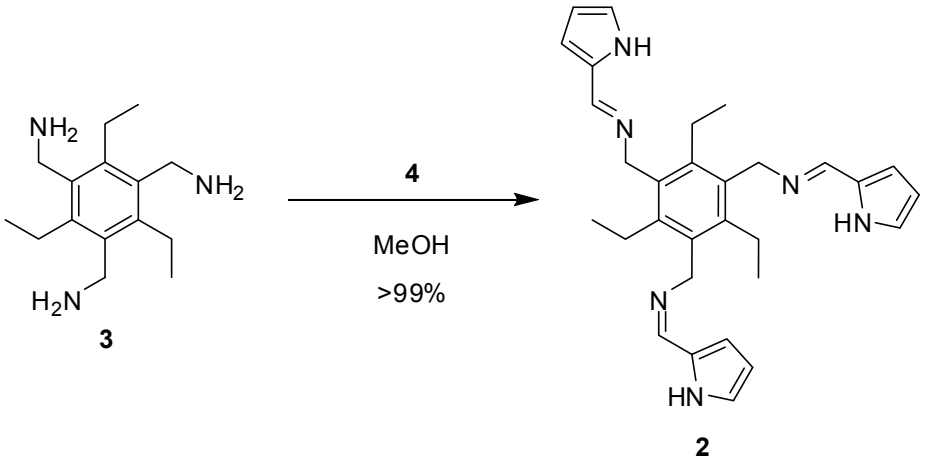

Pyrrole-2-carbaldehyde **4** (1.14 g, 12.0 mmol) and **3** (1.00 g, 4.01 mmol) were completely dissolved in 8 mL of MeOH. The mixture was stirred at room temperature for 20 h. The yellow precipitate was filtred and washed several times with CH_3OH to give a white powder that was dried at 50 °C under vacuum for 4 h to yield **2** (1.24 g, 64%) as pure solid. To obtain an analytically pure sample, the solid was washed with $CHCl_3$ (3 x 5 mL), and dried at 50 °C under vacuum for 4 h to yield **2** (604 mg, 31%) as a white powder. M.p.: dec. >201 °C; ^{1}H-NMR ($CDCl_3$, 400 MHz): δ 7.98 (s, 3H), 6.80 (m, 3H), 6.41-6.40 (m, 3H), 6.19-6.18 (m, 3H), 4.82 (s, 6H), 2.72 (q, *J* = 7.2 Hz, 6H), 1.22 (t, *J* = 7.2 Hz, 9H); ^{13}C-NMR ($CDCl_3$, 50 MHz): δ 150.67, 143.16, 132.80, 130.48, 121.29, 113.63, 109.56, 56.66, 23.14, 15.99. HRMS: calcd for $C_{30}H_{36}N_6$ + H: 481.30742; found: 481.30743. MS *m/z* (%): 480 (29), 398 (21), 387 (35), 386 (100), 372

(10), 371 (40), 358 (14), 357 (51), 306 (13), 294 (13), 293 (25), 292 (30), 291 (23), 277 (25), 263 (29), 212 (13), 198 (10), 185 (10), 170 (10), 169 (16), 156 (13), 155 (15), 143 (12), 141 (11), 129 (10), 128 (10), 95 (12), 80 (32), 79 (14), 52 (10).

1,3,5-*tris*(cyanomethyl)-2,4,6-triethylbenzene (13).[74]

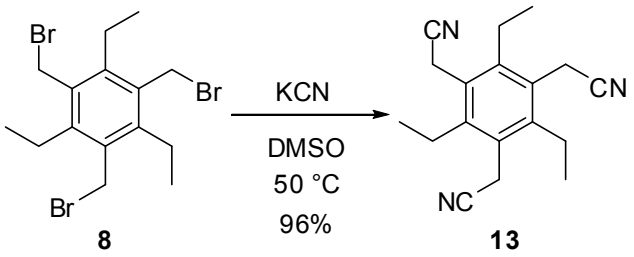

8 **13**

Potassium cyanide (1.19 g, 18.3 mmol) was dissolved in 35 mL of dry DMSO under nitrogen atmosphere and heated at 50 °C for a few minutes. To the solution was added **8** (2.6 g, 5.90 mmol), and the mixture was stirred at 50 °C for 15 min than cooled at room temperature and stirred for a night. The reaction mixture was poured into 40 mL of ice water and extracted with CH_2Cl_2 (3 x 30 mL). The combined organic layers were washed with Brine (4 x 40 mL), then dried over Na_2SO_4 and concentrated to give **13** (1.59 g, 96%) as a white powder. M.p.: 208-210 °C (lit. 220-222 °C).[75] ^{1}H-NMR ($CDCl_3$, 200 MHz): δ 3.73 (s, 6H), 2.83 (q, *J* = 7.6 Hz, 6H), 1.29 (t, *J* = 7.6 Hz, 9H).

1,3,5-*tris*(2'-aminoethyl)-2,4,6-triethylbenzene (14).[76;77]

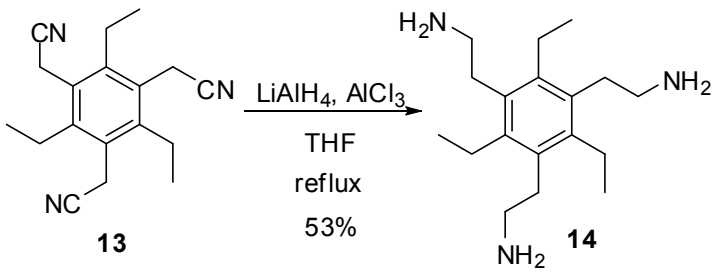

13 **14**

To 4 mL of THF cooled at 0 °C was slowly added under stirring solid $LiAlH_4$ (326 mg, 8.59 mmol). To the resulting suspension was added quickly at 0 °C under stirring a solution of $AlCl_3$ (1.15 g, 8.59 mmol) in 13 mL of THF. A

solution of **13** (600 mg, 2.15 mmol) in 22 mL of THF was added to the mixture under stirring in 15 min at 0 °C. The reaction mixture was heated at reflux for 3 h under vigorous stirring, during which time a gel is formed. The reaction mixture was then cooled at 0 °C and, in order, were slowly added 340 µL of H_2O, 260 µL of NaOH 20% and 1.20 mL of H_2O. Evolution of hydrogen was observed during these additions and the resulting suspension was filtred on a gooch filter. The grey powder was suspended in 150 mL of KOH 40% and extracted with CH_2Cl_2 (3 x 50 mL), dried over Na_2SO_4 and concentrated to give 580 mg of crude as a white solid which was purified by flash column chromatography on silica gel (CH_2Cl_2/MeOH/NH_3 30%, 66:33:7) to yield **14** (334 mg, 53%). M.p.: dec. >120 °C (lit. Dec >220 °C).[75] ^{1}H-NMR ($CDCl_3$/CD_3OD 90:10, 200 MHz): δ 3.13 (bs, NH_2 + H_2O), 2.72 (m, 12H), 2.56 (q, *J* = 7.6 Hz, 6H), 1.13 (t, *J* = 7.6 Hz, 9H). ^{13}C-NMR (50 MHz, CD_3OD): δ 139.38, 132.57, 42.72, 32.19, 22.20, 15.24.

1,3,5-*tris*(2-(2'-pyrrolylmethylen)-aminoethyl)-2,4,6-triethylbenzene (11).

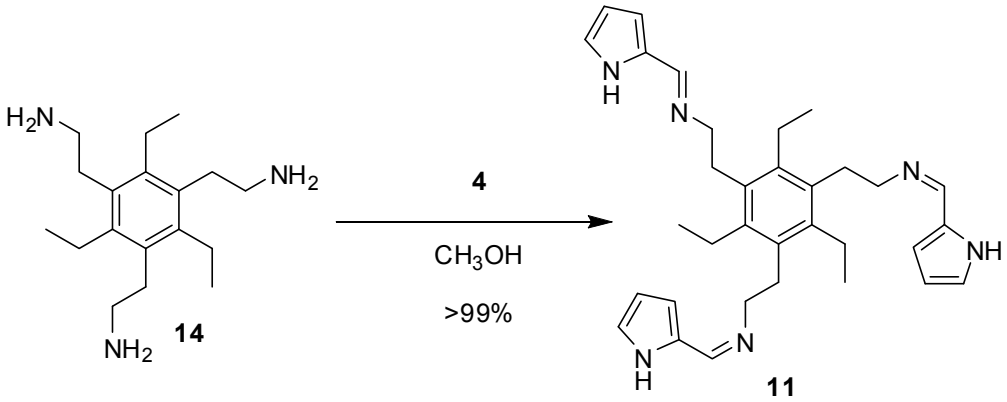

14 (118 mg, 0.41 mmol) and **4** (127 mg, 1.33 mmol) were completely dissolved in CH_3OH (1 mL). The solution was stirred overnight at room temperature, during which time a white precipitate was formed. The suspension was filtred and washed with CH_3OH to yield pure **11** (186 mg, 87%). To obtain an analytically pure sample, the solid was suspended in CH_3CN, filtred and washed several times with CH_3CN to yield the desired analytically pure **11** (135 mg, 64%). M.p.: dec. >186 °C; ^{1}H-NMR ($CDCl_3$, 400 MHz): δ 7.93 (s, 3H), 6.87 (m, 3H), 6.47-6.46 (m, 3H), 6.24-6.23 (m, 3H), 3.62-3.58 (m, 6H), 2.96-2.92 (m,

6H), 2.71 (q, *J* = 7.2 Hz, 6H), 1.18 (t, *J* = 7.2 Hz, 9H); ^{13}C-NMR ($CDCl_3$, 400 MHz): δ 151.28, 139.86, 133.06, 130.06, 121.56, 114.02, 109.69, 61.97, 31.12, 23.09, 15.92. MS *m/z* (%): 522 (21), 413 (12), 349 (21), 214 (10), 108 (10), 107 (53), 80 (100), 53 (16). Anal. Calcd for $C_{33}H_{42}N_6$: C, 75.82; H, 8.10; N, 16.08. Found: C, 74.99; H, 8.18; N, 15.97. HRMS: calcd for $[C_{33}H_{42}N_6 + 2H]^{2+}$: *m/z* 262.18082; found: 262.17982.

1,3,5-*tris*(2-(2'-pyrrolylmethyl)-aminoethyl)-2,4,6-triethylbenzene (12).

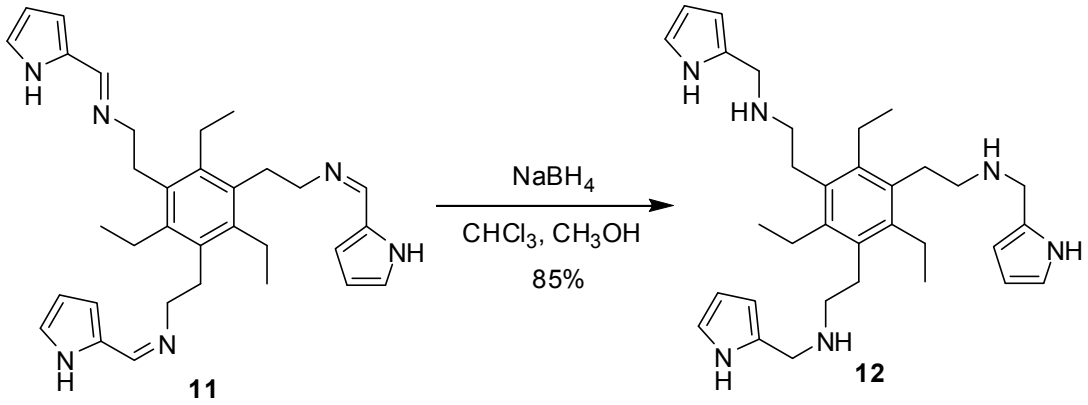

A suspension of **11** in CH_3OH was diluted with 300 µL of $CHCl_3$ and solid $NaBH_4$ was added. Evolution of hydrogen and dissolution of the suspension were observed during the addition. The reaction mixture was stirred for 30 min at room temperature, then diluted with 10 mL of CH_2Cl_2 and poured into a mixture of water (45 mL) and brine (5 mL). The mixture was extracted with CH_2Cl_2 (3 x 10 mL), dried over Na_2SO_4 and concentrated to give pure **12** (170 mg, 85%) as a white powder. M.p.: dec. >58 °C; ^{1}H-NMR ($CDCl_3$, 200 MHz): δ 8.51 (bs, 3H), 6.74-6.71 (m, 3H), 6.15-6.11 (m, 3H), 6.03 (m, 3H), 3.83 (s, 6H), 2.76 (bs, 12H), 2.59 (q, *J* = 7.4 Hz, 6H), 1.61 (bs, NH + H_2O), 1.16 (t, *J* = 7.4 Hz, 9H); ^{13}C-NMR ($CDCl_3$, 50 MHz): δ 139.48, 133.24, 130.27, 117.22, 108.02, 106.23, 50.71, 46.72, 30.17, 22.88, 15.95. HRMS: calcd for $C_{33}H_{48}N_6$ + H: 529.40132; found: 529.39966.

1,2,4,5-*tetrakis*(azidomethyl)benzene (17).

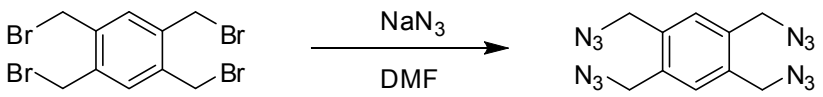

16 **17**

To a solution of **16** (2.50 g, 5.56 mmol) in DMF (17 mL), under nitrogen atmosphere, NaN_3 (2.89 g, 44.5 mmol) was added. Reaction mixture was stirred for 20 h at RT, than poured into water (300 mL), filtred and washed with fresh water to yeald crude **17** (1.76 g) as a white solid that was used for next reaction without any further purification. M.p.: 51-52 °C. ^{1}H NMR (200 MHz, $CDCl_3$): δ 7.40 (s, 2H), 4.47 (s, 8H). ^{13}C NMR (50 MHz, $CDCl_3$): δ 134.50, 131.25, 51.81.

1,2,4,5-*tetrakis*(aminomethyl)benzene (18).

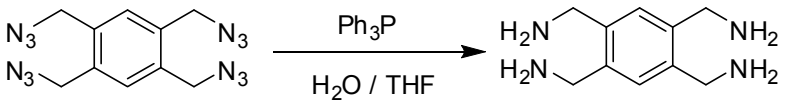

17 **18** 79%

To a solution of crude **17** (1.66 g, 5.56 mmol) and Ph_3P (11.7 g, 44.5 mmol) in THF (30 mL), H_2O (4 g, 222 mmol) was added and reaction was stirred at RT overnight. The solution was concentrated and the crude obtained was divide up CH_2Cl_2 and HCl 1M, then the layers were separated. The aqueous layer was extracted two times with fresh CH_2Cl_2, alkalised with KOH 40% and extracted several times with ethyl acetate. The organic layers were dried over Na_2SO_4 and concentrated to give pure **18** (784 mg, 79% over 2 steps) as a white solid. M.p.: dec. >128 °C. ^{1}H NMR (200 MHz, D_2O): δ 7.57 (s, 2H); 4.29 (s, 8H). ^{13}C NMR (50 MHz, CD_3OD): δ 138.53, 128.85, 42.14.

1,2,4,5-*tetrakis*((pyrrol-2-yl)methylamino)methyl)benzene (15).

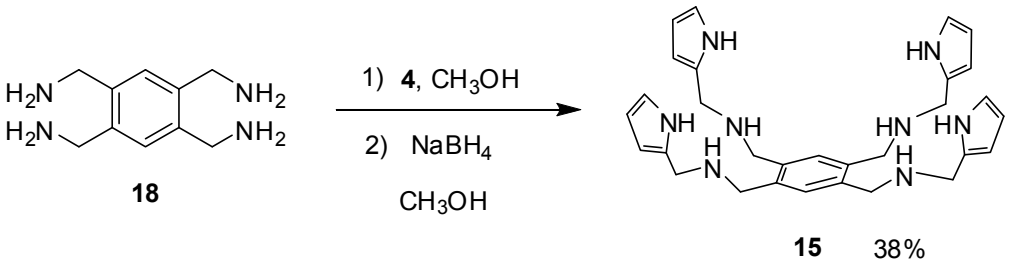

A solution of **18** (138 mg, 0.710 mmol) and **4** (405 mg, 4.26 mmol) in CH_3OH (12 mL) was stirred at RT overnight. To the obtained suspension $NaBH_4$ (242 mg, 6.39 mmol) was added and evolution of H_2 was observed. The reaction mixture was stirred for 2 h at RT, then concentrated and divide up $CHCl_3$ and H_2O + Brine. The organic layer was collected and the aqueous layer extracted two times with $CHCl_3$. The organic layers were washed with Brine, dried over Na_2SO_4 and concentrated to give crude **15**, that was purified by flash column chromatography on silica gel ($CHCl_3/CH_3OH/NH_3$ 33%, 77:23:5) to yield pure **15** (138 mg, 38%). To obtain an analytically pure sample, the solid was suspended in CH_3CN (10 mL), filtred and washed with CH_3CN (5 mL) to yield the desired analytically pure **15** (81 mg, 22%). M.p.: dec. >140 °C. ^{1}H NMR (200 MHz, DMSOd6): δ 10.48 (bs, 4H), 7.17 (s, 2H), 6.57-6.56 (m, 4H), 5.87-5.86 (m, 4H), 5.83-5.82 (m, 4H), 3.60 (s, 8H), 3.58 (s, 8H), 3.32 (bs, H_2O+4H). ^{13}C NMR (50 MHz, DMSOd6): δ 137.30, 130.90, 117.08, 107.41, 106.21, 79.64, 50.23, 46.09. Anal. Calcd for $C_{30}H_{38}N_8$+3/2H_2O: C, 67.01; H, 7.69; N, 20.84; O, 4.46. Found C, 67.28; H, 7.39; N, 21.16. ESI-MS *m/z* (%): 511.17 (100) $[M+H]^+$.

Receptor (19).

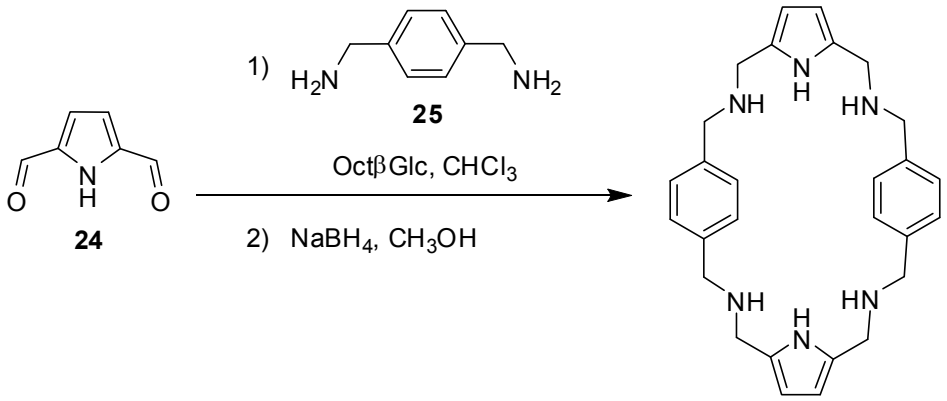

Octyl β-D-mannopyranoside (848 mg, 2.90 mmol), **24** (179 mg, 1.45 mmol) and **25** (197 mg, 1.45 mmol) were completely dissolved in $CHCl_3$ (24 mL). The solution was stirred overnight at RT, then $NaBH_4$ (126 mg, 3.34 mmol) suspended in 6 mL of CH_3OH was added. Evolution of H_2 was observed. The raction mixture was diluted with $CHCl_3$ (20 mL) and washed three times with water, dired over Na_2SO_4 and concentrated to give crude **19**, that was purified by flash column chromatography on silica gel ($CHCl_3/CH_3OH$, 80:20, then $CHCl_3/CH_3OH/NH_3$ 33%, 82:18:2) to yield pure **19** (239 mg, 71%) as a pale yellow glassy solid. M.p.: dec. >155 °C. ^1H NMR (200 MHz, $CDCl_3$): δ 9.27 (bs, 2H), 7.31 (s, 8H), 5.96-5.94 (m, 4H), 3.86 (s, 8H), 3.71 (s, 8H), 2.93 (bs, 4H+H_2O). ^{13}C NMR (50 MHz, $CDCl_3$): δ 138.62, 129.53, 128.27, 106.09, 52.40, 46.19. ESI-MS *m/z* (%): 455.00 (100) $[M+H]^+$. Anal. calcd for $C_{28}H_{34}N_6$+1/2H_2O : C, 72.54; H, 7.61; N, 18.13, O, 1.73; found: C, 72.13; H, 7.38; N, 17.97.

Receptor (27).

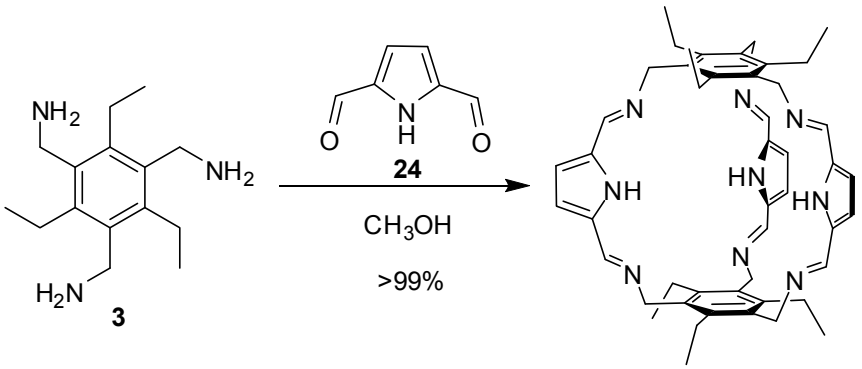

27

Pyrrole-2,5-dicarbaldehyde **24** (200 mg, 1.62 mmol) and 1,3,5-tris(aminomethyl)-2,4,6-triethylbenzene **3** (270 mg, 1.08 mmol) were dissolved in 15 mL of methanol. The mixture was stirred overnight at RT. The resulting yellow precipitate was filtered and washed with methanol to yield 402 mg (quantitative) of **27** as a pale yellow solid. The solid was purified to analytical grade by washing with several portions of CH_3CN. M.p.: dec. >210°C. ^1H NMR (400 MHz, $CDCl_3/CD_3OD$ 97:3): δ 7.78 (s, 6H), 6.62 (s, 6H), 4.77 (s, 12H), 2.68 (bs, 3H + H_2O), 2.43 (m, 12H), 1.51 (t, J = 7.2 Hz, 18H). ^{13}C NMR (100 MHz, $CDCl_3/CD_3OD$ 97:3): δ 151.86, 143.45, 132.53, 132.15, 113.41, 55.62, 22.60, 15.77. ESI-MS *m/z* (%): 760.5 (100) $[M+H]^+$, 782.5 (6) $[M+Na]^+$, 798.4 (4) $[M+K]^+$. HRMS: calcd for $C_{48}H_{57}N_9$ + H: 760.48097; found: 760.48071.

Receptor (26).

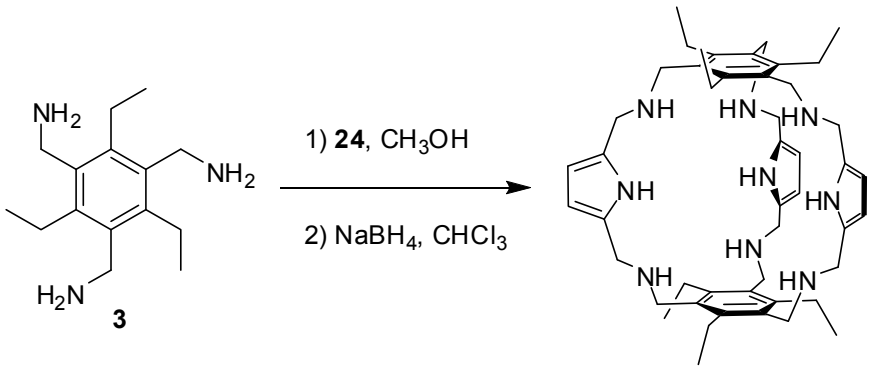

26 >99%

24 (900 mg, 7.31 mmol) and **3** (1.21 g, 4.87 mmol) were dissolved in 75 mL of methanol. The mixture was stirred overnight at RT. To the resulting yellow suspension was added 25 mL of trichloromethane and then, portionwise, solid $NaBH_4$ (636 mg, 16.8 mmol). An evolution of hydrogen and dissolution of the suspension was noted during the addition of $NaBH_4$. The yellow solution was stirred at RT for 30 min, then diluted with trichloromethane, washed with several portions of water, and dried over Na_2SO_4. Evaporation of the solvent gave 1.90 g of a yellow solid with quantitative yield. The solid was purified to analytical grade by washing with several portions of methanol and then dried at 40°C under reduced pressure to give 1.33 g of a pale yellow solid. Methanolic mother liquors contained essentially lower grade **26**. Residual methanol (1 equiv, most likely complexed) was removed by co-distillation with dichloromethane. M.p.: dec. >130°C. ^{1}H NMR (400 MHz, $CDCl_3$, assignments based on 2D-gDQCOSY experiments): δ 8.49 (bs, 3H; NH (Pyrr)), 5.87 (d, *J* = 2.4 Hz, 6H; CH (Pyrr)), 3.84 (s, 12H; CH_2Pyrr), 3.73 (s, 12H; CH_2Bn), 2.66 (q, *J* = 7.6 Hz, 12H; CH_2(Et)), 1.23 (t, *J* = 7.6 Hz, 12H; CH_3 (Et)), 0.83 (bs, 6H; NH); ^{13}C NMR (100 MHz, $CDCl_3$): δ = 141.60, 134.17, 129.88, 104.70, 48.35, 47.73, 22.56, 16.79; ESI-MS *m/z* (%): 772.6 (100) $[M+H]^+$, 794.6 (26) $[M+Na]^+$, 810.5 (3) $[M+K]^+$. HRMS: calcd for $C_{48}H_{69}N_9$ + H: 772.57487; found: 772.57503.

1,3,5-*tris*[methyl-((5-(5,5-dimethyl-1,3-dioxan-2-yl)-2-pirrolylmethyl)-amino)]-2,4,6-triethylbenzene (28).

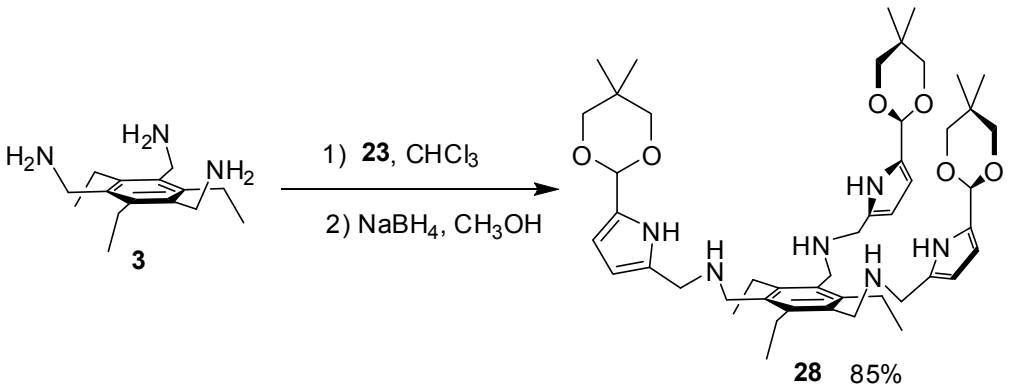

A mixture of **3** (150 mg, 0.60 mmol) and **23** (377 mg, 1.80 mmol) was dissolved in $CHCl_3$ (5 mL) and stirred overnight at room temperature. To the solution, diluited with CH_3OH (8 mL), was slowly added solid $NaBH_4$ (72 mg, 1.89 mmol). The reaction mixture was stirred at room temperature for 30 min and then poured into a solution of water (50 mL) and Brine (25 mL) and extracted with CH_2Cl_2 (3 x 25 mL). The combined organic layers were washed with water (2 x 25 mL), dried over Na_2SO_4 and concentrated to give 558 mg of crude product as a yellow solid, which was purified by flash column chromatography on silica gel ($CH_2Cl_2/CH_3OH/NH_3$ 33% 9:1:0.1) to afford **28** (423 mg, 85%) as a pale yellow powder. M.p. dec 74 °C; ^{1}H-NMR (400 MHz, $CDCl_3$): δ 8.71 (bs, 3H), 6.14-6.12 (m, 3H), 6.00-5.99 (m, 3H); 5.44 (s, 3H), 3.88 (s, 6H), 3.72-3.58 (m, 12H), 3.69 (s, 6H), 2.72 (q, *J* = 7.2 Hz, 6H), 1.50 (bs, 3H + H_2O), 1.25 (s, 9H), 1.17 (t, *J* = 7.2 Hz, 9H), 0.78 (s, 9H). ^{13}C-NMR (100 MHz. $CDCl_3$): δ 142.32, 134.07, 130.63, 128.23, 106.16, 77.31, 47.33, 47.20, 30.21, 23.06, 22.69, 21.90, 16.88. HRMS: calcd for $C_{48}H_{72}N_6O_6$ + H: 829.55861; found: 829.55896. ESI-MS *m/z* (%): 851 (15) $[M+Na]^+$, 829 (100) $[M+H]^+$. Anal. calcd for $C_{48}H_{72}N_6O_6$: C, 69.53; H, 8.75; N, 10.14; found: C, 69.22; H, 8.79; N, 10.01.

Methyl 5-formyl-pyrrole-2-carboxylate (33). [78]

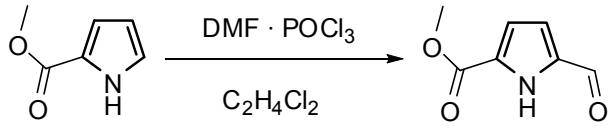

In a reaction flask DMF (1.28 g, 17.6 mmol) was cooled at 0 °C. Under stirring $POCl_3$ was added in 10 min, maintaining the temperature low than 20 °C. The reaction was warmed at RT and stirred for 15 min, diluted with $C_2H_4Cl_2$ (4 mL) and cooled again at 0 °C. Under stirring a solution of methyl 1H-pyrrole-3-carboxylate **32** (2.00 g, 16.0 mmol) in 7 mL $C_2H_4Cl_2$ was added in 15 min. The reaction mixture was warmed at 90 °C for 20 min and envelope of HCl was observed. The reaction was cooled at RT and a solution of $CH_3COONa{\cdot}3H_2O$ (12g, 88.0 mmol) in 16 mL of H_2O was added, then reaction was refluxed for 15 min under vigorous stirring. Reaction mixture was cooled at RT and the two layers were separated. The aqueous layer was extracted with CH_2Cl_2 (3 x 10 mL), the organic layers collected were washed with Na_2CO_3 ss, dried over dry Na_2CO_3, filtered and concentrated to give crude **33**, that was purified by flash column chromatography on silica gel (ethyl acetate/petroleum ether 40:60) to afford **33** (1.45 g, 60%) as a white powder. M.p. 94.5-95.5 °C (lit. 90-93 °C).[79] ^{1}H NMR (200 MHz, $CDCl_3$): δ 9.95 (bs, 1H), 9.67 (s, 3H), 6.97-6.91 (m, 2H), 3.92 (s, 3H). ^{13}C NMR (50 MHz, $CDCl_3$): δ 180.16, 119.67, 115.66, 52.37.

1,3,5-*tris*[methyl-((methyl(5-caboxylate))-2-pirrolylmethyl)-amino)]-2,4,6-triethylbenzene (29).

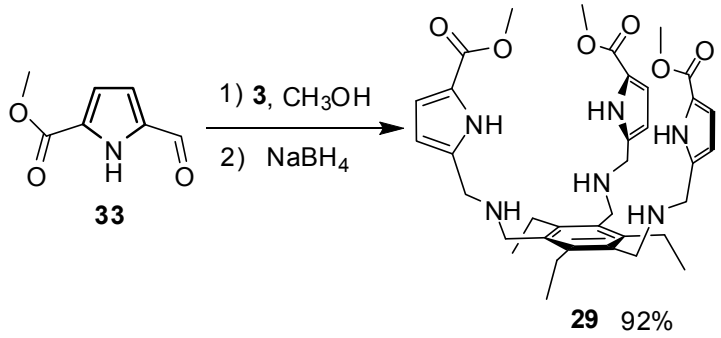

In a reaction flask a solution of **3** (180 mg, 0.722 mmol) and **33** (332 mg, 2.17 mmol) in CH_3OH (7 mL) was stirred overnight at RT, then $NaBH_4$ was

added, with observed evolution of H_2, and stirred for 20 min. The reaction mixture was diluted with CH_2Cl_2 (70 mL) and washed three times with water. The organic layers were dried over Na_2SO_4 and concentrated to give 468 mg of crude product as a white solid, which was purified by flash column chromatography on silica gel ($CH_3Cl/CH_3OH/NH_3$ 33% 9:1:0.1) to afford **29** (441 mg, 92%) as a bight white powder. M.p. 80-82 °C. ^{1}H NMR (200 MHz, $CDCl_3$): δ 9.63 (bs, 3H), 6.83-6.82 (m, 3H), 6.09-6.08 (m, 3H), 3.85 (s, 6H), 3.82 (s, 9H), 3.65 (s, 6H), 2.66 (q, *J* = 7.2 Hz, 6H), 1.63 (bs, 3H+H_2O), 1.12 (t, *J* = 7.2 Hz, 9H). ^{13}C NMR (50 MHz, $CDCl_3$): δ 161.36, 142.31, 136.35, 133.66, 121.55, 115.73, 108.47, 51.43, 47.23, 47.06, 22.85, 17.04. ESI-MS *m/z* (%) 661.08 (100) $[M+H]^+$, 682.92 (99) $[M+Na]^+$, 699.00 (88) $[M+K]^+$, 1342.50 (36) $[M+M+Na]^+$. Anal. calcd for $C_{36}H_{48}N_6O_6$ + 3/2H_2O : C, 62.86; H, 7.47; N, 12.22; O, 17.45 found: C, 62.90; H, 7.43; N, 12.08.

1,3,5-*tris*[methyl-((5-formyl-2-pirrolylmethyl)-amino)]-2,4,6-triethylbenzene (30).

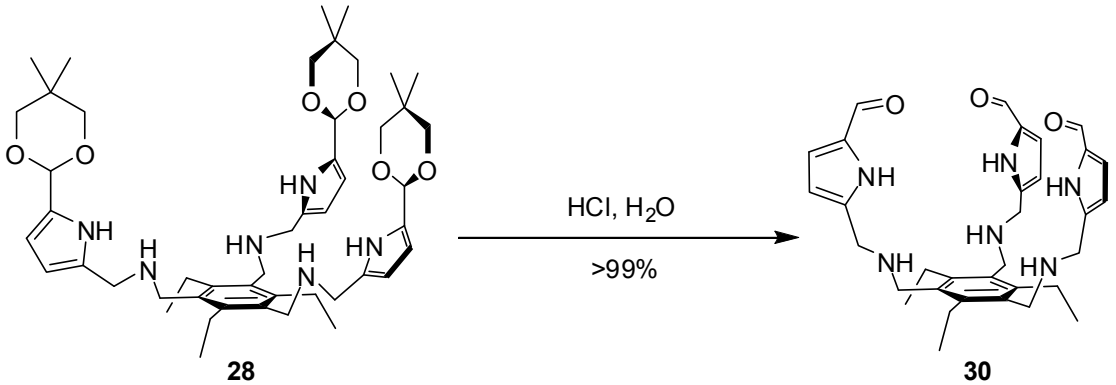

28 **30**

To a suspension of **28** (417 mg, 0.503 mmol) in 17 mL of water, HCl 1M was added drop wise until *p*H = 2. The solution was stirred for 1 h at RT, then cooled at 0 °C, diluted with CH_2Cl_2 and alkalized with NaOH 1 M (80 mL). The organic layer was separated and aqueous layer extracted with CH_2Cl_2 (2 x 30 mL). The collected organic layers were washed with water (2 x 40 mL), dried over Na_2SO_4 and concentrated to give pure **30** (270 mg, 94%) as a pale yellow glassy solid. M.p. 80-81 °C. ^{1}H NMR (200 MHz, $CDCl_3$): δ 10.50 (bs, 3H), 9.35 (s, 3H), 6.86-6.84 (m, 3H), 6.16-6.14 (m, 3H), 3.84 (s, 6H), 3.60 (s, 6H), 2.58 (q,

J = 7.2 Hz, 6H), 2.07 (bs, 3H + H_2O), 1.04 (t, *J* = 7.2 Hz, 9H). ^{13}C NMR (50 MHz, $CDCl_3$): δ 178.29, 142.11, 140.02, 132.97, 132.06, 121.76, 109.65, 46.45, 46.31, 22.34, 16.50. ESI-MS *m/z* (%) 571.17 (100) $[M+H]^+$. Anal. calcd for $C_{33}H_{42}N_6O_3$ + H_2O: C, 67.32; H, 7.53; N, 14.27; O, 8.41; found: C, 67.61; H, 7.63; N, 13.91.

1,3,5-*tris*[methyl-((propyl(5-pirrolylmethyl)amino)-2-methyl)-amino)]-2,4,6-triethylbenzene (31).

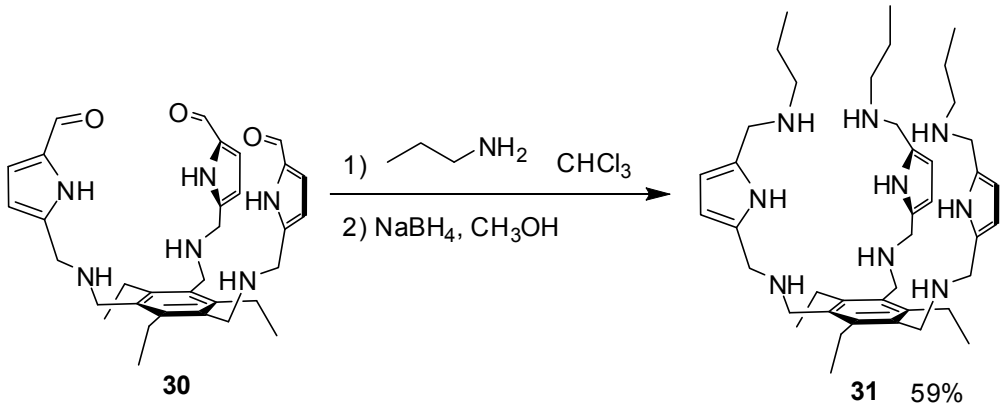

A solution of **30** (120 mg, 0.222 mmol) and $PrNH_2$ (79 mg, 1.33 mmol) in $CHCl_3$ (2 mL) was stirred overnight at RT. To the solution $NaBH_4$ (50 mg, 1.33 mmol) extemporary suspended in CH_3OH (2 mL) was added. The reaction mixture was stirred for 1.5 h at RT, poured into Brine (20 mL) and extracted with $CHCl_3$ (3 x 10 mL). The organic layers were washed with water (2 x 10 mL), dried over Na_2SO_4 and concentrated to give 150 mg of crude product as a pale yellow solid, which was purified by flash column chromatography on silica gel ($CH_3Cl/CH_3OH/NH_3$ 33% 70:30:6) to afford **31** (91 mg, 59%) as a pale yellow solid. M.p. 55-56 °C. ^1H NMR (200 MHz, $CDCl_3$): δ 9.06 (bs, 3H), 5.93-5.89 (m, 6H), 3.82 (s, 6H), 3.66 (s, 12H), 2.68 (q, *J* = 7.4 Hz, 6H), 2.56 (t, *J* = 7.4 Hz, 6H), 1.50 (tq, J_t = 7.4 Hz, J_q = 7.4 Hz, 6H), 1.13 (t, *J* = 7.4 Hz, 9H), 0.90 (t, *J* = 7.4 Hz, 9H). ^{13}C NMR (50 MHz, $CDCl_3$): δ 141.99, 133.93, 130.22, 129.76, 106.13, 105.97, 51.14, 47.50, 47.03, 46.65, 23.10, 22.76, 17.12, 11.97. ESI-MS *m/z* (%) 700.08 (100) $[M+H]^+$, 1398.58 (20) $[M+M+H]^+$, 1435.92 (33) $[M+M+K]^+$. Anal. calcd for $C_{42}H_{69}N_9$ + $2H_2O$: C, 68.53; H, 10.00; N, 17.13; O, 4.35; found: C, 68.73; H, 10.14; N, 16.80.

4,6-triethylbenzene-1,3,5-tricarbaldehyde (36).

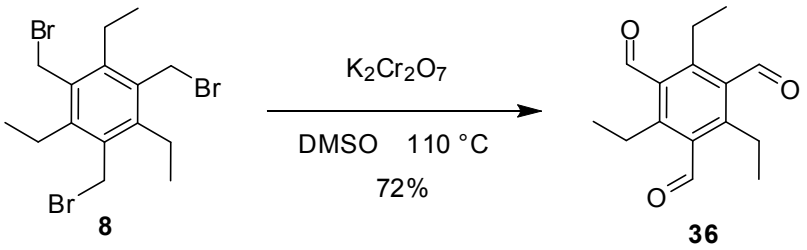

Potassium dichromate (24.0 g, 81.5 mmol) was suspended in dry DMSO (175 mL) and heated under vigorous stirring at 30 °C until dissolution. Under a mild nitrogen atmosphere **8** (8.00g, 18.1 mmol) was added and the reaction mixture was heated to 110 °C for 2 h. The reaction was poured into 700 mL of NaOH 10 M and extracted with CH_2Cl_2 (3 x 200 mL). The combined organic layers were washed with water (3 x 200 mL), dried over Na_2SO_4 and concentrated to give pure **36** (3.20 g, 72%) as a pale yellow powder. M.p. dec 54-56 °C. ^{1}H-NMR ($CDCl_3$, 200 MHz): δ 10.61 (s, 3H), 3.00 (q, *J* = 7.4 Hz, 6H), 1.27 (t, *J* = 7.4 Hz, 9H). ^{13}C-NMR (50 MHz, $CDCl_3$): δ 193.98, 149.13, 134.01, 22.72, 16.68.[80]

1,3,5-*tris*[methyl-(*tert*-butoxycarbonyl-*trans*-1,2-diaminocyclohexyl)]-2,4,6-triethylbenzene (38).

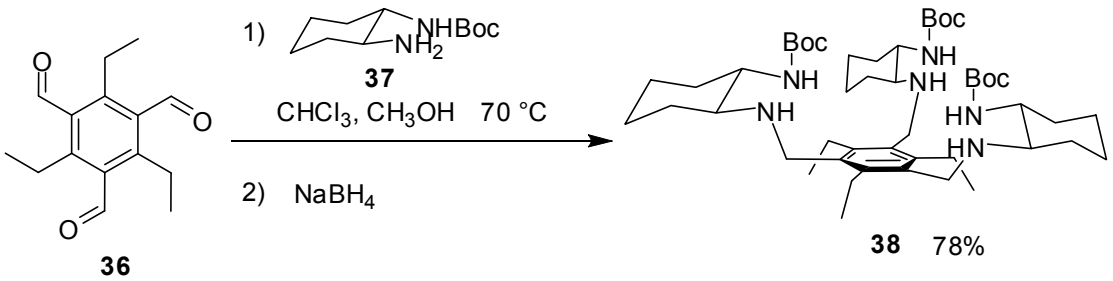

A mixture of *tert*-butoxycarbonyl-*trans*-1,2-diaminocyclohexane **37** (1.27 g, 5.93 mmol) and **36** (443 mg, 1.80 mmol) was dissolved in $CHCl_3$/CH_3OH 1:1 (16 mL) and stirred 7.5 h at 70 °C. The reaction mixture was cooled at RT and $NaBH_4$ (214 mg, 5.67 mmol) was slowly added. The solution was stirred for 1 h during which evolution of hydrogen was observed, then was poured into a

solution of water (50 mL) and Brine (50 mL) and extracted $CHCl_3$ (3 x 30 mL). The combined organic layers were washed with water (2 x 30 mL), dried over Na_2SO_4 and concentrated to give 1.68 g of crude **38** as a yellow solid, which was purified firstly by flash column chromatography on silica gel ($CHCl_3/CH_3OH/NH_3$ acq, 93:7:0.8), then by flash column chromatography on silica gel (NH_3 acq, saturated solution in $CHCl_3$) to afford pure **38** (1.19 g, 78%) as a white powder. ***R*-38**: m.p. 211-212 °C. ^{1}H-NMR ($CDCl_3$, 200 MHz): δ 4.76 (bs, 3H), 3.86-3.80 (m, 3H), 3.58-3.53 (m, 3H), 3.28-3.15 (m, 3H), 2.88- 2.69 (m, 6H), 2.46-2.38 (m, 3H), 2.23-2.16 (m, 6H), 1.75-1.65 (m, 6H), 1.41 (s, 27H), 1.30-1.20 (m, 12H + 3H), 1.24 (m, 9H). ^{13}C-NMR (50 MHz, $CDCl_3$): δ 155.76, 142.13, 134.21, 79.05, 61.20, 54.51, 44.69, 32.55, 31.38, 28.59, 24.69, 24.69, 22.66, 17.29. ***S*-38**: m.p. 203-204 °C; ^{1}H-NMR ($CDCl_3$, 200 MHz): δ 4.74 (bs, 3H), 3.86-3.80 (m, 3H), 3.58-3.53 (m, 3H), 3.28-3.15 (m, 3H), 2.88- 2.69 (m, 6H), 2.47-2.37 (m, 3H), 2.28-2.10 (m, 6H), 1.75-1.65 (m, 6H), 1.41 (s, 27H), 1.30-1.20 (m, 12H + 3H), 1.24 (m, 9H). ^{13}C-NMR (50 MHz, $CDCl_3$): δ 155.79, 142.11, 134.21, 79.06, 61.19, 54.49, 44.65, 32.55, 31.35, 28.59, 24.71, 24.71, 22.66, 17.29.

1,3,5-*tris*[methyl-(*trans*-1,2-diaminocyclohexyl)]-2,4,6-triethylbenzene (39).

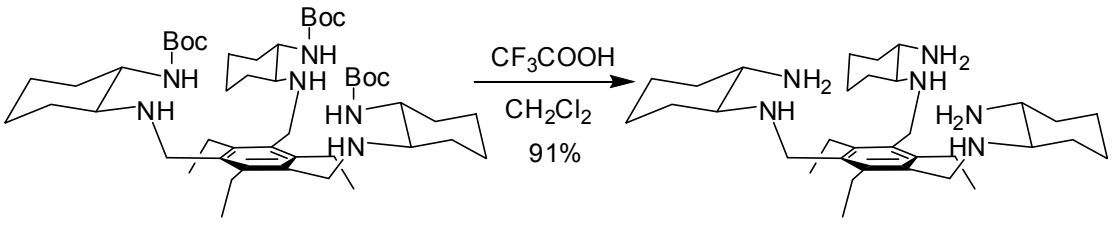

38 **39**

To a solution of **38** (1.20g, 1.43 mmol) in CH_2Cl_2 (6 mL) was slowly added trifluoroacetic acid (10.6 g, 92.7 mmol). A mild exothermic reaction occurred with gas evolution. The reaction solution was stirred for 1.5 h at RT then poured into ice water (20 mL) and cooled while a solution of KOH 50% (100 mL) was slowly added. The two phases were separeted and the water layer was extracted with CH_2Cl_2 (4 x 25 mL). The organic layers were combined, dried over Na_2SO_4, and concentrated to give pure **39** (700 mg, 91%)

as a pale yellow solid. ***R*-39**: m.p. 70-71 °C. ^{1}H-NMR ($CDCl_3$, 200 MHz): δ 3.98-3.93 (m, 3H), 3.53-3.47 (m, 3H), 3.04-2.85 (m, 3H), 2.80-2.62 (m, 3H), 2.41-2.30 (m, 6H), 2.20-2.09 (m, 3H), 1.92-1.69 (m, 9H), 1.42 (bs, 9H, H_2O + NH_2), 1.34-0.93 (m, 12H), 1.24 (m, 9H). ^{13}C-NMR (50 MHz, $CDCl_3$): δ 141.92, 134.45, 64.65, 5541, 45.06, 35.59, 31.47, 25.63, 25.28, 22.61, 17.16. $[\alpha]^{25}_D$ = -63.1 (c = 0.255). HRMS: calcd for $C_{33}H_{60}N_6$ + H^+: 541.49522; found: 541.49457. ESI-MS *m/z* (%): 541.55 (100) $[M+H]^+$. Anal. calcd for $C_{33}H_{60}N_6$ + $2H_2O$: C, 68.70; H, 11.18; N, 14.57; O, 5.55; found: C, 68.78; H, 11.93; N, 14.18. ***S*-39**: m.p. 70-71 °C. ^{1}H-NMR ($CDCl_3$, 400 MHz): δ 3.96-3.93 (m, 3H), 3.51-3.49 (m, 3H), 2.98-2.89 (m, 3H), 2.77-2.68 (m, 3H), 2.38-2.29 (m, 6H), 2.17-2.11 (m, 3H), 1.90-1.87 (m, 3H), 1.79-1.69 (m, 6H), 1.44 (bs, 9H, H_2O + NH_2), 1.35-1.21 (m, 9H), 1.24 (m, 9H), 1.03-0.97 (m, 3H). ^{13}C-NMR (50 MHz, $CDCl_3$): δ 141.89, 134.48, 64.65, 55.44, 45.06, 35.60, 31.46, 25.66, 25.30, 22.64, 17.19. $[\alpha]^{25}_D$ = +63.2 (c = 0.280). HRMS: calcd for $C_{33}H_{60}N_6$ + H^+: 541.4952; found: 541.4961. ESI-MS *m/z* (%): 541.40 (100) $[M+H]^+$. Anal. calcd for $C_{33}H_{60}N_6$ + $2H_2O$: C, 68.70; H, 11.18; N, 14.57; O, 5.55; found: C, 68.74; H, 11.63; N, 14.20.

1,3,5-*tris*[methyl-((2-pyrrolylmethyl)-*trans*-1,2-diaminocyclohexyl)]-2,4,6-triethylbenzene (34).

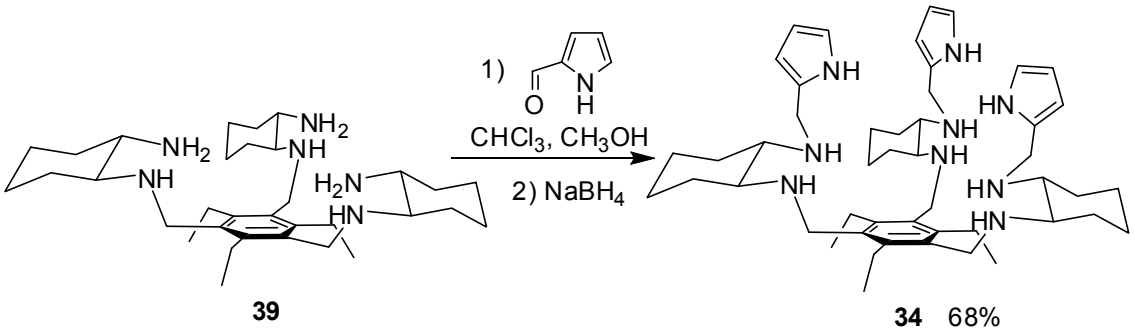

39 **34** 68%

A solution of **39** (362 mg, 0.669 mmol) and pyrrol-2-carboxaldehyde (210 mg, 2.21 mmol) in $CHCl_3$/CH_3OH 1:1 (6 mL) was stirred at RT overnight. To the reaction mixture $NaBH_4$ (96 mg, 2.54 mmol) was added. The solution was stirred for 1 h, poured on H_2O + Brine (50 mL) and extracted with $CHCl_3$ (3 x 25 mL). The organic layers were washed three times with water, dried over Na_2SO_4 and concentrated to give crude **34** as a glassy solid, that was purified by flash

column chromatography on silica gel (NH_3 33% saturated solution in $CHCl_3$) to afford pure **34** (294 mg, 68%) as a pale yellow solid. ***R*-34**: m.p. 79-80 °C. ^{1}H-NMR ($CDCl_3$, 400 MHz): δ 9.14 (bs, 3H), 6.58-6.56 (m, 3H), 6.05-6.03 (m, 3H), 5.94 (m, 3H), 3.90-3.85 (m, 6H), 3.62-3.59 (m, 3H), 3.49-3.46 (m, 3H), 2.79-2.73 (q, *J* = 7.6 Hz, 6H), 2.32-2.15 (m, 12H), 1.81-1.75 (m, 6H), 1.33-1.02 (m, 12H), 1.18 (t, *J* = 7.6 Hz, 9H). ^{13}C-NMR (50 MHz, $CDCl_3$): δ 141.80, 134.48, 131.10, 116.89, 107.65, 105.62, 62.43, 61.22, 44.93, 44.89, 31.73, 31.73, 25.33, 25.16, 22.64, 17.18. $[\alpha]^{28}_D$ = -119 (c = 0.21). HRMS: calcd for $C_{48}H_{75}N_9$ + H^+: 778.6218; found: 778.6233. ESI-MS *m/z* (%): 814.36 (11) $[M{\cdot}2H_2O+H]^+$, 778.45 (100) $[M+H]^+$. Anal. calcd for $C_{48}H_{75}N_9$ + $2H_2O$: C, 70.81; H, 9.78; N, 15.48; O, 3.93; found: C, 71.35; H, 10.10; N, 15.47. ***S*-34**: m.p. 80-81 °C. ^{1}H-NMR (CD_3CN, 400 MHz): δ 9.18 (bs, 3H), 6.57-6.55 (m, 3H), 5.96-5.94 (m, 3H), 5.86 (m, 3H), 3.87-3.79 (m, 6H), 3.58-3.55 (m, 3H), 3.49-3.46 (m, 3H), 2.84-2.71 (m, 6H), 2.30-2.11 (m, 12H + H_2O), 1.79-1.73 (m, 6H), 1.34-1.22 (m, 6H), 1.16 (t, *J* = 7.6 Hz, 9H), 1.13-1.01 (m, 6H). ^{13}C-NMR (50 MHz, $CDCl_3$): δ 141.98, 134.03, 130.41, 117.36, 107.42, 106,01, 62.19, 60.84, 44.63, 43.71, 31.50, 31.44, 25.21, 25.16, 22.78, 17.64. $[\alpha]^{28}_D$ = +121 (c = 0.280). HRMS: calcd for $C_{48}H_{75}N_9$ + H^+: 778.6218; found: 778.6218. ESI-MS *m/z* (%):814.27 (14) $[M{\cdot}2H_2O+H]^+$, 778.45 (100) $[M+H]^+$. Anal. calcd for $C_{48}H_{75}N_9$ + $2H_2O$: C, 70.81; H, 9.78; N, 15.48; O, 3.93; found: C, 71.93; H, 9.91; N, 15.50.

2-*tert*-butoxycarbonyl-2,3-diamino-2,3-dimethylbutane (43).

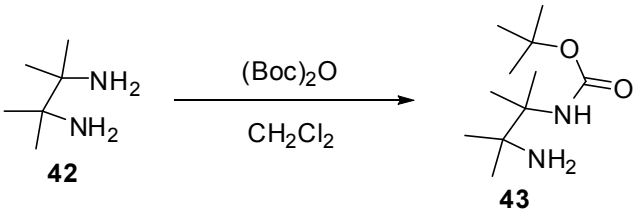

42 **43**

To a solution of **42** (3.00 g, 25.8 mmol) in CH_2Cl_2 (50 mL) was added under stirring a solution of $(Boc)_2O$ (2.82 g, 12.9 mmol) in CH_2Cl_2 (80 mL) in 2 h. The reaction mixture was stirred for 5 h at RT then filtered. The mother liquor was washed with NaOH 1 M (2 x 70 mL), dried over Na_2SO_4 and concentrated to give crude **43** as an oil, that was purified by crystallization in H_2O (10 mL).

The solid was filtered and washed several times with water. The mother liquors were poured into NaOH 1M (150 mL) and extracted with CH_2Cl_2 (3 x 50 mL). The organic layers were dried over Na_2SO_4 and concentrated to give pure **43** (2.36 g, 85%) as a white crystalline powder. M.p. 47-48°C. ^{1}H NMR (200 MHz, $CDCl_3$): δ 5.69 (bs, 1H), 1.74 (bs, 2H), 1.42 (s, 9H), 1.32 (s, 6H), 1.13 (s, 6H). ^{13}C NMR (50 MHz, $CDCl_3$): δ 155.42, 78.30, 57.47, 55.09, 28.62, 26.68, 22.05.

1,3,5-*tris*(methanylylidene(2-*tert*-butoxycarbonyl-2,3-diamino-2,3-dimethylbutane)]-2,4,6-triethylbenzene (44).

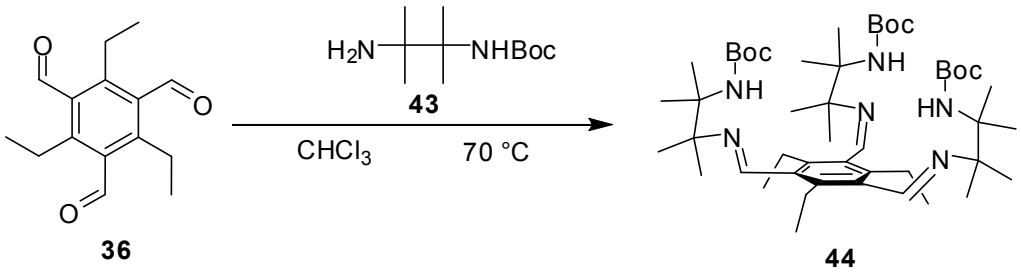

36 **44**

A solution of **43** (845 mg, 3.91 mmol) and **36** (162 mg, 0.658 mmol) in $CHCl_3$ (1.5 mL) was stirred at 70 °C for 36 h. The solution was concentrated to give crude **44**, which was purified by flash column chromatography on silica gel ($CH_3Cl/CH_3OH/NH_3$ 33% 95:5:1) to afford **44** (380 mg, 69%) as a pale yellow solid. M.p. 140-142°C. ^{1}H NMR (200 MHz, $CDCl_3$): δ 8.69 (s, 3H), 5.89 (bs, 3H,), 2.71 (q, 6H), 1.39 (bs, 45H), 1.29 (s, 18H), 1.12 (s, 9H). ^{13}C NMR (50MHz, $CDCl_3$): δ 157.46, 155.41, 141.30, 134.21, 78.20, 66.54, 58.15, 28.65, 23.31, 22.78, 22.32, 15.24.

1,3,5-*tris*(methanylylidene(2,3-diamine-2,3-dimethylbutane)]-2,4,6-triethylbenzene (45).

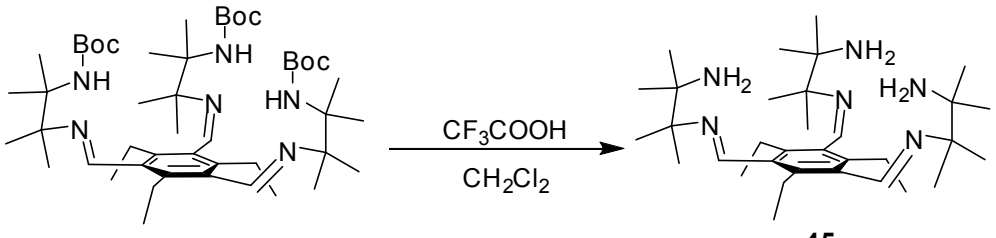

44 **45**

To a solution of **44** (260 mg, 0.309 mmol) in CH_2Cl_2 (1.5 mL), TFA (2.14 g, 18.8 mmol) was added dropwise. The solution was stirred for 3 h at RT, cooled at 0 °C and diluted with CH_2Cl_2 (8 mL). To reaction mixture sodium methoxide (1.70 g, 31.5 mmol) was added and the precipitated filtered and washed with CH_2Cl_2. The mother liquors were concentrated to give **45** (160 mg, 95%) as a pale yellow oil. Product was used without further purification for the next reaction. ^{1}H NMR (200 MHz, $CDCl_3$): δ 8.67 (s, 3H), 2.73 (q, 6H), 1.50 (bs, 6H), 1.28 (s, 18H) 1.16 (s, 18H), 1.07 (s, 9H). ^{13}C NMR (50MHz, $CDCl_3$): δ 157.18, 140.82, 134.48, 66.24, 54.83, 26.35, 23.13, 22.95, 15.22.

1,3,5-*tris*(methyl((2-pyrrolylmethyl)2,3-diamine-2,3-dimethylbutane)]-2,4,6-triethylbenzene (40).

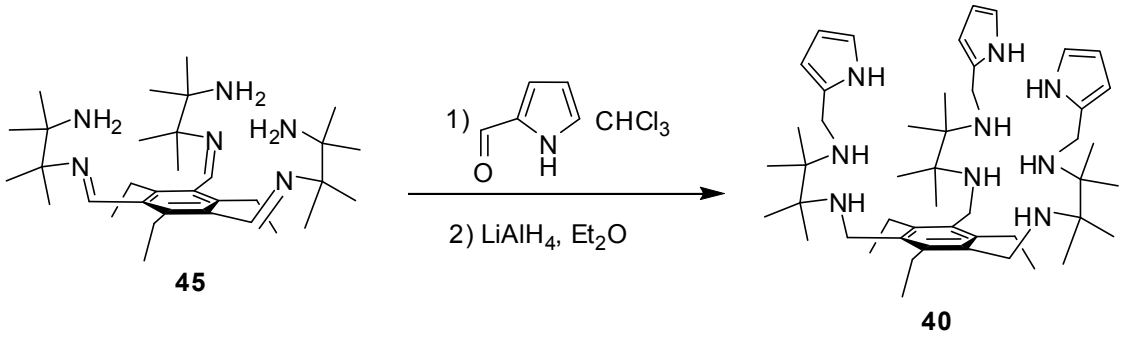

To a solution of **45** (160 mg, 0.296 mmol) in $CHCl_3$ (1.5 mL), pyrrole-2-carbaldehyde (126 mg, 1.33 mmol) was added. The reaction mixture was stirred at 70 °C for 5 days, concentrated, redissolved in dry Et_2O. (2.0 mL) and added dropwise under nitrogen atmosphere to a suspension of $LiAlH_4$ (520 mg, 13.7 mmol) in dry Et_2O (3.0 mL) at 0 °C. The reaction mixture was warmed at RT and stirred for 2.5 h, cooled again at 0 °C and diluted with Et_2O (5 mL). To the suspension were added in sequence 520 μL of H_2O, 520 μL of NaOH 15%, then 1560 μL of H_2O to obtain a powder suspension, that was filtered and washed with fresh Et_2O (50 mL). The mother liquors were washed with water (2 x 30 mL), dried over Na_2SO_4 and concentrated to give crude **40**, that was purified by flash column chromatography on silica gel (NH_3 33% saturated solution in $CHCl_3$) to afford pure **38** (74 mg, 32%) as a pale yellow solid. M.p. 83-85°C. ^{1}H NMR (200 MHz, $CDCl_3$): δ 8.69 (bs, 3H), 6.50-6.60 (m, 3H), 6.11-

6.06 (m, 3H), 5.92 (s, 3H,), 3.69-3.66 (m, 12H) 2.78 (q, 6H), 1.23 (m, 27H), 1.08 (s, 18H). ^{13}C NMR (100 MHz, $CDCl_3$): δ 142.50, 134.85, 132.46, 116.26, 107.81, 104.49, 58.86, 58.54, 40.20, 39.60, 22.12, 20.93, 20.56, 16.82.

***tert*-butyl 2-aminoethylcarbamate (47).**[81]

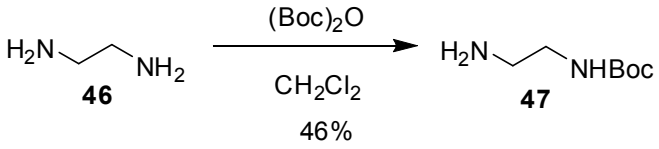

To a solution of **46** (1.10 g, 18.3 mmol) in CH_2Cl_2 (30 mL), a solution of $(Boc)_2O$ (2.00 g, 9.15 mmol) in CH_2Cl_2 (60 mL) was added under vigorous stirring in 2 h. The suspension was stirred for 5 h at RT then filtered. The mother liquors were concentrated, suspended in H_2O, filtered and washed many times with fresh water. The aqueous layers were extracted with ethyl acetate. The collected organic layers were washed with water, dried over Na_2SO_4 and concentrated to give pure **47** (670 mg, 46%) as a yellow oil. ^{1}H NMR (200 MHz, $CDCl_3$): δ 4.96 (bs, 1H), 3.20-3.11 (m, 2H), 2.81-2.75 (m, 2H), 1.50 (bs, 2H), 1.43 (s, 9H). ^{13}C NMR (50 MHz, $CDCl_3$): δ 156.08, 78.97, 43.46, 41.90, 28.48.

1,3,5-*tris*[methyl-(*tert*-butoxycarbonyl-1,2-diaminoethyl)]-2,4,6-triethylbenzene (48).

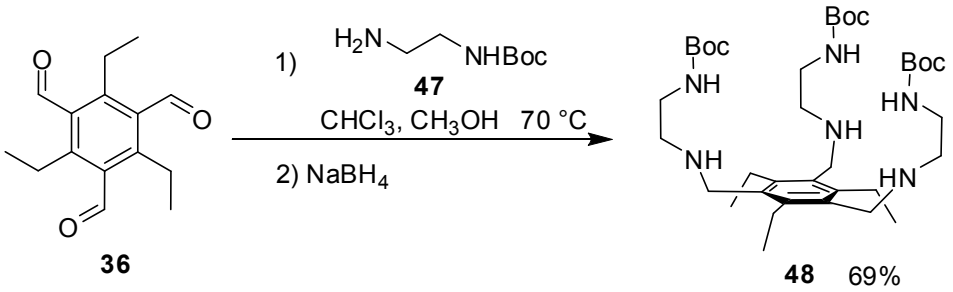

A solution of **36** (312 mg, 1.27 mmol) and **47** (670 mg, 4.18 mmol) in $CHCl_3/CH_3OH$ 1:1 (12 mL) was heated at 70 °C and stirred for 7.5 h, then cooled at RT. To the reaction mixture $NaBH_4$ (237 mg, 6.27 mmol) was added,

and the solution was stirred for 1 h at RT, then poured into water + brine and extracted with $CHCl_3$. The organic layers were washed with water, dried over Na_2SO_4 and concentrated to give crude **48**, that was purified by flash column chromatography on silica gel ($CHCl_3/CH_3OH/NH_3$ 33%, 90:10:1) to afford pure **48** (591 mg, 69%) as a white powder. M.p. 62-63 °C. ^{1}H NMR (200 MHz, $CDCl_3$): δ 5.09 (bs, 3H), 3.71 (s, 6H), 3.26-3.20 (m, 6H), 2.89-2.71 (m, 12H), 1.45 (s, 27H + 3H), 1.25-1.17 (m, 9H). ^{13}C NMR (50 MHz, $CDCl_3$): δ 155.98, 142.28, 133.59, 79.15, 49.88, 47.50, 40.23, 28.61, 23.08, 17.13.

1,3,5-*tris*[methyl-(1,2-diaminoethyl)]-2,4,6-triethylbenzene (49).

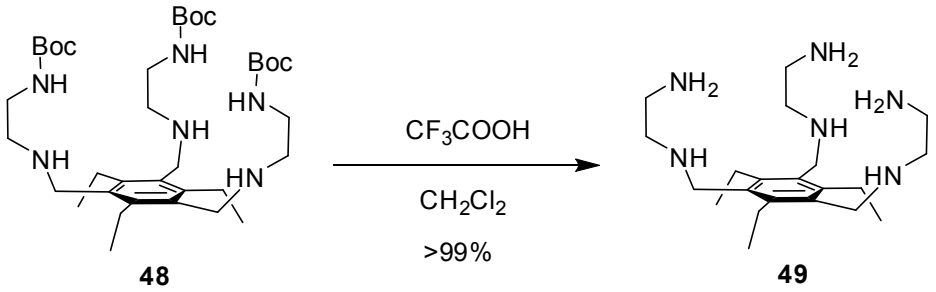

48 **49**

To a solution of **48** (591 mg, 0.870 mmol) in CH_2Cl_2 (4 mL), TFA (6.66 g, 58.4 mmol) was added. Reaction mixture was stirred at RT for 1.5 h, poured into icy water, alkalized with KOH 40% (100 mL) and extracted with CH_2Cl_2 (4 x 25 mL). The organic layers were dried over Na_2SO_4 and concentrated to give **49** (330 mg, >99%) as a pale yellow oil, that was used for next reaction without any further purification. ^{1}H NMR (200 MHz, $CDCl_3$): δ 3.71 (s, 6H), 2.86-2.75 (m, 18H), 1.27-1.93 (m, 9H).

1,3,5-*tris*[methyl-(2-(2'-pyrrolylmethyl)-1,2-diaminoethyl)]-2,4,6-triethylbenzene (41).

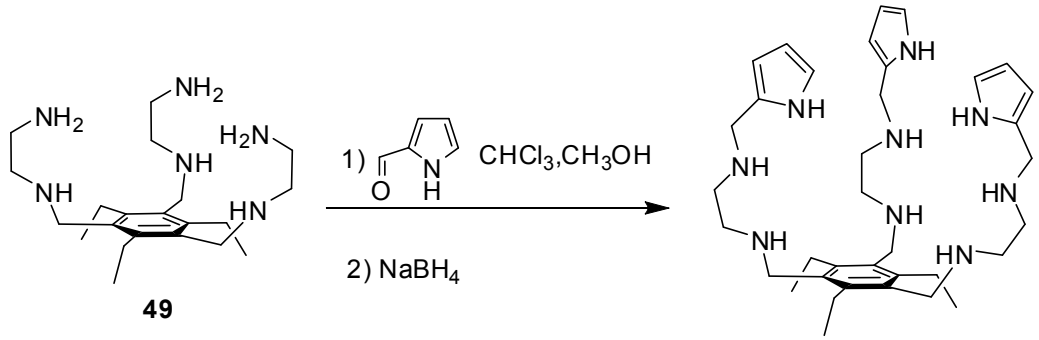

49 **41** 41%

A solution of **49** (330 mg, 0.872 mmol) and pyrrole-2-carboxaldehyde (373 mg, 3.92 mmol) in $CHCl_3/CH_3OH$ 1:1 (8 mL) was stirred for 14 h at RT, then $NaBH_4$ was added, and reaction was stirred for 1 h, poured into 50 mL of water + brine, and extracted with CH_2Cl_2 (3 x 25 mL). The organic layers were washed three times with water, dried over Na_2SO_4 and concentrated to give crude **41**, that was purified by flash column chromatography on silica gel ($CHCl_3/CH_3OH/NH_3$ 33%, 77:23:5) to afford pure **41** (220 mg, 41%) as a white powder. M.p. 47-48 °C. ^{1}H NMR (400 MHz, CD_3CN): δ 9.23 (bs, 3H), 6.65-6.63 (m, 3H), 6.00-5.98 (m, 3H), 5.92-5.90 (m, 3H), 3.70 (s, 6H), 3.68 (s, 6H), 2.82-2.76 (m, 12H), 2.70-2.67 (m, 6H), 2.18 (NH + H_2O), 1.19-1.16 (m, 9H). ^{13}C NMR (50 MHz, $CDCl_3$): δ 141.95, 133.95, 129.97, 117.36, 107.82, 106.39, 49.73, 48.65, 47.62, 46.32, 22.95, 17.10. ESI-MS *m/z* (%): 616.25 (100) $[M+H]^+$, 1230.50 (25) $[M+M+H]^+$. Anal. calcd for $C_{36}H_{57}N_9$ + $3H_2O$: C, 64.54; H, 9.48; N, 18.82; O, 7.16; found: C, 64.64; H, 9.08; N, 18.42.

Hexamino Pyrrolic Tripodal Compound (51).

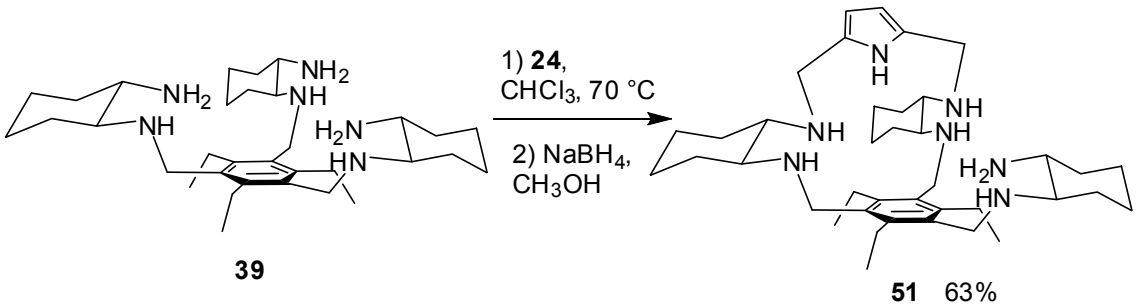

39 **51** 63%

A mixture of **39** (850 mg, 1.57 mmol) and **24** (174 mg, 1.41 mmol) was dissolved in $CHCl_3$ (30 mL). The solution was stirred at reflux overnight. The reaction mixture was cooled at RT and freshly suspended $NaBH_4$ (234 mg, 6.20 mmol) in CH_3OH was added. The solution was stirred for 1 h during which evolution of hydrogen was observed, then was poured into water (100 mL) and Brine (50 mL) and extracted $CHCl_3$ (3 x 50 mL). The combined organic layers were washed with water (3 x 50 mL), dried over Na_2SO_4 and concentrated to give 1.37 g of crude **51** as a yellow solid, which was purified by flash column chromatography on silica gel ($CHCl_3$/CH_3OH/NH_3 acq, 88:12:1.8) to afford pure **51** (560 mg, 63%) as a pale yellow solid. ***R*-51**: m.p. 162-164 °C. ^{1}H-NMR ($CDCl_3$, 400 MHz): δ 8.87 (bs, 1H), 5.84 (s, 2H), 4.01-3.90 (m, 4H), 3.75-3.67 (m, 2H), 3.56-3.39 (m, 4H), 3.15-3.10 (m, 1H), 2.94-2.83 (m, 5H), 2.62-2.60 (m, 1H), 2.39-0.85 (m, 45H). ^{13}C-NMR (50 MHz, $CDCl_3$): δ 141.93, 141.93, 141.22, 134.48, 134.45, 134.45, 130.95, 129.99, 105.38, 104.84, 64.18, 64.12, 60.84, 60.09, 57.71, 55.51, 45.98, 45.04, 44.37, 43.86, 40.00, 35.42, 32.13, 31.76, 31.72, 31.52, 30.55, 25.72, 25.69, 25.54, 25.46, 25.25, 24.95, 22.68, 22.58, 22.49, 17.44, 17.06, 16.88. $[\alpha]^{26}_D$ = -84.2 (c = 0.120). HRMS: calcd for $C_{39}H_{65}N_7$ + H^+: 632.5374; found: 632,5375. ESI-MS *m/z* (%):632.54 (100) $[M+H]^+$, 316.77 (72) $[M+2H]^+$. Anal. calcd for $C_{39}H_{65}N_7$ + $3H_2O$: C, 68.28; H, 10.43; N, 14.29; O, 7.00; found: C, 68.32; H, 10.25; N, 14.08. ***S*-51**: m.p. 161-163 °C. ^{1}H-NMR (CD_3CN, 400 MHz): δ 9.07 (bs, 1H), 5.74 (s, 2H), 3.94-3.86 (m, 4H), 3.74-3.64 (m, 2H), 3.50-3.33 (m, 4H), 3.22-3.15 (m, 1H), 2.89-2.74 (m, 5H), 2.60-2.55 (m, 1H), 2.36-1.70 (m, 24H), 1.50-0.95 (m, 21H). ^{13}C-NMR (100 MHz, $CDCl_3$): δ 141.89, 141.98, 141.11, 134.54, 134.54, 134.48, 130.92, 130.17, 105.32, 104.81, 64.40, 64.13, 60.85, 60.17, 57.71, 55.53, 46.03, 45.16, 44.39, 43.95, 39.99, 35.54, 32.16, 31.88, 31.87, 31.49, 30.59, 25.79, 25.72, 25.59, 25.48, 25.28, 24.95, 22.68, 22.56, 22.48, 17.47, 17.09, 16.88. $[\alpha]^{26}_D$ = +81.1 (c = 0.09). HRMS: calcd for $C_{39}H_{65}N_7$ + H^+: 632.5374; found: 632.5368. ESI-MS *m/z* (%): 668.51 (47) $[M{\cdot}H_2O+H]^+$, 632.54 (100) $[M+H]^+$. Anal. calcd for $C_{39}H_{65}N_7$ + $2H_2O$ + 1/2 $CHCl_3$: C, 65.19; H, 9.63; N, 13.47; O, 4.40; found: C, 64.85; H, 9.84; N, 13.25.

Hexamino Dipyrrolic Tripodal Receptor (52).

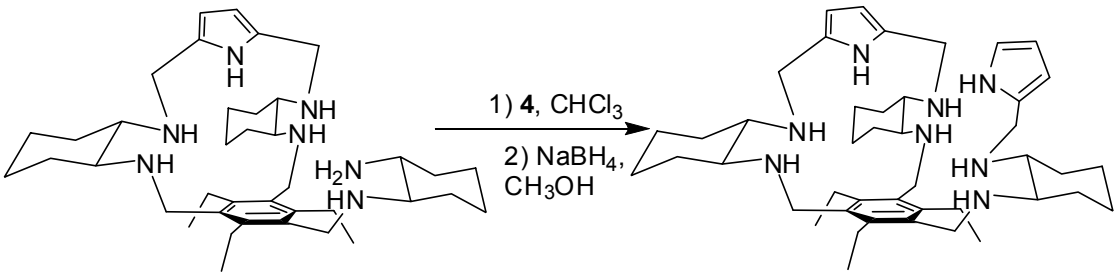

51 **52** 50%

A mixture of **51** (515 mg, 0.815 mmol) and **4** (137 mg, 1.44 mmol) was dissolved in $CHCl_3$ (20 mL) and stirred at RT overnight. To the reaction mixture was added freshly suspended $NaBH_4$ (68 mg, 2.33 mmol) in CH_3OH. The solution was stirred for 1 h during which evolution of hydrogen was observed, then was poured into water (100 mL) and Brine (50 mL) and extracted $CHCl_3$ (3x50 mL). The combined organic layers were washed with water (3x50 mL), dried over Na_2SO_4 and concentrated to give 600 mg of crude **52** as a yellow solid, which was purified by flash column chromatography on silica gel ($CHCl_3/CH_3OH/NH_3$ acq, 93:7:1) to afford analytical pure **52** (290 mg, 50%) as a pale yellow solid. ***R*-52**: m.p. 170 °C (dec). ^{1}H-NMR (CD_3CN, 400 MHz): δ 9.72 (bs, 1H), 9.28 (bs, 1H), 6.61-6.58 (m, 1H), 5.96-5.93 (m, 1H), 5.88-5.87 (m, 1H), 5.76-5.73 (m, 2H), 3.95-3.80 (m, 5H), 3.76-3.67 (m, 2H), 3.58-3.33 (m, 5H), 3.22-3.14 (m, 1H), 2.88-2.71 (m, 5H), 2.61-2.55 (m, 1H), 2.39-1.68 (m, 24H +H_2O), 1.49-0.98 (m, 21H). ^{13}C-NMR (50 MHz, $CDCl_3$): δ 141.98, 141.86, 141.23, 134.47, 134.34, 134.23, 131.01, 130.90, 130.11, 117.14, 107.41, 105.88, 105.36, 104.91, 63.95, 61.93, 61.17, 60.97, 60.02, 57.91, 45.78, 44.90, 44.43, 43.88, 43.84, 40.11, 32.16, 32.01, 31.78, 31.71, 31.44, 30.67, 25.75, 25.53, 25.51, 25.42, 24.92, 24.01, 22.78, 22.48, 22.46, 17.42, 17.04, 16.92. $[\alpha]^{25}_D$ = -96.0 (c = 0.175). HRMS: calcd for $C_{44}H_{70}N_8$ + H^+: 711,5796; found: 711.5796. ESI-MS *m/z* (%):711.58 (100) $[M+H]^+$. Anal. calcd for $C_{44}H_{70}N_8$ + $3H_2O$: C, 69.07; H, 10.01; N, 14.65; O, 6.27; found: C, 69.00; H, 9.75; N, 14.34. ***S*-52**: m.p. 170 °C (dec). ^{1}H-NMR (CD_3CN, 900 MHz): δ 9.40 (bs, 1H), 9.08 (bs, 1H), 6.58-6.59 (m, 1H), 5.95-5.94 (m, 1H), 5.86-5.85 (m, 1H), 5.75-5.73 (m, 2H), 3.94-3.90 (m, 2H), 3.87-3.85 (m, 2H), 3.81-3.80 (m, 1H), 3.73-3.65 (m,

2H), 3.56-3.54 (m, 1H), 3.50-3.48 (m, 1H), 3.46-3.45 (m, 1H), 3.42-3.41 (m, 1H), 3.34-3.33 (m, 1H), 3.22-3.18 (m, 1H), 2.90-2.73 (m, 5H), 2.60-2.56 (m, 1H), 2.35-1.72 (m, 23H+H_2O), 1.49-1.46 (m, 1H), 1.33-0.95 (m, 20H). ^{13}C-NMR (100 MHz, $CDCl_3$): δ 142.08, 141.91, 141.19, 134.74, 134.62, 134.50, 131.10, 130.99, 130.28, 116.93, 107.63, 105.67, 105.32, 104.79, 63.93, 61.92, 61.35, 60.79, 60.14, 57.51, 45.81, 44.93, 44.28, 43.85, 43.84, 39.77, 32.02, 31.99, 31.76, 31.57, 31.45, 30.37, 25.65, 25.44, 25.31, 25.30, 24.82, 22.74, 22.56, 22.32, 22.29, 17.34, 16.88, 16.68. $[\alpha]^{23}_D$ = +93.5 (c = 0.200). HRMS: calcd for $C_{44}H_{70}N_8$ + H^+: 711,5796; found: 711.5798. ESI-MS *m/z* (%):711.58 (100) $[M+H]^+$. Anal. calcd for $C_{44}H_{70}N_8$ + $2H_2O$: C, 70.74; H, 9.98; N, 15.00; O, 4.28; found: C, 70.27; H, 10.20; N, 14.26.

Titrations and Data Analysis.

Titrations were performed in 5 mm NMR tubes using Hamilton microsyringes, following a previously described technique.[28] To avoid interference of traces of acid in solution, $CDCl_3$ and CD_3CN were additionally treated by eluting through a short column of alumina right before use. Mathematical analysis of data and graphic presentation of results was performed using the HypNMR 2006 program,[82] handling general host-guest association equilibria under fast exchange regime on the NMR time scale. Calculation and refinement of cumulative binding constants β_i from the set of binding isotherms was achieved by simultaneous fit of all the available signals to the general expression for the observed chemical shift δ of a nucleus under fast exchange conditions, which is the weighted average of the shifts δ_i of the nucleus in all the species present at equilibrium:

$$\delta = \sum_i f_i \delta_i$$

where

$$f_i = \frac{x_i C_i}{T_X}$$

with T_x standing for the total concentration of the reagent containing the nucleus, x_i for the stoichiometric coefficient of the reagent in the *i*-th species and C_i its equilibrium concentration. The mass balance equation for each reagent, expressed as a function of cumulative binding constants β_i provides a system

$$T_A = [A] + \sum_i a_i C_i = [A] + \sum_i a_i \beta_i [A]^{a_i} [B]^{b_i} ...$$

$$T_B = [B] + \sum_i b_i C_i = [B] + \sum_i b_i \beta_i [A]^{a_i} [B]^{b_i} ...$$

.....

of *n* equations which can be solved for the *n* unknown reagent concentrations. The program performs simultaneous fit of multiple signals to models involving multiple equilibria through a Gauss-Newton-Marquardt least-squares fitting of the experimental data by minimizing the error square sum

$$U = \sum_i w_i (\delta_i^{obs} - \delta_i^{calcd})^2$$

U, where w_i represents the statistical weight assigned to each observed point, δ_i^{obs} and δ_i^{calcd} are the *i*-th observed and calculated chemical shifts,

respectively. The refinement process yields best-fit values for equilibrium constants β_i and individual chemical shifts δ_i for each nucleus in each chemical species. BC_{50} values and species distributions were computed from log β_i values using the "BC_{50} Calculator" program[27].

Experimental result, data analysis and titration plots are reported hereafter for a selection of binding studies.

Numbering scheme of the signals monitored in the titration experiments:

Receptor (R)

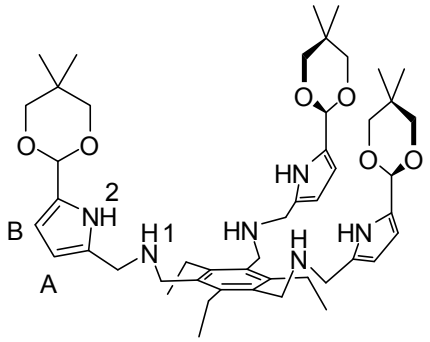

28

Glycoside (G)

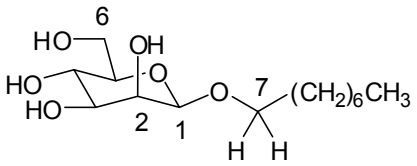

OctαMan

OctβMan

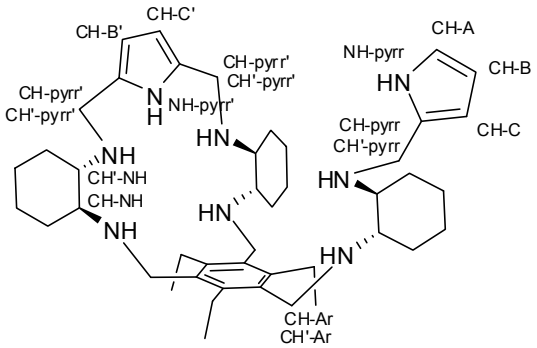

***S*-52** ***R*-52**

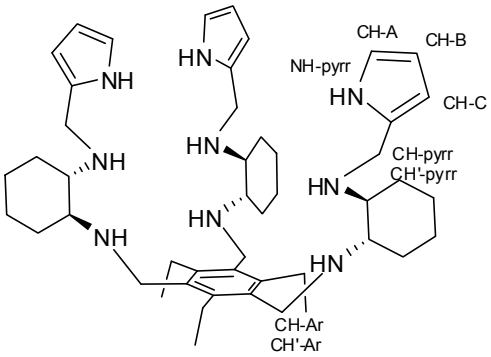

***S*-34** ***R*-34**

28 + OctαMan in CD_3CN (400 MHz)

Data Table

R = **28** G = OctαMan [G] = 1.22E-03 mol L^{-1}

R mol L^{-1}	CH-1 G	CH-7 G	CH-4 G	CH-5 G	NH-2 R	CH(acet) R
0.00E+00	4.7092	3.6707	3.5075	3.4444	-	-
1.06E-03	4.6747	3.6571	3.3366	-	9.2675	5.4173
1.47E-03	4.6638	-	3.2844	-	9.2651	5.4173
2.03E-03	4.6502	-	3.2184	3.3901	9.2621	5.4172
2.66E-03	4.6371	-	3.1545	3.3694	9.2586	5.4171
3.28E-03	4.6256	-	3.0986	3.3515	9.2563	5.4170
3.78E-03	4.6175	-	3.0590	-	9.2531	5.4169
4.36E-03	4.6089	-	3.0168	3.3334	9.2509	5.4168
5.04E-03	4.5999	-	2.9733	-	9.2488	5.4167
5.66E-03	4.5925	-	2.9369	3.3156	9.2462	5.4166
6.36E-03	4.5850	-	2.9005	3.3084	9.2446	5.4165
7.14E-03	4.5774	3.5783	2.8640	3.2993	9.2421	5.4163
8.02E-03	4.5699	3.5732	2.8269	3.2921	9.2396	5.4161
9.01E-03	4.5625	3.5678	2.7911	3.2836	9.2370	5.4159
1.01E-02	4.5549	3.5627	2.7549	3.2753	9.2349	5.4156
1.14E-02	4.5479	3.5580	2.7198	3.2679	9.2334	5.4154
1.28E-02	4.5409	3.5531	-	3.2601	9.2317	5.4152
1.43E-02	4.5342	3.5485	-	3.2527	9.2300	5.4148
1.61E-02	4.5277	3.5441	2.6209	3.2458	9.2284	5.4144
1.81E-02	4.5214	3.5397	2.5900	3.2388	9.2271	5.4141

Results page

```
 no. of spectra            20
 no. of resonance values  100
 no. of resonant nuclei     6

   sigma = 0.00133020653         RMS weighted residual = 0.00124073405

       stoich            value   relative    log    standard
       coeff                     std devn    beta   deviation

 Beta  1  1 refined  1.7095E+002  0.0062    2.2329   0.0027

 Individual chemical shifts

        +
                     R                          G
 ============================================================
        +        value    error         value    error
CH-1    +                                4.7083   0.0007
CH-7    +                                3.6707   0.0013
CH-4    +                                3.5015   0.0010
CH-5    +                                3.4444   0.0010
NH-2    +       9.2054   0.0011
CH(acet +       5.4133   0.0010
        +
                   1,1
 ================================
        +        value    error
CH-1    +       4.4589   0.0010
CH-7    +       3.4954   0.0010
CH-4    +       2.2856   0.0026
CH-5    +       3.1695   0.0011
NH-2    +       9.6137   0.0099
CH(acet +       5.4431   0.0089
```

Titration Plots

Experimental (symbols) and calculated (lines) chemical shifts
(Only the glycoside signals are shown)

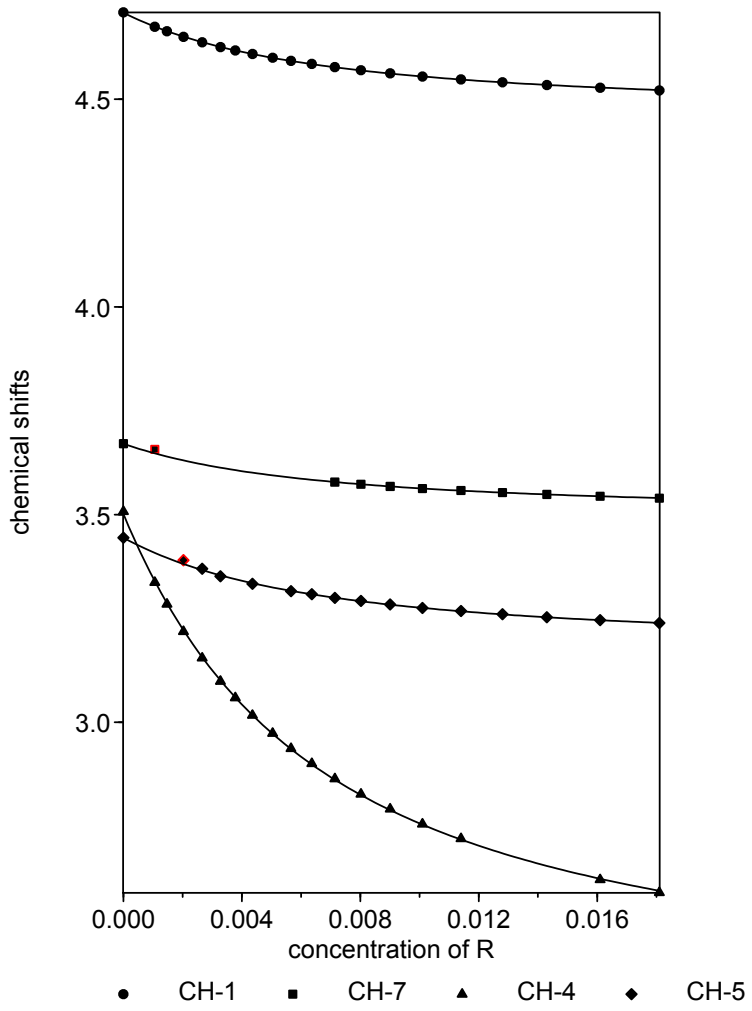

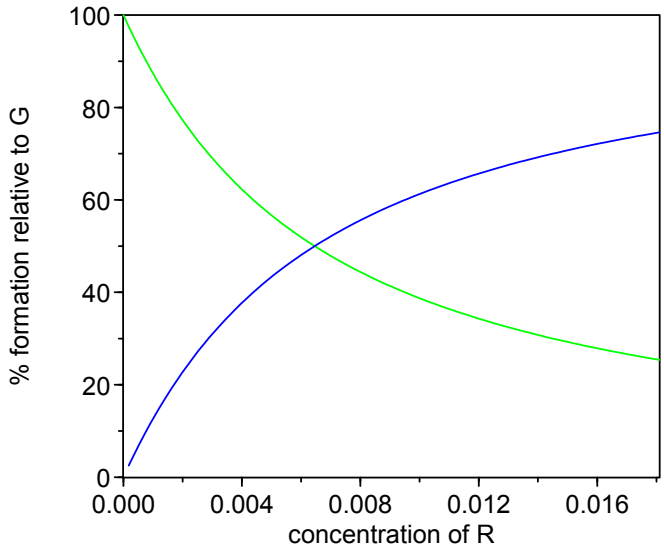

28 + OctβMan in CD_3CN (900 MHz)

Data Table

R = **28** G = OctβMan [G] = 1.01E-03 mol L^{-1}

R mol L^{-1}	CH-1 G	CH-2 G	CH-6 G	CH-7' G	CH-4 G	CH-3 G	CH-5 G	CH2-8 G
0.00E+00	4.4535	3.7556	3.7410	3.4918	3.4140	3.3466	3.1260	1.5633
2.25E-04	4.4433	3.7670	3.7118	3.4979	-	3.3290	3.0941	1.5597
3.12E-04	4.4398	3.7705	3.7022	3.5001	3.2088	3.3229	3.0835	1.5585
4.27E-04	4.4353	3.7746	3.6902	3.5028	3.1455	3.3154	3.0705	1.5571
5.79E-04	4.4301	3.7794	3.6758	3.5059	-	3.3065	-	1.5553
7.75E-04	4.4241	3.7846	3.6590	3.5097	2.9839	3.2961	3.0372	1.5532
1.03E-03	4.4173	3.7902	3.6405	3.5142	2.8852	3.2847	3.0168	1.5508
1.34E-03	4.4104	3.7950	-	3.5192	2.7820	3.2729	2.9961	1.5484
1.73E-03	4.4038	3.7997	-	3.5245	2.6796	3.2614	2.9754	1.5461
2.22E-03	4.3978	-	-	3.5300	2.5835	3.2506	2.9568	1.5446
2.80E-03	4.3930	-	-	3.5354	-	3.2421	2.9414	-
3.48E-03	4.3897	3.8019	-	3.5403	2.4344	3.2348	2.9296	1.5412
4.29E-03	4.3872	-	-	-	-	3.2296	2.9209	-
5.21E-03	4.3858	3.7952	-	3.5446	2.3407	3.2262	2.9152	1.5408
6.26E-03	4.3847	-	-	-	-	3.2235	2.9110	-
7.42E-03	4.3844	3.7910	-	3.5440	2.2968	3.2222	2.9088	1.5409
8.67E-03	4.3843	3.7906	-	3.5547	2.2805	3.2210	2.9072	1.5409
1.00E-02	4.3843	3.7903	-	3.5573	2.2697	3.2205	2.9059	1.5404

R mol L^{-1}	NH-2 R	CH-A R	CH-B R	CH(acet) R	CH3(acet) R	CH3(Et) R	CH3(acet) R
0.00E+00	-	-	-	-	-	-	-
2.25E-04	9.5497	6.0083	5.9575	5.3984	1.2059	0.9923	0.7439
3.12E-04	9.5459	6.0080	-	5.3986	1.2066	0.9927	0.7444
4.27E-04	9.5397	6.0078	-	5.3989	1.2074	0.9932	0.7449
5.79E-04	9.5332	6.0076	-	5.3991	1.2084	0.9938	0.7455
7.75E-04	9.5242	6.0073	5.9557	5.3994	1.2096	0.9949	0.7462
1.03E-03	9.5126	6.0072	5.9552	5.3997	1.2110	0.9966	0.7471
1.34E-03	9.5015	6.0068	5.9544	5.4000	1.2125	0.9986	0.7481
1.73E-03	9.4905	6.0066	5.9535	5.4004	1.2142	1.0010	0.7492
2.22E-03	9.4777	6.0063	5.9521	5.4007	1.2159	1.0039	0.7503
2.80E-03	9.4642	6.0058	5.9507	5.4009	1.2176	1.0068	0.7514
3.48E-03	9.4501	6.0055	5.9491	5.4011	1.2193	1.0098	0.7525
4.29E-03	9.4360	6.0051	5.9475	5.4012	1.2208	1.0123	0.7534
5.21E-03	9.4277	6.0046	5.9459	5.4011	1.2221	1.0146	0.7541
6.26E-03	9.4159	6.0043	5.9445	5.4010	1.2231	1.0163	0.7547
7.42E-03	9.4092	6.0040	5.9434	5.4008	1.2240	1.0177	0.7552
8.67E-03	9.4034	6.0037	5.9425	5.4006	1.2247	1.0190	0.7555
1.00E-02	9.4008	6.0035	5.9416	5.4003	1.2252	1.0195	0.7558

Results page

```
no. of spectra            18
no. of resonance values  230
no. of resonant nuclei    15

   sigma =    0.0010          RMS weighted residual =   0.00087741046

       stoich            value   relative    log    standard
       coeff                     std devn    beta   deviation

 Beta  1  1 refined   1.3072E+03  0.0472    3.1163   0.0205
 Beta  2  1 refined   2.5256E+05  0.1989    5.4024   0.0864

 Individual chemical shifts

        +
                     R                         G
 ========================================================
        +        value    error          value    error
CH-1    +                                 4.4534   0.0006
CH-2    +                                 3.7572   0.0007
CH-6    +                                 3.7407   0.0009
CH-7'   +                                 3.4919   0.0006
CH-4    +                                 3.4078   0.0008
CH-3    +                                 3.3460   0.0006
CH-5    +                                 3.1246   0.0006
CH2-8   +                                 1.5632   0.0006
NH-2    +       9.3593   0.0025
CH-A    +       6.0015   0.0022
CH-B    +       5.9318   0.0024
CH(acet +       5.3978   0.0022
CH3(ace +       1.2288   0.0022
CH3(Et) +       1.0312   0.0022
CH3(ace +       0.7575   0.0022
        +
                   1,1                       2,1
 ========================================================
        +        value    error          value    error
CH-1    +       4.3690   0.0019          4.3900   0.0023
CH-2    +       3.8389   0.0016          3.7581   0.0053
CH-6    +       3.5005   0.0084          3.6354   0.0700
CH-7'   +       3.5406   0.0020          3.5708   0.0021
CH-4    +       2.2115   0.0258          2.2428   0.0099
CH-3    +       3.2046   0.0030          3.2234   0.0025
CH-5    +       2.8747   0.0049          2.9137   0.0041
CH2-8   +       1.5341   0.0015          1.5437   0.0017
NH-2    +       9.7112   0.0082          9.5771   0.0138
CH-A    +       6.0134   0.0014          6.0146   0.0106
CH-B    +       5.9781   0.0022          5.9969   0.0136
CH(acet +       5.3982   0.0014          5.4193   0.0112
CH3(ace +       1.1863   0.0016          1.2118   0.0106
CH3(Et) +       0.9583   0.0024          0.9641   0.0120
CH3(ace +       0.7321   0.0014          0.7516   0.0106
```

Titration Plots

Experimental (symbols) and calculated (lines) chemical shifts
(Only the glycoside signals are shown)

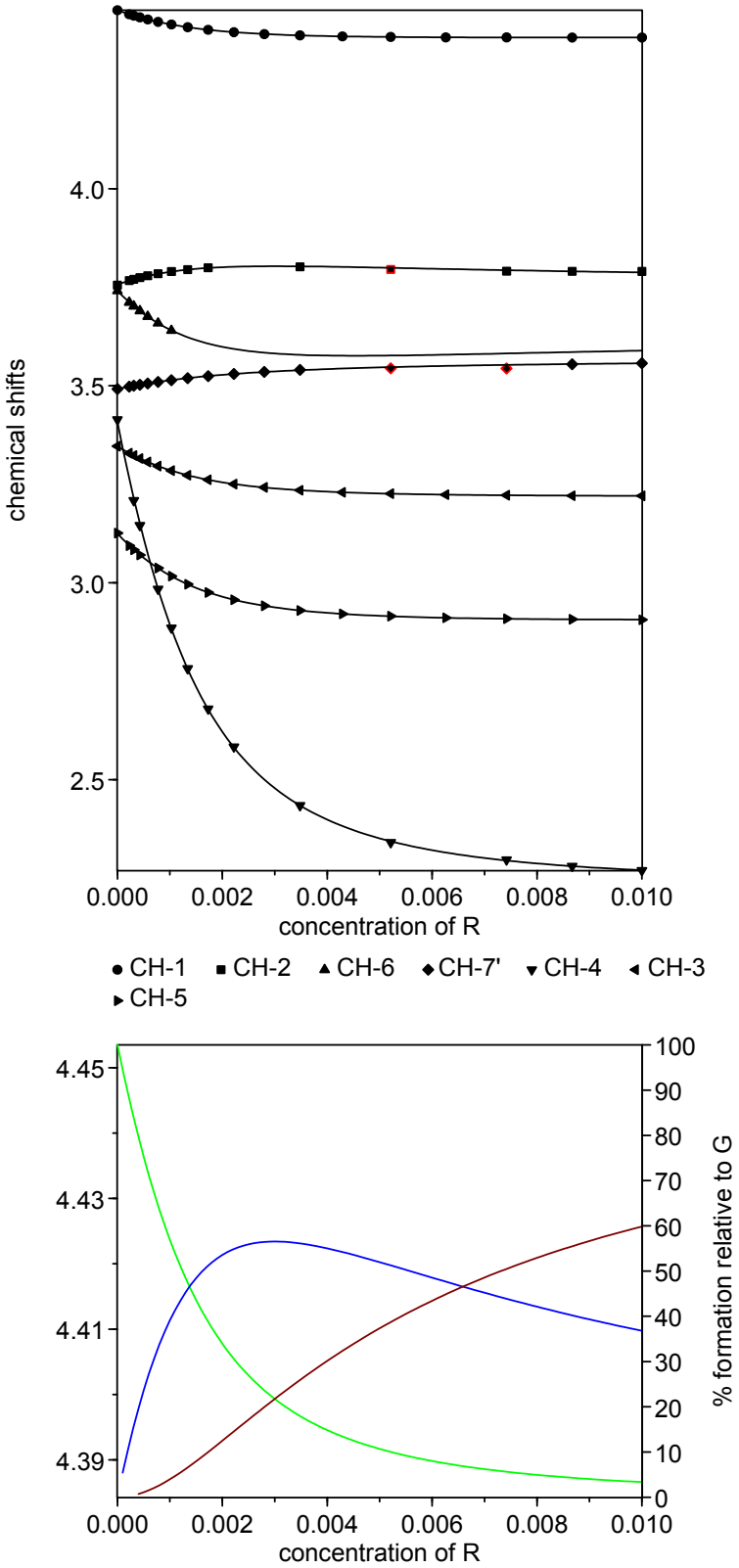

R-52 + OctαMan (CD_3CN, 298 K, 400 MHz)

Titration Data Table

R = ***R*-52** G = **OctαMan** [G] = 1.09 10^{-3} mol L^{-1}

R mol L^{-1}	G mol L^{-1}	CH-1 G	CH-2 G	CH-7 G	CH-3 G	CH-4 G	CH-7' G
0.00E+00	1.09E-03	4.7084	3.7179	3.6817	3.5773	3.5084	3.4105
4.01E-04	1.09E-03	4.6492	3.6872	3.6334	3.5020	3.2587	3.3612
5.01E-04	1.09E-03	4.6366	3.6805	3.6237	3.4865	3.2056	3.3505
6.00E-04	1.09E-03	4.6246	3.6746	3.6139	3.4708	3.1556	3.3407
8.01E-04	1.09E-03	4.6036	3.6637	3.5966	3.4436	3.0668	3.3231
1.00E-03	1.09E-03	4.5852	3.6542	3.5819	3.4191	2.9891	3.3079
1.25E-03	1.09E-03	4.5653	3.6453	3.5659	3.3935	2.9055	3.2907
1.50E-03	1.09E-03	4.5494	3.6361	-	3.3726	-	3.2773
1.80E-03	1.09E-03	4.5346	3.6292	3.5412	-	-	3.2651
2.11E-03	1.09E-03	4.5224	3.6204	3.5309	3.3383	2.7248	3.2550
2.41E-03	1.09E-03	4.5128	3.6168	-	-	2.6833	3.2468
2.70E-03	1.09E-03	4.5052	3.6122	3.5090	3.3122	2.6517	3.2404
3.10E-03	1.09E-03	4.4972	3.6102	-	3.3061	2.6174	3.2337
3.50E-03	1.09E-03	4.4909	3.6086	-	3.2989	2.5909	3.2282
3.89E-03	1.09E-03	4.4858	3.6047	-	3.2917	2.5697	3.2244
4.42E-03	1.09E-03	4.4806	3.6020	-	3.2850	2.5476	3.2196
4.88E-03	1.09E-03	4.4771	3.6003	-	3.2801	2.5326	3.2164
5.50E-03	1.09E-03	4.4732	3.5983	-	3.2759	2.5158	-
6.11E-03	1.09E-03	4.4704	3.5970	-	3.2726	2.5028	-
6.79E-03	1.09E-03	4.4676	3.5955	-	3.2700	2.4910	3.2087
7.50E-03	1.09E-03	4.4653	3.5948	-	3.2672	2.4813	3.2064
8.34E-03	1.09E-03	4.4632	3.5938	-	3.2649	2.4715	-
9.20E-03	1.09E-03	4.4612	3.5929	-	3.2634	2.4638	-

R mol L^{-1}	G mol L^{-1}	NH-Pyrr R	NH-Pyrr' R	CH-A R	CH-B R	CH-Pyrr R	CH-NH R	CH'-NH R
0.00E+00	1.09E-03	-	-	-	-	-	-	-
4.01E-04	1.09E-03	10.2474	9.9109	6.6504	5.9069	3.9593	2.6824	2.5370
5.01E-04	1.09E-03	10.2296	9.8938	6.6492	5.9058	3.9566	2.6792	2.5327
6.00E-04	1.09E-03	10.2115	9.8744	6.6479	5.9046	3.9534	2.6764	2.5284
8.01E-04	1.09E-03	10.1752	9.8386	6.6452	5.9022	3.9473	2.6708	2.5190
1.00E-03	1.09E-03	10.1393	9.8012	6.6426	5.9007	3.9412	2.6645	2.5097
1.25E-03	1.09E-03	10.0931	9.7545	6.6394	5.8980	3.9336	2.6573	2.4987
1.50E-03	1.09E-03	10.0504	9.7123	6.6364	5.8961	3.9265	2.6507	2.4886
1.80E-03	1.09E-03	10.0027	9.6643	6.6330	5.8936	3.9186	2.6437	2.4765
2.11E-03	1.09E-03	9.9582	9.6197	6.6300	5.8912	3.9117	2.6368	2.4659
2.41E-03	1.09E-03	9.9173	6.5797	6.6271	5.8893	3.9050	2.6311	2.4557
2.70E-03	1.09E-03	9.8834	9.5450	6.6247	5.8874	3.8993	-	2.4475
3.10E-03	1.09E-03	9.8398	9.5021	6.6217	5.8849	3.8923	-	2.4372
3.50E-03	1.09E-03	9.8055	9.4670	6.6192	5.8833	3.8872	-	2.4290
3.89E-03	1.09E-03	9.7728	9.4366	6.6170	5.8817	3.8824	2.6094	2.4219
4.42E-03	1.09E-03	9.7391	9.4014	6.6147	5.8801	3.8767	2.6046	2.4137
4.88E-03	1.09E-03	9.7132	9.3758	6.6128	5.8788	3.8719	2.6013	2.4080
5.50E-03	1.09E-03	9.6844	9.3468	6.6106	5.8774	3.8689	2.5968	2.4008
6.11E-03	1.09E-03	9.6598	9.3227	6.6092	5.8768	3.8643	2.5935	2.3954
6.79E-03	1.09E-03	9.6362	9.2989	6.6076	5.8754	3.8605	2.5910	2.3900
7.50E-03	1.09E-03	9.6161	9.2783	6.6061	5.8744	3.8572	2.5880	2.3855
8.34E-03	1.09E-03	9.5951	9.2564	6.6045	5.8732	3.8542	2.5856	2.3809
9.20E-03	1.09E-03	9.5788	9.2389	6.6030	5.8722	3.8516	2.5832	2.3765

Results page

```
 no. of spectra            23
 no. of resonance values  266
 no. of resonant nuclei    13

Chi-squared = 108.62

   Sigma = 0.00079618583        RMS weighted residual = 0.00073225928

       stoich            value   relative    log    standard
       coeff                      std devn    beta   deviation

 Beta  1  1 refined  3.0760E+003  0.0231    3.4880   0.0100  (  RG  )
 Beta  2  1 refined  8.7900E+005  0.0570    5.9440   0.0248  ( R2G )

 Individual chemical shifts

                     R                          G
 ========================================================
        +        value    error          value    error
CH-1    +                                 4.7074   0.0006
CH-2    +                                 3.7174   0.0006
CH-7    +                                 3.6812   0.0007
CH-3    +                                 3.5776   0.0006
CH-4    +                                 3.5038   0.0006
CH-7'   +                                 3.4097   0.0006
NH-Pyrr +       9.3674   0.0025
NH-Pyrr +       9.0297   0.0025
CH-A    +       6.5886   0.0014
CH-B    +       5.8632   0.0013
CH-Pyrr +       3.8202   0.0014
CH-NH   +       2.5573   0.0015
CH'-NH  +       2.3306   0.0014
        +
                   1,1                        2,1
 ========================================================
        +        value    error          value    error
CH-1    +       4.4863   0.0016          4.4442   0.0008
CH-2    +       3.6027   0.0010          3.5858   0.0008
CH-7    +       3.4999   0.0022          3.4778   0.0078
CH-3    +       3.2899   0.0020          3.2424   0.0009
CH-4    +       2.5734   0.0061          2.3905   0.0016
CH-7'   +       3.2251   0.0014          3.1882   0.0011
NH-Pyrr +      10.5920   0.0080         10.3974   0.0145
NH-Pyrr +      10.2555   0.0080         10.0574   0.0144
CH-A    +       6.6745   0.0008          6.6604   0.0047
CH-B    +       5.9240   0.0007          5.9071   0.0046
CH-Pyrr +       4.0145   0.0014          3.9713   0.0049
CH-NH   +       2.7327   0.0013          2.6773   0.0053
CH'-NH  +       2.6192   0.0019          2.5519   0.0052

 Correlation coefficients*1000

       1    2
   1
   2  942

 Parameters are numbered as follows
    1 beta 1,1
    2 beta 2,1
```

Titration Plots

Experimental (symbols) and calculated (lines) chemical shifts

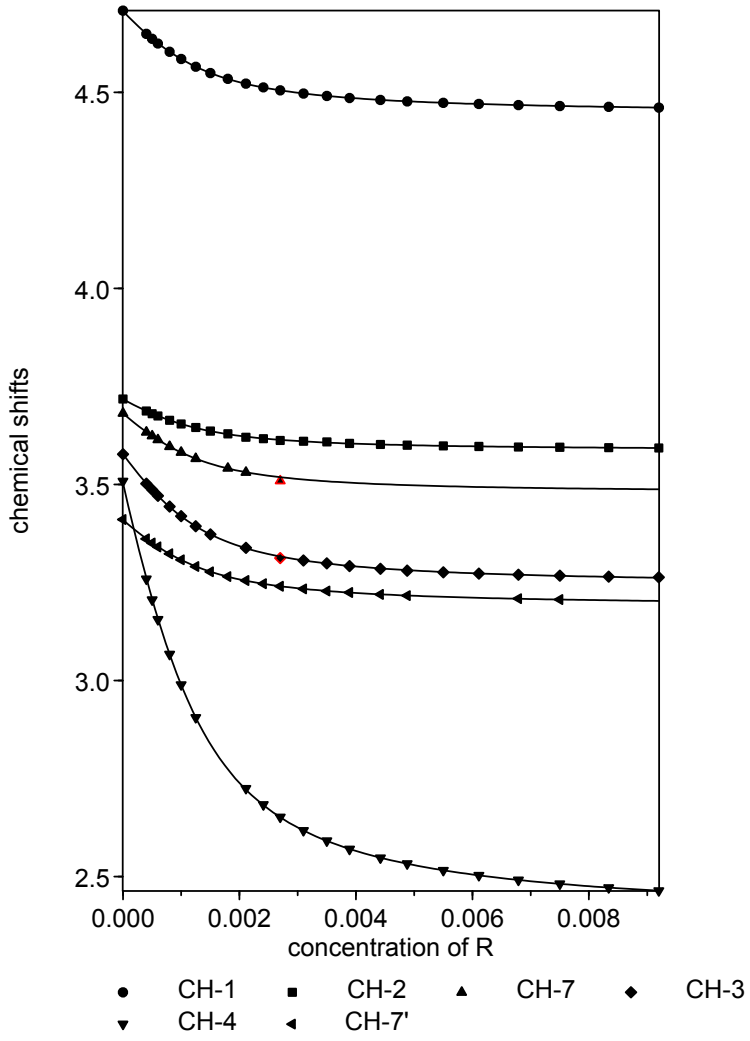

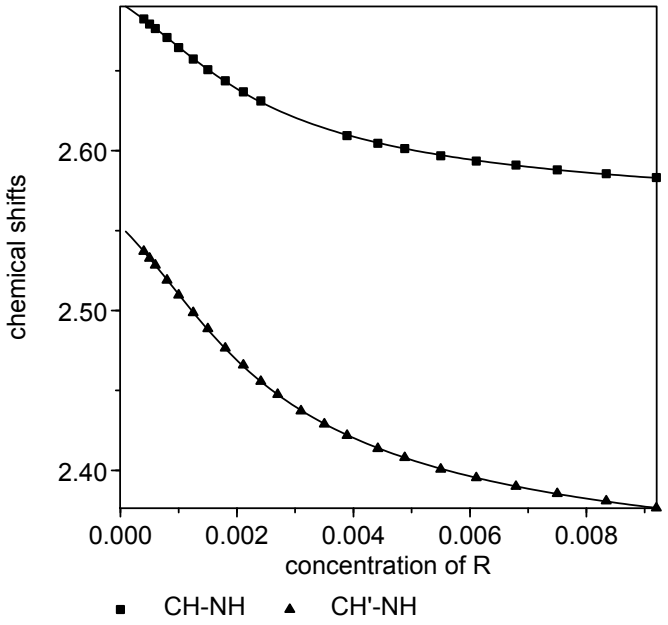
chemical shifts
2.60
2.50
2.40
0.000
0.002
0.004
0.006
0.008
concentration of R
CH-NH
CH'-NH

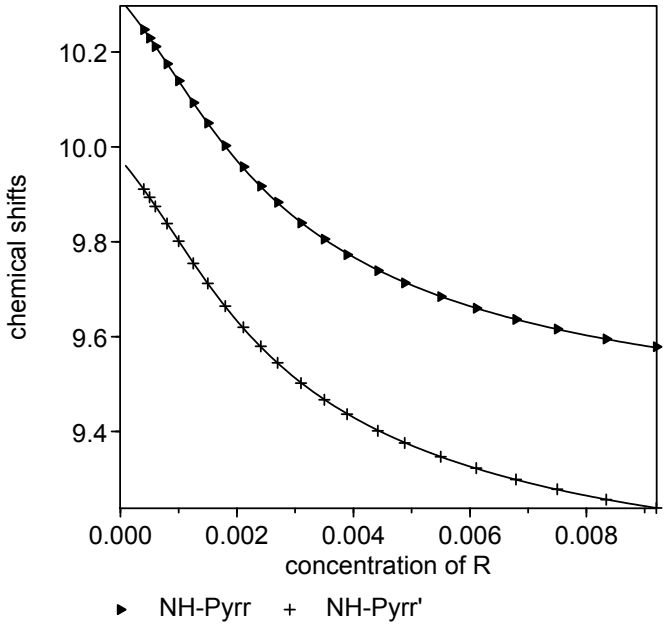
chemical shifts
10.2
10.0
9.8
9.6
9.4
0.000
0.002
0.004
0.006
0.008
concentration of R
NH-Pyrr
NH-Pyrr'

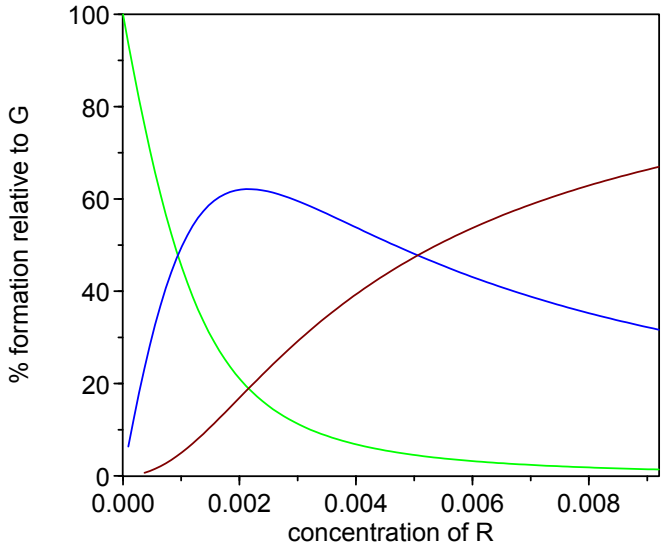
100
80
60
40
20
0
% formation relative to G
0.000
0.002
0.004
0.006
0.008
concentration of R

S-52 + OctαMan (CD_3CN, 298 K, 400 MHz)

Titration Data Table

R = ***S*-52** G = **OctαMan** [G] = 9.83 10^{-4} mol L^{-1}

R mol L^{-1}	G mol L^{-1}	CH-1 G	CH-2 G	CH-7 G	CH-4 G	CH-7' G
0.00E+00	9.83E-04	4.7081	3.7175	3.6816	3.5080	3.3864
4.01E-04	9.83E-04	4.6585	3.6853	3.6294	3.2341	3.3389
5.00E-04	9.83E-04	4.6480	3.6806	3.6186	3.1775	3.3289
6.00E-04	9.83E-04	4.6384	3.6770	3.6085	3.1255	3.3198
7.00E-04	9.83E-04	4.6293	3.6714	3.5990	3.0753	3.3107
8.01E-04	9.83E-04	4.6206	3.6657	3.5903	3.0287	3.3028
9.99E-04	9.83E-04	4.6061	3.6570	3.5751	2.9502	3.2888
1.25E-03	9.83E-04	4.5907	3.6473	3.5586	2.8655	3.2742
1.50E-03	9.83E-04	4.5792	3.6396	3.5477	-	3.2630
1.80E-03	9.83E-04	4.5683	3.6324	3.5291	2.7478	3.2531
2.11E-03	9.83E-04	4.5600	3.6262	3.5279	2.7049	3.2453
2.41E-03	9.83E-04	4.5534	3.6213	3.5212	2.6709	3.2390
2.70E-03	9.83E-04	4.5485	3.6177	3.5161	2.6452	3.2345
3.10E-03	9.83E-04	4.5432	3.6130	3.4865	2.6185	3.2293
3.50E-03	9.83E-04	4.5391	3.6091	-	2.5980	3.2255
3.89E-03	9.83E-04	4.5358	3.6056	-	2.5817	3.2226
4.39E-03	9.83E-04	4.5324	3.6014	-	2.5654	3.2193
4.91E-03	9.83E-04	4.5298	3.5979	-	2.5520	3.2163
5.50E-03	9.83E-04	4.5273	3.5951	-	2.5410	3.2150
6.12E-03	9.83E-04	4.5251	3.5921	-	2.5316	3.2129
6.80E-03	9.83E-04	4.5234	3.5885	-	2.5238	-
7.50E-03	9.83E-04	4.5218	-	-	2.5167	-
8.34E-03	9.83E-04	4.5202	-	-	2.5105	-

R mol L^{-1}	G mol L^{-1}	NH-Pyrr R	NH-Pyrr' R	CH-A R	CH-B R	CH-Pyrr R	CH-NH R	CH'-NH R
0.00E+00	9.83E-04	-	-	-	-	-	-	-
4.01E-04	9.83E-04	10.2093	9.9600	6.6325	5.9056	3.9082	2.6920	2.4766
5.00E-04	9.83E-04	10.1894	9.9399	6.6313	5.9047	3.9052	2.6873	2.4719
6.00E-04	9.83E-04	10.1711	9.9194	6.6304	5.9037	3.9018	2.6845	2.4692
7.00E-04	9.83E-04	10.1529	9.8969	6.6292	5.9023	3.8986	2.6799	2.4637
8.01E-04	9.83E-04	10.1313	9.8739	6.6285	5.9008	3.8955	2.6765	2.4595
9.99E-04	9.83E-04	10.0930	9.8301	6.6261	5.8991	3.8893	2.6687	2.4522
1.25E-03	9.83E-04	10.0490	9.7778	6.6237	5.8965	3.8822	2.6607	2.4433
1.50E-03	9.83E-04	10.0048	9.7264	6.6210	5.8939	3.8750	2.6516	2.4347
1.80E-03	9.83E-04	9.9569	9.6729	6.6185	5.8910	3.8675	2.6428	2.4254
2.11E-03	9.83E-04	9.9161	9.6261	6.6164	5.8890	3.8608	2.6356	2.4185
2.41E-03	9.83E-04	9.8802	9.5845	6.6144	5.8870	3.8551	2.6286	2.4113
2.70E-03	9.83E-04	9.8492	9.5501	6.6128	5.8856	3.8505	2.6228	2.4056
3.10E-03	9.83E-04	9.8117	9.5087	6.6108	5.8831	3.8446	-	2.3992
3.50E-03	9.83E-04	9.7821	9.4747	6.6092	5.8813	3.8395	-	2.3939
3.89E-03	9.83E-04	9.7571	9.4467	6.6079	5.8804	3.8371	-	2.3892
4.39E-03	9.83E-04	9.7303	9.4160	6.6063	5.8788	3.8324	2.6014	2.3844
4.91E-03	9.83E-04	9.7047	9.3881	6.6051	5.8774	3.8286	2.5982	2.3801
5.50E-03	9.83E-04	9.6838	9.3637	6.6038	5.8761	3.8253	2.5942	2.3763
6.12E-03	9.83E-04	9.6631	9.3417	6.6027	5.8752	3.8224	2.5912	2.3729
6.80E-03	9.83E-04	9.6459	9.3213	6.6016	5.8743	3.8199	2.5882	2.3698
7.50E-03	9.83E-04	9.6251	9.3010	6.6006	5.8735	3.8175	2.5861	2.3674
8.34E-03	9.83E-04	9.6120	9.2842	6.5996	5.8726	3.8150	2.5834	2.3644

Results page

```
 no. of spectra            23
 no. of resonance values  249
 no. of resonant nuclei    12

Chi-squared =  96.99

   sigma = 0.00067477191         RMS weighted residual = 0.00062115295

       stoich            value   relative    log    standard
       coeff                     std devn    beta   deviation

 Beta  1  1 refined  3.2837E+003  0.0224    3.5164   0.0097  (  RG  )
 Beta  2  1 refined  7.3413E+005  0.0782    5.8658   0.0340  (  R2G  )

 Individual chemical shifts

                     R                          G
 ============================================================
        +        value    error          value    error
CH-1    +                                 4.7081   0.0005
CH-2    +                                 3.7154   0.0005
CH-7    +                                 3.6814   0.0006
CH-4    +                                 3.5065   0.0006
CH-7'   +                                 3.3863   0.0005
NH-Pyrr +       9.4262   0.0032
NH-Pyrr +       9.0829   0.0032
CH-A    +       6.5897   0.0014
CH-B    +       5.8636   0.0014
CH-Pyrr +       3.7905   0.0014
CH-NH   +       2.5581   0.0015
CH'-NH  +       2.3385   0.0014
        +
                   1,1                        2,1
 ============================================================
        +        value    error          value    error
CH-1    +       4.5338   0.0013          4.5056   0.0009
CH-2    +       3.6194   0.0010          3.5588   0.0017
CH-7    +       3.4990   0.0016          3.4778   0.0042
CH-4    +       2.5510   0.0059          2.4531   0.0017
CH-7'   +       3.2197   0.0012          3.1953   0.0012
NH-Pyrr +      10.5365   0.0075         10.3820   0.0243
NH-Pyrr +      10.3322   0.0083         10.1077   0.0242
CH-A    +       6.6503   0.0006          6.6420   0.0060
CH-B    +       5.9236   0.0006          5.9079   0.0059
CH-Pyrr +       3.9586   0.0012          3.9110   0.0062
CH-NH   +       2.7499   0.0013          2.6747   0.0065
CH'-NH  +       2.5355   0.0013          2.4609   0.0060

 Correlation coefficients*1000

       1    2
   1
   2  951

 Parameters are numbered as follows
    1 beta 1,1
    2 beta 2,1
```

Titration Plots

Experimental (symbols) and calculated (lines) chemical shifts

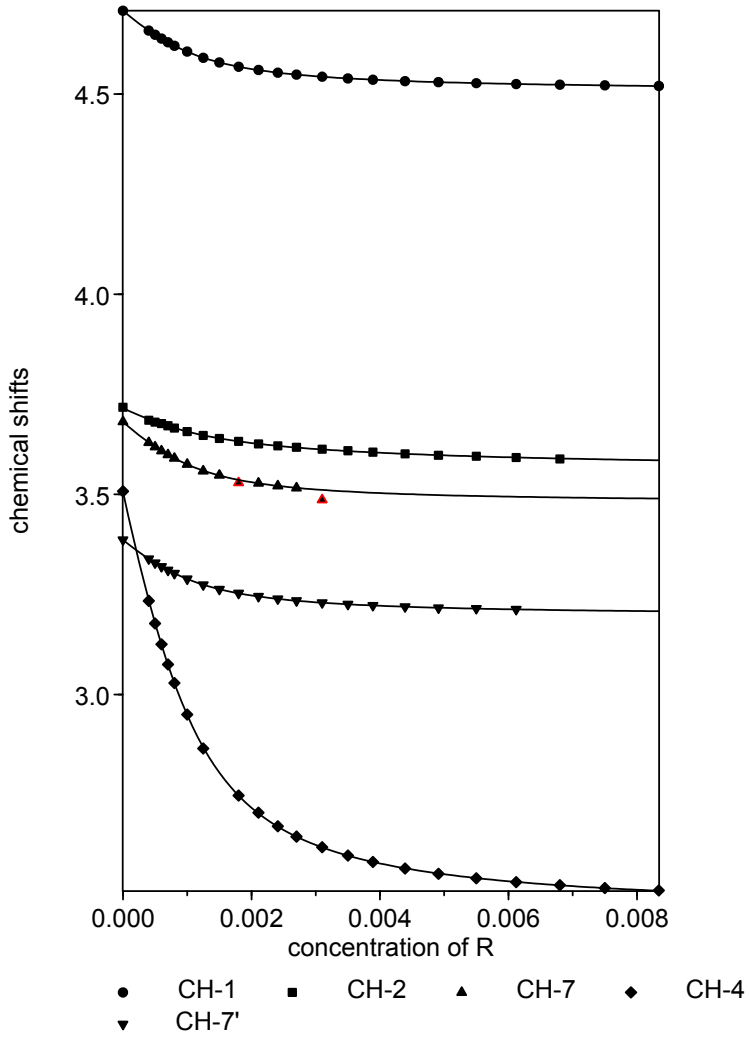

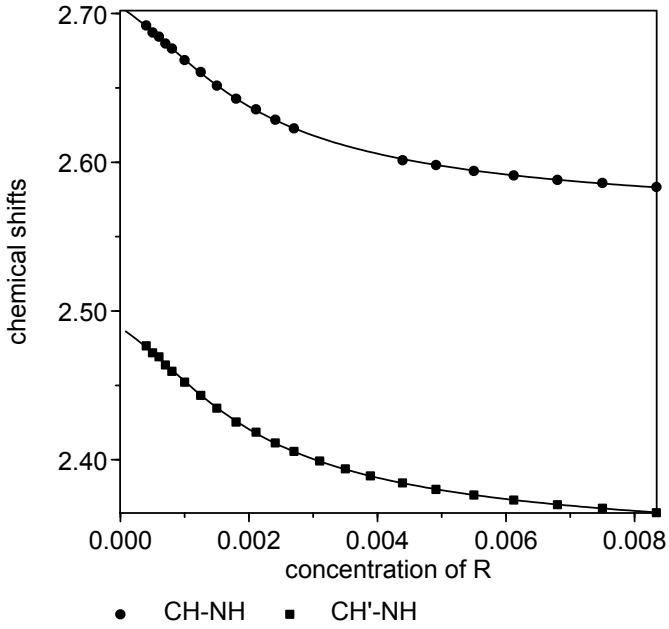
2.70
2.60
2.50
2.40
chemical shifts
0.000
0.002
0.004
0.006
0.008
concentration of R
CH-NH
CH'-NH

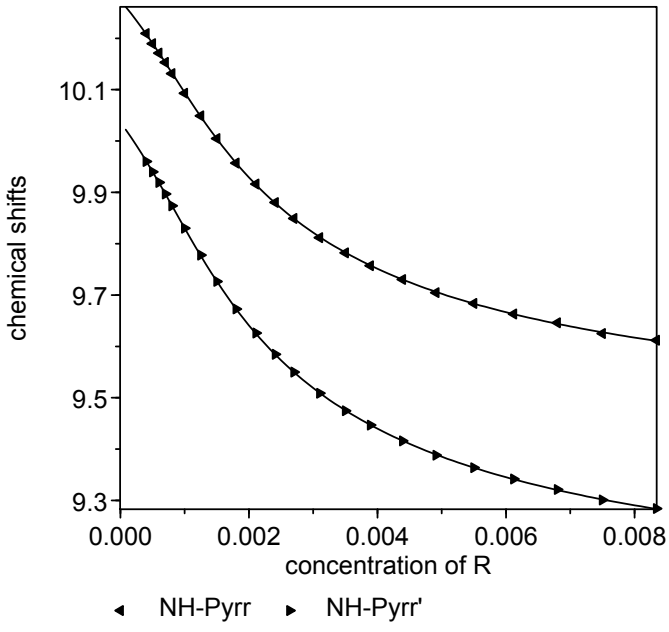
10.1
9.9
9.7
9.5
9.3
chemical shifts
0.000
0.002
0.004
0.006
0.008
concentration of R
NH-Pyrr
NH-Pyrr'

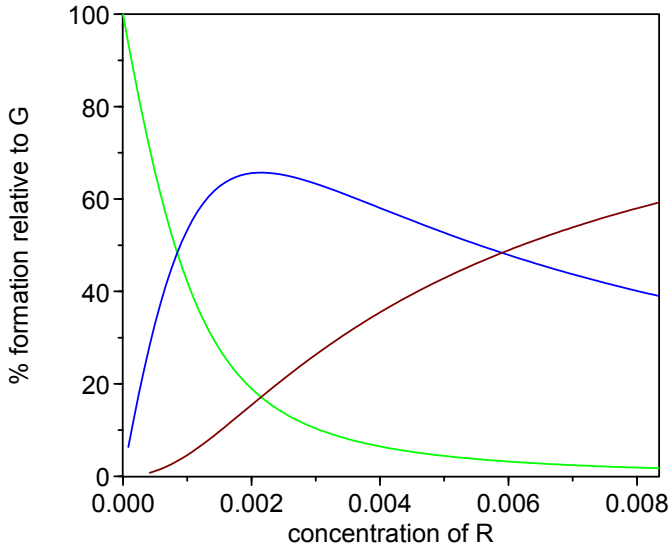
100
80
60
40
20
0
% formation relative to G
0.000
0.002
0.004
0.006
0.008
concentration of R

R-52 + OctβMan (CD_3CN, 298 K, 400 MHz)

Titration Data Table

R = ***R*-52** G = **OctβMan**

Set 1: [G] = 0 –1.94 10^{-2} mol L^{-1} [R] = 0 – 5.60 10^{-3} mol L^{-1}

G mol L^{-1}	R mol L^{-1}	CH-1 G	CH-7 G	CH-6 G	CH-7' G	CH-4 G	CH-3 G	CH-5 G
0.00E+00	5.60E-03	-	-	-	-	-	-	-
8.86E-04	5.34E-03	4.3191	-	3.5962	3.3977	2.5587	3.1408	-
2.00E-03	5.02E-03	4.3307	3.7336	3.5989	3.4069	-	3.1606	2.8997
3.04E-03	4.72E-03	4.3439	3.7443	3.6026	3.4179	2.7003	3.1791	2.9224
4.25E-03	4.37E-03	4.3602	3.7579	3.6086	3.4315	2.7939	3.2035	2.9514
5.37E-03	4.05E-03	4.3764	3.7713	3.6212	3.4449	2.8864	3.2267	2.9796
6.59E-03	3.70E-03	4.3934	3.7850	3.6410	3.4587	2.9810	3.2520	-
7.88E-03	3.33E-03	4.4086	3.7976	3.6603	3.4714	3.0739	3.2725	3.0286
9.18E-03	2.95E-03	4.4217	3.8082	3.6772	3.4822	3.1471	3.2900	3.0557
1.05E-02	2.58E-03	4.4325	3.8169	3.6915	3.4907	3.2068	3.3049	3.0751
1.17E-02	2.22E-03	4.4409	3.8239	3.7031	3.4979	3.2551	3.3174	3.0897
1.28E-02	1.89E-03	4.4482	3.8296	3.7126	3.5036	3.2937	3.3286	3.1016
1.39E-02	1.59E-03	4.4538	3.8341	3.7203	3.5082	-	-	3.1109
1.48E-02	1.32E-03	4.4584	3.8377	3.7265	3.5118	-	-	3.1197
1.57E-02	1.06E-03	4.4621	3.8407	3.7316	3.5148	3.3795	-	3.1263
1.65E-02	8.35E-04	4.4653	3.8431	3.7360	3.5173	3.3963	3.3444	3.1312
1.72E-02	6.41E-04	4.4678	3.8452	3.7392	3.5193	3.4098	3.3486	3.1353
1.77E-02	4.80E-04	4.4698	3.8467	3.7420	3.5209	3.4206	3.3516	3.1389
1.94E-02	0.00E+00	4.4752	3.8510	3.7467	3.5252	3.4497	3.3553	3.1482

G mol L^{-1}	R mol L^{-1}	NH-Pyrr R	NH-Pyrr' R	CH-A R	CH-B R	CH-Pyrr R	CH'-NH R
0.00E+00	5.60E-03	9.6574	9.2082	6.5973	5.8724	3.9443	2.3529
8.86E-04	5.34E-03	9.7643	9.3898	6.6067	5.8784	3.9528	2.3937
2.00E-03	5.02E-03	9.8857	9.6003	6.6175	5.8854	3.9628	2.4418
3.04E-03	4.72E-03	9.9869	9.7755	6.6266	5.8913	3.9713	2.4819
4.25E-03	4.37E-03	10.0797	9.9385	6.6351	5.8968	3.9791	2.5194
5.37E-03	4.05E-03	10.1429	10.0497	6.6409	5.9007	3.9847	2.5455
6.59E-03	3.70E-03	10.1909	10.1349	6.6457	5.9043	3.9889	2.5663
7.88E-03	3.33E-03	10.2222	10.1964	6.6490	5.9068	3.9920	2.5808
9.18E-03	2.95E-03	-	-	6.6514	5.9089	3.9945	2.5919
1.05E-02	2.58E-03	-	-	6.6531	5.9103	3.9959	2.5994
1.17E-02	2.22E-03	-	-	6.6545	5.9118	3.9973	2.6057
1.28E-02	1.89E-03	-	-	6.6556	5.9130	3.9983	2.6094
1.39E-02	1.59E-03	10.2838	10.3034	6.6564	5.9140	3.9991	2.6135
1.48E-02	1.32E-03	10.2843	10.3096	6.6571	5.9148	3.9996	2.6172
1.57E-02	1.06E-03	10.2881	10.3149	6.6574	5.9154	4.0003	2.6194
1.65E-02	8.35E-04	10.2890	10.3170	6.6581	5.9163	4.0005	2.6223
1.72E-02	6.41E-04	10.2866	10.3165	6.6586	5.9177	4.0010	2.6264
1.77E-02	4.80E-04	10.2883	10.3124	6.6595	5.9191	4.0015	2.6320
1.94E-02	0.00E+00	-	-	-	-	-	-

Set 2: [G] = 0 – 9.66 10^{-3} mol L^{-1} [R] = 0 – 5.60 10^{-3} mol L^{-1}

G mol L^{-1}	R mol L^{-1}	CH-1 G	CH-7 G	CH-6 G	CH-7' G	CH-4 G	CH-3 G	CH-5 G
0.00E+00	5.60E-03	-	-	-	-	-	-	-
4.42E-04	5.34E-03	4.3143	-	3.5951	3.3936	-	-	-
9.97E-04	5.02E-03	4.3211	3.7254	3.5962	3.3991	2.5712	3.1452	-
1.52E-03	4.72E-03	4.3281	3.7314	3.5981	3.4048	2.6101	3.1560	2.8950
2.12E-03	4.37E-03	4.3381	3.7394	3.6003	3.4129	2.6679	3.1725	2.9125
2.68E-03	4.05E-03	4.3480	3.7476	3.6044	3.4211	2.7485	3.1857	2.9297
3.29E-03	3.69E-03	4.3607	3.7579	3.6088	3.4315	2.8207	3.2028	2.9509
3.93E-03	3.32E-03	4.3748	3.7694	3.6190	3.4432	2.8756	3.2236	2.9760
4.58E-03	2.94E-03	4.3894	3.7814	3.6356	3.4551	2.9567	3.2447	-
5.22E-03	2.57E-03	4.4031	3.7927	3.6527	3.4665	-	3.2644	-
5.83E-03	2.22E-03	4.4086	3.7968	3.6599	3.4705	-	3.2716	-
6.41E-03	1.89E-03	4.4225	3.8086	3.6780	3.4826	3.1497	3.2904	3.0568
6.93E-03	1.58E-03	4.4331	3.8171	3.6920	3.4910	3.2081	3.3052	3.0750
7.40E-03	1.31E-03	4.4415	3.8239	3.7033	3.4980	3.2552	3.3171	3.0897
7.84E-03	1.06E-03	4.4488	3.8299	3.7135	3.5040	3.2957	3.3290	3.1026
8.23E-03	8.30E-04	4.4549	3.8348	3.7214	3.5091	-	-	3.1130
8.77E-03	5.16E-04	4.4627	3.8411	3.7321	3.5153	3.3812	-	3.1267
9.66E-03	0.00E+00	4.4746	3.8506	-	3.5249	3.4462	3.3572	3.1472

G mol L^{-1}	R mol L^{-1}	NH-Pyrr R	NH-Pyrr' R	CH-A R	CH-B R	CH-Pyrr R	CH'-NH R
0.00E+00	5.60E-03	9.6485	9.2022	6.5964	5.8716	3.9441	2.3529
4.42E-04	5.34E-03	9.7049	9.2942	6.6012	5.8747	3.9482	2.3728
9.97E-04	5.02E-03	9.7728	9.4112	6.6070	5.8784	3.9538	2.3990
1.52E-03	4.72E-03	9.8395	9.5229	6.6131	5.8825	3.9591	2.4242
2.12E-03	4.37E-03	9.9139	9.6518	6.6197	5.8868	3.9651	2.4528
2.68E-03	4.05E-03	9.9750	9.7564	6.6250	5.8903	3.9703	2.4773
3.29E-03	3.69E-03	10.0376	9.8661	6.6308	5.8941	3.9756	2.5026
3.93E-03	3.32E-03	10.0923	9.9623	6.6358	5.8976	3.9801	2.5249
4.58E-03	2.94E-03	10.1369	10.0415	6.6401	5.9007	3.9845	2.5431
5.22E-03	2.57E-03	10.1702	10.1014	6.6436	5.9029	3.9875	2.5582
5.83E-03	2.22E-03	10.1821	10.1224	6.6447	5.9043	3.9888	2.5632
6.41E-03	1.89E-03	10.2068	10.1692	6.6474	5.9062	3.9911	2.5755
6.93E-03	1.58E-03	10.2223	10.2010	6.6490	5.9076	3.9928	2.5835
7.40E-03	1.31E-03	-	-	6.6504	5.9091	3.9941	2.5900
7.84E-03	1.06E-03	-	-	6.6515	5.9100	3.9952	2.5962
8.23E-03	8.30E-04	-	-	6.6525	5.9118	3.9963	2.6011
8.77E-03	5.16E-04	-	-	6.6544	5.9140	3.9976	2.6091
9.66E-03	0.00E+00	-	-	-	-	-	-

Results page

```
 no. of spectra            37
 no. of resonance values  398
 no. of resonant nuclei    13

Chi-squared = 227.81

   sigma = 0.00358156017         RMS weighted residual = 0.00332489378

       stoich            value   relative    log    standard
       coeff                     std devn    beta   deviation

 Beta  1  1 refined  7.5268E+002  0.0373    2.8766   0.0162  (  GR  )
 Beta  1  2 refined  2.0127E+004  0.4259    4.3038   0.1850  (  GR2  )
 Beta  1  3 refined  2.7416E+007  0.1829    7.4380   0.0794  (  GR3  )

 Individual chemical shifts

                     G                          R
 ============================================================
        +        value    error          value    error
CH-1    +       4.4743   0.0013
CH-7    +       3.8504   0.0014
CH-6    +       3.7497   0.0015
CH-7'   +       3.5247   0.0013
CH-4    +       3.4459   0.0016
CH-3    +       3.3571   0.0016
CH-5    +       3.1475   0.0015
NH-Pyrr +                                 9.6529   0.0023
NH-Pyrr +                                 9.2056   0.0024
CH-A    +                                 6.5964   0.0023
CH-B    +                                 5.8715   0.0023
CH-Pyrr +                                 3.9439   0.0023
CH'-NH  +                                 2.3515   0.0023
        +
                    1,1                        1,2
 ============================================================
        +        value    error          value    error
CH-1    +       4.2653   0.0091         4.3745   0.2722
CH-7    +       3.6829   0.0104         3.6940   0.3808
CH-6    +       3.4366   0.0102         5.1638   0.6734
CH-7'   +       3.3554   0.0090         3.3836   0.2732
CH-4    +       2.2435   0.0152         3.5355   0.5048
CH-3    +       3.0974   0.0101         2.5754   0.4353
CH-5    +       2.7749   0.0134         3.4199   0.5718
NH-Pyrr +      10.3372   0.0023        11.6860   0.7009
NH-Pyrr +      10.4025   0.0032        12.4421   1.1005
CH-A    +       6.6629   0.0015         6.6603   0.0862
CH-B    +       5.9188   0.0019         5.8294   0.0975
CH-Pyrr +       4.0052   0.0015         4.0042   0.0860
CH'-NH  +       2.6425   0.0018         2.6474   0.1281
```

```
        +
                    1,3
 ================================
        +        value    error
CH-1    +       4.3103   0.0387
CH-7    +       3.7259   0.0650
CH-6    +       3.4956   0.0441
CH-7'   +       3.3977   0.0383
CH-4    +       2.4009   0.0931
CH-3    +       3.2002   0.0509
CH-5    +       2.7865   0.1093
NH-Pyrr +       9.7378   0.0301
NH-Pyrr +       9.3475   0.0427
CH-A    +       6.6198   0.0212
CH-B    +       5.8975   0.0224
CH-Pyrr +       3.9632   0.0211
CH'-NH  +       2.4443   0.0239

 Correlation coefficients*1000

       1    2    3
   1
   2  222
   3  -40  -64

 Parameters are numbered as follows
    1 beta 1,1
    2 beta 1,2
    3 beta 1,3
```

Titration Plots

Experimental (symbols) and calculated (lines) chemical shifts

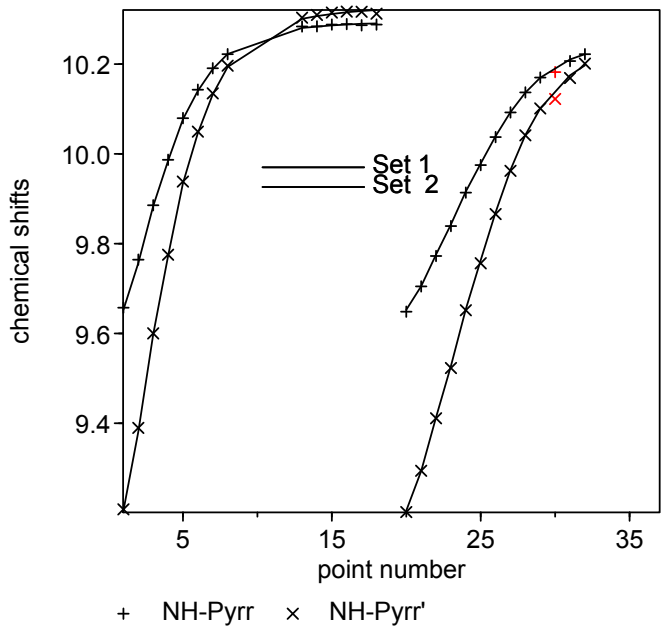

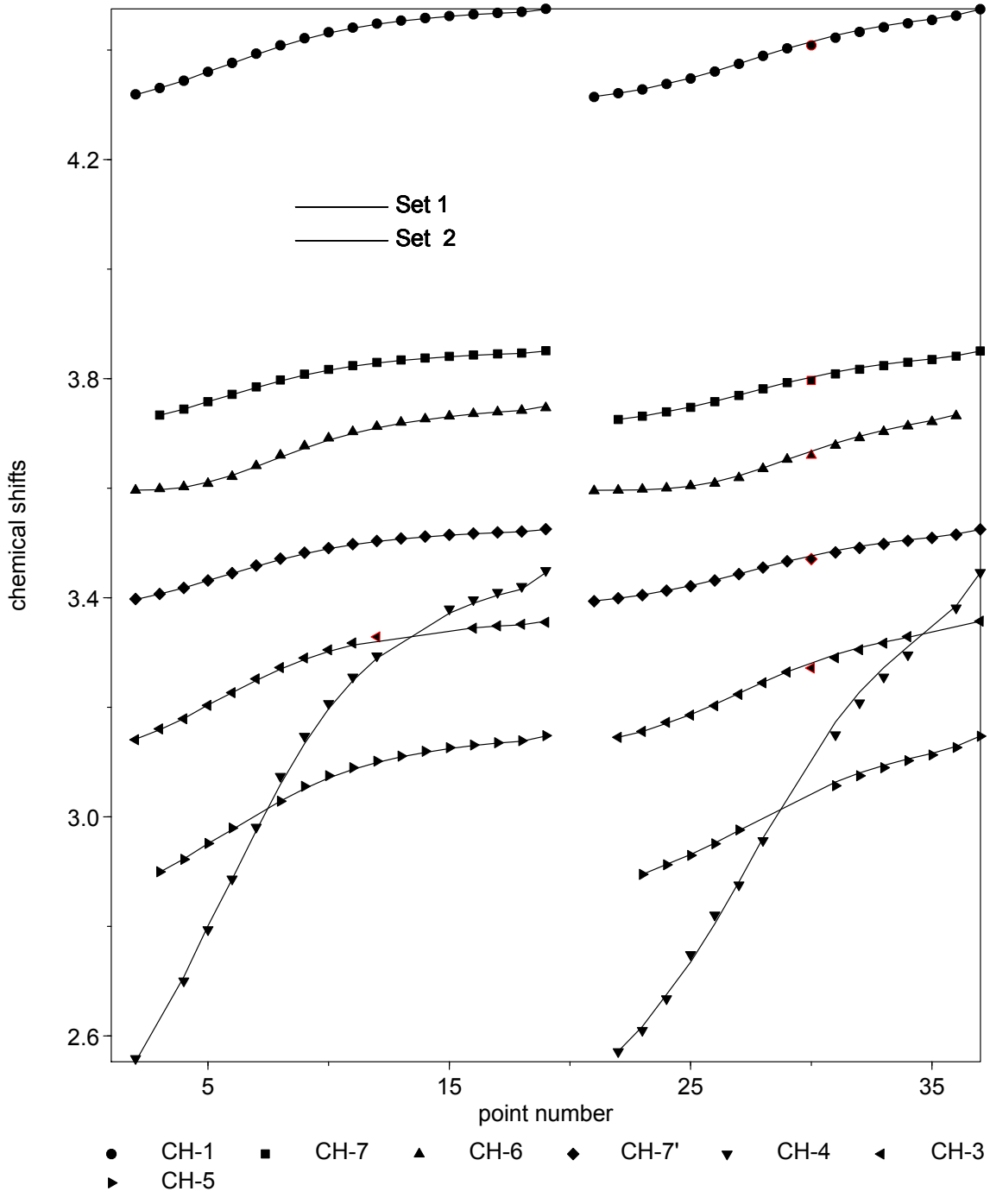
chemical shifts
4.2
3.8
3.4
3.0
2.6
Set 1
Set 2
5
15
25
35
point number
CH-1
CH-7
CH-6
CH-7'
CH-4
CH-3
CH-5

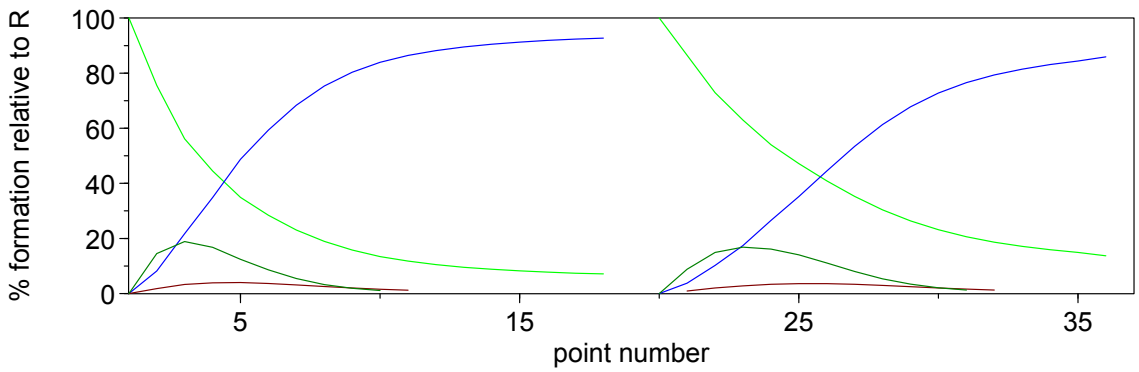
% formation relative to R
100
80
60
40
20
0
5
15
25
35
point number

S-52 + OctβMan (CD_3CN, 298 K, 900 MHz)

Titration Data Table

R = ***S*-52** G = **OctβMan** [G] = 1.54 10^{-3} mol L^{-1}

G mol L^{-1}	R mol L^{-1}	CH-1 G	CH-7 G	CH-2 G	CH-7' G	CH-3 G	CH-4 G	CH-5 G
0.00E+00	1.54E-03	-	-	-	-	-	-	-
1.50E-04	1.54E-03	4.2847	-	-	3.2867	3.1356	-	-
2.00E-04	1.54E-03	4.2854	3.7329	-	3.2877	3.1364	-	-
2.99E-04	1.54E-03	4.2871	3.7335	-	3.2896	3.1385	-	-
4.00E-04	1.54E-03	4.2888	3.7347	3.8261	3.2915	3.1405	-	-
6.01E-04	1.54E-03	4.2929	3.7368	3.8249	3.2962	3.1456	-	-
8.02E-04	1.54E-03	4.2976	3.7393	3.8242	3.3017	3.1513	-	-
1.10E-03	1.54E-03	4.3061	3.7438	3.8223	3.3119	3.1618	2.4377	2.8613
1.50E-03	1.54E-03	4.3202	3.7513	3.8186	3.3283	3.1792	2.5287	2.8849
2.00E-03	1.54E-03	4.3391	3.7614	3.8133	3.3505	3.2124	2.6475	2.9168
2.51E-03	1.54E-03	4.3568	3.7710	3.8082	3.3690	3.2234	2.7448	2.9472
3.01E-03	1.54E-03	4.3712	3.7787	3.8040	3.3880	3.2408	2.8256	2.9717
3.99E-03	1.54E-03	4.3920	3.7910	3.7984	3.4124	3.2662	2.9572	3.0061
5.01E-03	1.54E-03	4.4063	3.7985	3.7942	3.4291	3.2840	-	-
6.01E-03	1.54E-03	4.4161	3.8031	3.7915	3.4405	3.2957	3.1001	3.0480
7.02E-03	1.54E-03	4.4235	3.8072	3.7894	3.4449	3.3044	3.1441	3.0608
8.03E-03	1.54E-03	4.4292	3.8102	3.7878	3.4557	3.3113	3.1787	3.0703
8.99E-03	1.54E-03	4.4336	3.8126	3.7867	3.4607	3.3166	3.2046	3.0779
9.99E-03	1.54E-03	4.4373	3.8146	3.7858	3.4649	3.3211	3.2264	3.0844
1.20E-02	1.54E-03	4.4430	3.8177	3.7845	3.4715	3.3282	3.2599	3.0939
1.40E-02	1.54E-03	4.4472	3.8199	3.7835	3.4762	3.3336	3.2852	3.1013
1.60E-02	1.54E-03	4.4504	3.8216	3.7829	3.4799	3.3379	3.3049	3.1069
1.80E-02	1.54E-03	4.4530	3.8231	3.7823	3.4828	3.3414	3.3211	3.1109
2.02E-02	1.54E-03	4.4551	3.8243	3.7820	3.4852	-	-	3.1148

G mol L^{-1}	R mol L^{-1}	NH-Pyrr R	NH-Pyrr' R	CH-A R	CH-B R	CH-Pyrr R	CH-NH R	CH'-NH R
0.00E+00	1.54E-03	9.3964	9.0777	6.5922	5.8626	3.9336	2.5792	2.3320
1.50E-04	1.54E-03	9.5125	9.2315	6.5978	5.8682	3.9413	2.6011	2.3491
2.00E-04	1.54E-03	9.5438	9.2755	6.5994	5.8698	3.9491	2.6075	2.3539
2.99E-04	1.54E-03	9.6076	9.3631	6.6024	5.8728	3.9635	2.6196	2.3633
4.00E-04	1.54E-03	9.6688	9.4473	6.6053	5.8758	3.9776	2.6317	2.3723
6.01E-04	1.54E-03	9.7893	9.6093	6.6109	5.8818	4.0046	2.6545	2.3898
8.02E-04	1.54E-03	9.8953	9.7558	6.6161	5.8872	4.0291	2.6755	2.4058
1.10E-03	1.54E-03	10.0355	9.9478	6.6229	5.8942	4.0615	2.7035	2.4280
1.50E-03	1.54E-03	-	-	6.6298	5.9017	4.0949	-	2.4493
2.00E-03	1.54E-03	-	-	6.6353	5.9074	4.1215	2.7540	2.4669
2.51E-03	1.54E-03	-	-	6.6385	5.9109	4.1368	2.7672	2.4774
3.01E-03	1.54E-03	10.3884	10.4305	6.6405	5.9132	4.1457	2.7749	2.4836
3.99E-03	1.54E-03	10.4198	10.4812	6.6424	5.9157	4.1551	2.7831	2.4907
5.01E-03	1.54E-03	10.4375	10.5078	6.6436	5.9173	4.1598	2.7875	2.4946
6.01E-03	1.54E-03	10.4468	10.5229	6.6442	5.9180	4.1629	2.7901	2.4967
7.02E-03	1.54E-03	10.4521	10.5319	6.6446	5.9187	4.1647	2.7920	2.4986
8.03E-03	1.54E-03	10.4561	10.5397	6.6448	5.9193	4.1662	2.7930	2.4994
8.99E-03	1.54E-03	10.4585	10.5450	6.6452	5.9193	4.1673	2.7941	2.5002
9.99E-03	1.54E-03	10.4608	10.5498	6.6452	5.9198	4.1682	2.7946	2.5004
1.20E-02	1.54E-03	10.4628	10.5562	6.6455	5.9201	4.1695	2.7958	2.5012
1.40E-02	1.54E-03	10.4638	10.5603	6.6458	5.9213	4.1704	2.7966	2.5022
1.60E-02	1.54E-03	10.4645	10.5645	6.6459	5.9220	4.1713	2.7970	2.5025
1.80E-02	1.54E-03	10.4651	10.5699	6.6458	5.9219	4.1722	2.7972	2.5014
2.02E-02	1.54E-03	10.4645	10.5728	6.6459	5.9227	4.1729	2.7973	2.5015

Results page

```
 no. of spectra            24
 no. of resonance values  299
 no. of resonant nuclei    14

Chi-squared = 101.29

   sigma = 0.00151982251         RMS weighted residual = 0.00136164188

       stoich            value   relative    log    standard
       coeff                     std devn    beta   deviation

 Beta  1  1 refined  9.8876E+003  0.1204    3.9951    0.0523  (  GR  )
 Beta  2  1 refined  1.0885E+007  0.3109    7.0368    0.1350  (  G2R  )
 Beta  3  1 refined  1.1215E+010  0.3503   10.0498    0.1521  (  G3R  )

 Individual chemical shifts

                    G                          R
 ========================================================
        +        value    error         value    error
CH-1    +       4.4694   0.0017
CH-7    +       3.8316   0.0017
CH-2    +       3.7789   0.0018
CH-7'   +       3.5009   0.0018
CH-3    +       3.3608   0.0020
CH-4    +       3.4326   0.0024
CH-5    +       3.1433   0.0019
NH-Pyrr +                             9.4051   0.0010
NH-Pyrr +                             9.0858   0.0011
CH-A    +                             6.5926   0.0009
CH-B    +                             5.8626   0.0009
CH-Pyrr +                             3.9172   0.0011
CH-NH   +                             2.5802   0.0009
CH'-NH  +                             2.3330   0.0009
        +
                   1,1                        2,1
 ========================================================
        +        value    error         value    error
CH-1    +       4.2685   0.0016         4.3516   0.0045
CH-7    +       3.7235   0.0012         3.7682   0.0041
CH-2    +       3.8318   0.0014         3.8118   0.0044
CH-7'   +       3.2682   0.0018         3.3625   0.0049
CH-3    +       3.1158   0.0019         3.2188   0.0051
CH-4    +       2.1703   0.0103         2.8032   0.0109
CH-5    +       2.7850   0.0041         2.9601   0.0069
NH-Pyrr +      10.5448   0.0096        10.3581   0.0068
NH-Pyrr +      10.6482   0.0124        10.3595   0.0091
CH-A    +       6.6474   0.0021         6.6388   0.0039
CH-B    +       5.9206   0.0021         5.9084   0.0039
CH-Pyrr +       4.1795   0.0032         4.1361   0.0042
CH-NH   +       2.8029   0.0029         2.7687   0.0041
CH'-NH  +       2.5032   0.0025         2.4822   0.0040
        +
```

```
                  3,1
 ================================
        +        value    error
CH-1    +       4.4036   0.0032
CH-7    +       3.7971   0.0031
CH-2    +       3.7923   0.0033
CH-7'   +       3.4285   0.0035
CH-3    +       3.2793   0.0036
CH-4    +       2.9855   0.0047
CH-5    +       3.0157   0.0039
NH-Pyrr +      10.4743   0.0012
NH-Pyrr +      10.5821   0.0017
CH-A    +       6.6464   0.0009
CH-B    +       5.9225   0.0009
CH-Pyrr +       4.1740   0.0009
CH-NH   +       2.7992   0.0009
CH'-NH  +       2.5036   0.0009

 Correlation coefficients*1000


      1    2    3
   1
   2  984
   3  975  986

 Parameters are numbered as follows
    1 beta 1,1
    2 beta 2,1
    3 beta 3,1
```

Titration Plots

Experimental (symbols) and calculated (lines) chemical shifts

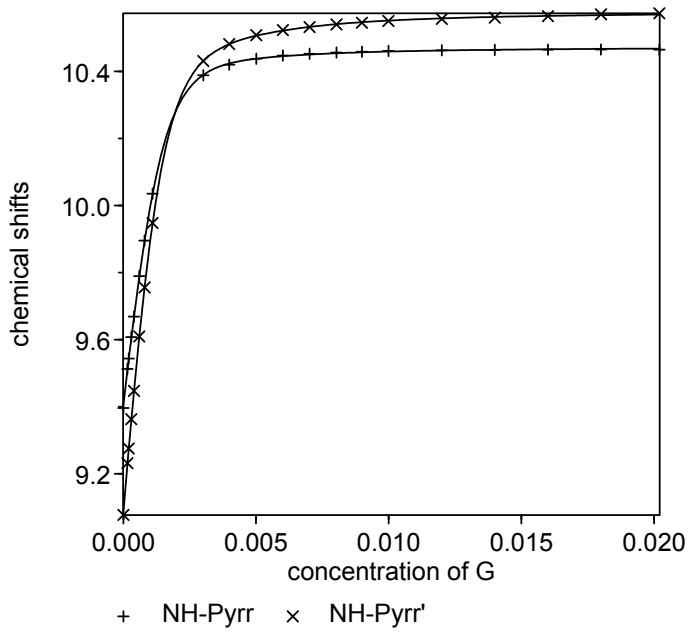

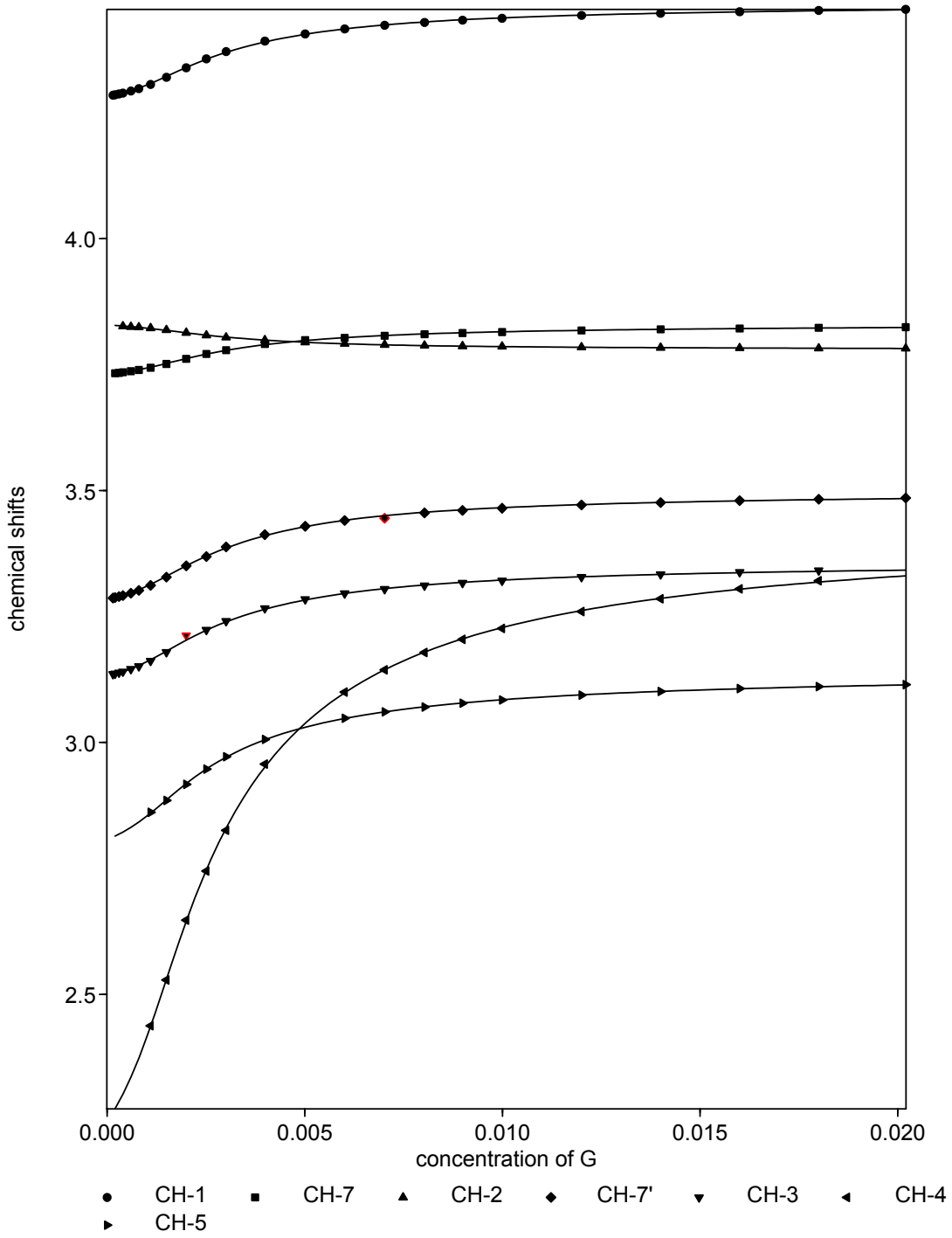
chemical shifts
4.0
3.5
3.0
2.5
0.000
0.005
0.010
0.015
0.020
concentration of G
CH-1
CH-7
CH-2
CH-7'
CH-3
CH-4
CH-5

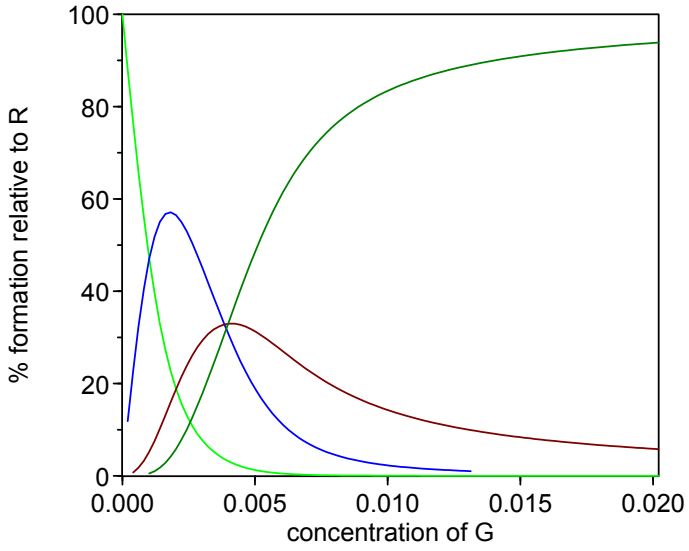
100
80
60
40
20
0
% formation relative to R
0.000
0.005
0.010
0.015
0.020
concentration of G

R-34 + OctαMan (CD_3CN, 298 K, 900 MHz)

Titration Data Table

R = ***R*-34** G = **OctαMan** [G] = 1.16 10^{-3} mol L^{-1}

R	G	CH-1 G	CH-2 G	CH-6 G	CH-7 G	CH-4 G	CH-5 G
4.98E-04	1.16E-03	4.6333	3.6671	3.6237	3.5866	3.2654	3.3779
6.64E-04	1.16E-03	4.6135	3.6539	3.5990	3.5660	3.1993	3.3605
8.29E-04	1.16E-03	4.5963	3.6424	3.5772	3.5482	3.1403	3.3456
9.94E-04	1.16E-03	4.5817	3.6326	3.5595	3.5329	3.0954	3.3330
1.33E-03	1.16E-03	4.5599	3.6181	3.5328	-	3.0363	3.3142
1.65E-03	1.16E-03	4.5464	3.6086	-	3.4970	3.0014	3.3026
1.98E-03	1.16E-03	4.5373	3.6027	-	3.4871	2.9801	3.2951
2.65E-03	1.16E-03	4.5271	3.5956	-	3.4765	2.9541	3.2865
3.30E-03	1.16E-03	4.5218	3.5915	-	3.4709	2.9410	3.2819
3.96E-03	1.16E-03	4.5186	3.5892	-	3.4675	2.9322	3.2791
4.63E-03	1.16E-03	4.5165	3.5876	-	3.4651	2.9270	3.2776
5.29E-03	1.16E-03	4.5150	3.5864	-	3.4634	2.9223	3.2766
5.97E-03	1.16E-03	4.5140	3.5859	-	3.4623	2.9193	3.2759
7.30E-03	1.16E-03	4.5127	3.5850	-	3.4608	2.9144	3.2746
8.64E-03	1.16E-03	4.5119	3.5844	-	3.4599	2.9113	3.2741
9.74E-03	1.16E-03	4.5115	3.5839	-	3.4594	2.9097	3.2738
1.11E-02	1.16E-03	4.5112	3.5845	-	3.4592	2.9077	3.2740

R	G	NH-Pyrr R	CH-A R	CH-C R	CH-B R	CH-Pyrr R
4.98E-04	1.16E-03	10.1888	6.6436	5.9645	5.9149	3.9779
6.64E-04	1.16E-03	10.1502	6.6403	5.9637	5.9127	3.9710
8.29E-04	1.16E-03	10.1076	6.6368	5.9629	5.9103	3.9633
9.94E-04	1.16E-03	10.0595	6.6330	5.9619	5.9079	3.9550
1.33E-03	1.16E-03	9.9597	6.6250	5.9601	5.9025	3.9377
1.65E-03	1.16E-03	9.8677	6.6178	5.9584	5.8978	3.9222
1.98E-03	1.16E-03	9.7860	6.6114	5.9570	5.8935	3.9086
2.65E-03	1.16E-03	9.6650	6.6019	5.9549	5.8873	3.8876
3.30E-03	1.16E-03	9.5823	6.5952	5.9533	5.8830	3.8735
3.96E-03	1.16E-03	9.5283	6.5904	5.9523	5.8800	3.8632
4.63E-03	1.16E-03	9.4880	6.5868	5.9516	5.8777	3.8545
5.29E-03	1.16E-03	9.4557	6.5838	5.9509	5.8759	3.8497
5.97E-03	1.16E-03	9.4316	6.5815	5.9505	5.8746	3.8461
7.30E-03	1.16E-03	9.3993	6.5780	5.9499	5.8726	3.8375
8.64E-03	1.16E-03	9.3773	6.5754	5.9493	5.8711	3.8324
9.74E-03	1.16E-03	9.3651	6.5738	5.9491	5.8704	3.8292
1.11E-02	1.16E-03	9.3525	6.5720	5.9489	5.8695	3.8260

R	G	CH-Ar R	CH'-Pyrr R	CH'-Ar R	CH-Et R
4.98E-04	1.16E-03	3.8152	3.5187	3.4984	2.7109
6.64E-04	1.16E-03	3.8167	3.5164	3.5011	2.7121
8.29E-04	1.16E-03	3.8182	3.5141	3.5038	2.7135
9.94E-04	1.16E-03	3.8199	3.5113	3.5071	2.7151
1.33E-03	1.16E-03	3.8235	3.5060	3.5127	2.7182
1.65E-03	1.16E-03	3.8267	3.5011	3.5179	2.7211
1.98E-03	1.16E-03	3.8296	3.4969	3.5234	2.7236
2.65E-03	1.16E-03	3.8339	3.4905	3.5307	2.7275
3.30E-03	1.16E-03	3.8369	3.4862	3.5356	2.7301
3.96E-03	1.16E-03	3.8391	3.4831	3.5391	2.7321
4.63E-03	1.16E-03	3.8409	3.4808	3.5419	2.7337
5.29E-03	1.16E-03	3.8421	3.4790	3.5439	2.7349
5.97E-03	1.16E-03	3.8433	3.4775	3.5456	2.7360
7.30E-03	1.16E-03	3.8448	3.4755	3.5479	2.7376
8.64E-03	1.16E-03	3.8461	3.4740	3.5495	2.7388
9.74E-03	1.16E-03	3.8468	3.4731	3.5505	2.7397
1.11E-02	1.16E-03	3.8476	3.4722	3.5515	2.7406

Results page

```
 no. of spectra            17
 no. of resonance values  240
 no. of resonant nuclei    15

   Chi-squared = 188.13

   sigma = 0.00031366673         RMS weighted residual = 0.00026937015

       stoich            value   relative    log    standard
       coeff                     std devn    beta   deviation

 Beta  1  1 refined  7.3455E+003  0.0258    3.8660   0.0112  (  RG  )
 Beta  2  1 refined  1.9709E+006  0.1206    6.2947   0.0524  (  R2G  )
 Beta  1  2 refined  1.3060E+006  0.1209    6.1159   0.0525  (  RG2  )

 Individual chemical shifts

                     R                          G
 ============================================================
        +        value    error          value    error
CH-1    +                                4.7071   0.0016
CH-2    +                                3.7144   0.0016
CH-6    +                                3.7132   0.0080
CH-7    +                                3.6634   0.0017
CH-4    +                                3.5654   0.0024
CH-5    +                                3.4427   0.0016
NH-Pyrr +       9.2809   0.0028
CH-A    +       6.5602   0.0007
CH-C    +       5.9470   0.0007
CH-B    +       5.8638   0.0007
CH-Pyrr +       3.8039   0.0007
CH-Ar   +       3.8532   0.0007
CH'-Pyr +       3.4660   0.0007
CH'-Ar  +       3.5584   0.0007
CH-Et   +       2.7467   0.0007
        +
                   1,1                        2,1
 ============================================================
        +        value    error          value    error
CH-1    +       4.5135   0.0010          4.5088   0.0004
CH-2    +       3.5862   0.0008          3.5820   0.0004
CH-6    +       3.4651   0.0194          3.5287   0.0980
CH-7    +       3.4632   0.0010          3.4558   0.0004
CH-4    +       2.9287   0.0020          2.8954   0.0007
CH-5    +       3.2741   0.0008          3.2723   0.0004
NH-Pyrr +      10.3845   0.0047          9.5396   0.0232
CH-A    +       6.6565   0.0010          6.6221   0.0029
CH-C    +       5.9673   0.0009          5.9552   0.0027
CH-B    +       5.9237   0.0009          5.8904   0.0027
CH-Pyrr +       4.0077   0.0014          3.9131   0.0029
CH-Ar   +       3.8091   0.0009          3.8238   0.0028
CH'-Pyr +       3.5271   0.0009          3.4960   0.0027
CH'-Ar  +       3.4880   0.0009          3.5261   0.0027
CH-Et   +       2.7060   0.0009          2.7123   0.0029


        +
```

```
                  1,2
 ================================
        +        value    error
CH-1    +       4.5625   0.0137
CH-2    +       3.6370   0.0115
CH-6    +       3.5862   0.1292
CH-7    +       3.5069   0.0149
CH-4    +       2.3548   0.0963
CH-5    +       3.3092   0.0131
NH-Pyrr +      10.2413   0.0244
CH-A    +       6.6786   0.0106
CH-C    +       5.9724   0.0089
CH-B    +       5.9323   0.0093
CH-Pyrr +       4.0336   0.0134
CH-Ar   +       3.8014   0.0092
CH'-Pyr +       3.5420   0.0096
CH'-Ar  +       3.4807   0.0094
CH-Et   +       2.6917   0.0094

 Correlation coefficients*1000

      1    2    3
  1
  2  861
  3  229  -98
```

Titration Plots

Experimental (symbols) and calculated (lines) chemical shifts
(Only the glycoside signals are shown)

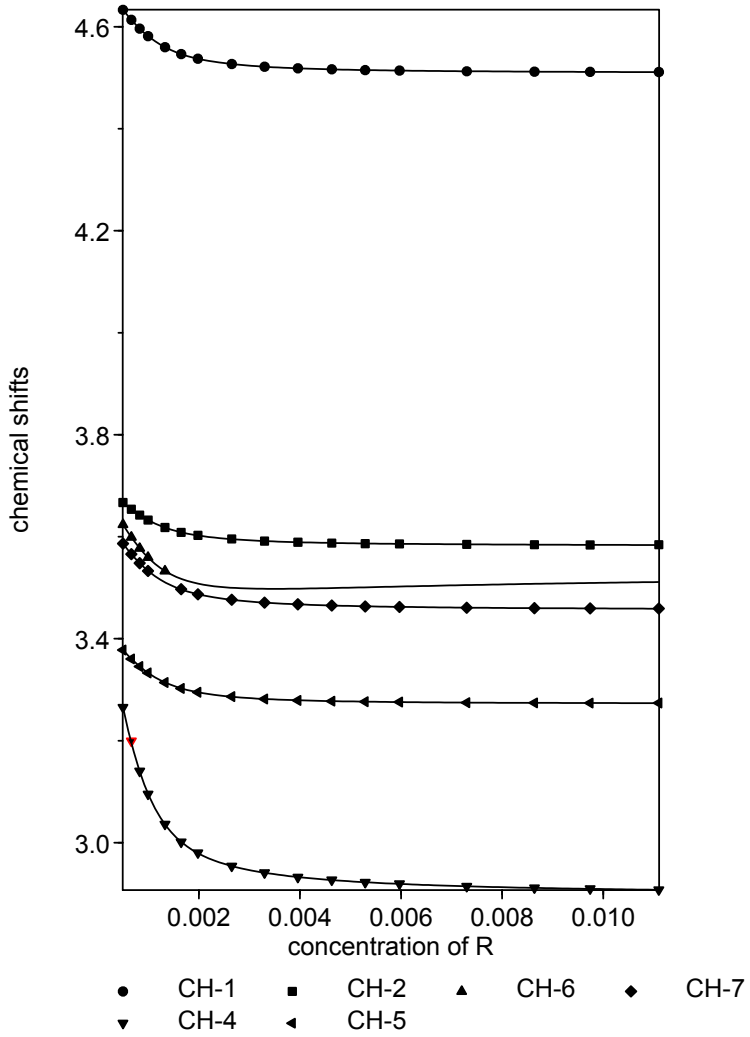

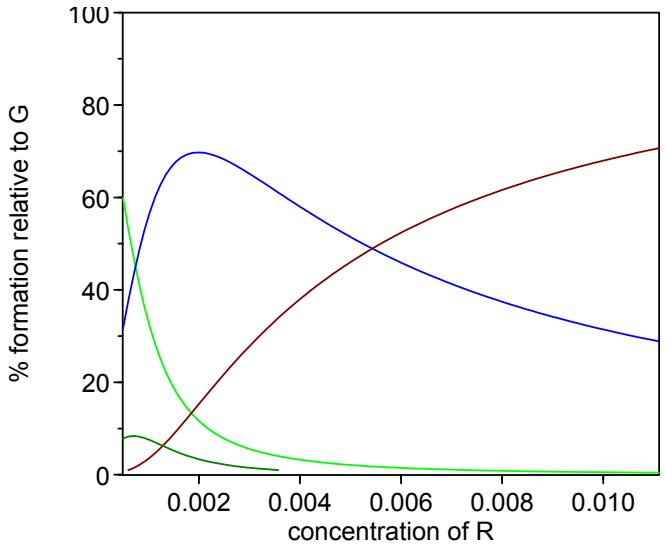

R-34 + OctβMan (CD_3CN, 298 K, 400 MHz)

Titration Data Table

R = ***R*-34** G = **OctβMan** [G] = 1.00 10^{-3} mol L^{-1}

R	G	CH-1 G	CH-7 G	CH-7' G	CH-4 G	CH-5 G
0.00E+00	1.00E-03	4.4751	3.8525	3.5257	3.4407	3.1466
4.01E-04	1.00E-03	4.4541	3.8129	3.4859	3.2759	3.1304
6.01E-04	1.00E-03	4.4451	3.7958	3.4688	3.2080	3.1233
8.02E-04	1.00E-03	4.4371	3.7806	3.4536	3.1480	-
1.00E-03	1.00E-03	4.4299	3.7671	3.4401	3.0874	-
1.25E-03	1.00E-03	4.4220	3.7522	3.4251	3.0290	3.1089
1.50E-03	1.00E-03	4.4149	3.7387	3.4114	2.9744	3.1029
1.75E-03	1.00E-03	4.4083	-	3.3991	2.9249	3.0979
2.00E-03	1.00E-03	4.4027	3.7148	3.3884	2.8804	3.0937
2.51E-03	1.00E-03	4.3930	3.6959	3.3703	-	3.0863
3.03E-03	1.00E-03	4.3850	3.6817	3.3549	-	3.0805
4.02E-03	1.00E-03	4.3735	3.6616	3.3337	2.6608	3.0718
5.01E-03	1.00E-03	4.3652	3.6463	3.3184	2.5991	3.0658
6.01E-03	1.00E-03	4.3589	3.6346	3.3068	2.5526	3.0611
7.01E-03	1.00E-03	4.3540	3.6261	3.2981	2.5178	3.0572
8.02E-03	1.00E-03	4.3501	3.6192	3.2914	2.4896	3.0544
8.98E-03	1.00E-03	4.3470	3.6136	3.2857	2.4675	3.0514
9.98E-03	1.00E-03	4.3442	3.6089	3.2810	2.4482	3.0503
1.10E-02	1.00E-03	4.3419	3.6050	3.2768	2.4315	3.0494
1.20E-02	1.00E-03	4.3400	3.6016	3.2733	2.4171	3.0477
1.33E-02	1.00E-03	4.3378	3.5975	3.2693	2.4015	3.0460
1.53E-02	1.00E-03	4.3348	-	3.2650	2.3841	3.0435
1.73E-02	1.00E-03	4.3326	-	3.2617	2.3717	3.0420

R	G	NH-Pyrr R	CH-A R	CH-C R	CH-B R	CH-Pyrr R	CH-Ar R	CH-Et R
0.00E+00	1.00E-03	-	-	-	-	-	-	-
4.01E-04	1.00E-03	9.5855	6.5985	5.9566	5.8845	3.8562	3.8283	2.7330
6.01E-04	1.00E-03	9.5638	6.5964	5.9561	5.8830	3.8526	3.8285	2.7340
8.02E-04	1.00E-03	9.5448	6.5949	5.9556	5.8817	3.8493	3.8290	2.7347
1.00E-03	1.00E-03	9.5269	6.5933	5.9552	5.8807	3.8464	3.8296	2.7354
1.25E-03	1.00E-03	9.5084	6.5913	5.9546	5.8798	3.8433	3.8303	2.7361
1.50E-03	1.00E-03	9.4918	6.5898	5.9544	5.8786	3.8405	3.8310	2.7367
1.75E-03	1.00E-03	9.4748	6.5883	5.9539	5.8774	3.8380	3.8318	2.7374
2.00E-03	1.00E-03	9.4586	6.5869	5.9537	5.8766	3.8353	3.8325	2.7381
2.51E-03	1.00E-03	9.4332	6.5844	5.9530	5.8752	3.8323	3.8323	2.7392
3.03E-03	1.00E-03	9.4118	6.5824	5.9525	5.8739	3.8283	3.8340	2.7402
4.02E-03	1.00E-03	9.3829	6.5792	5.9516	5.8719	3.8230	3.8356	2.7414
5.01E-03	1.00E-03	9.3599	6.5768	5.9514	5.8705	3.8191	3.8369	2.7427
6.01E-03	1.00E-03	9.3426	6.5748	5.9507	5.8698	3.8159	3.8378	2.7435
7.01E-03	1.00E-03	9.3309	6.5734	5.9505	5.8689	3.8135	3.8386	2.7442
8.02E-03	1.00E-03	9.3200	6.5719	5.9502	5.8682	3.8114	3.8395	2.7450
8.98E-03	1.00E-03	9.3121	6.5709	5.9500	5.8679	3.8099	-	2.7456
9.98E-03	1.00E-03	9.3052	6.5699	5.9499	5.8672	3.8084	-	2.7462
1.10E-02	1.00E-03	9.2994	6.5691	5.9498	5.8669	3.8072	-	2.7467
1.20E-02	1.00E-03	9.2933	6.5682	5.9499	5.8666	3.8060	-	2.7472
1.33E-02	1.00E-03	9.2873	6.5672	5.9498	5.8660	3.8048	-	2.7478
1.53E-02	1.00E-03	9.2830	6.5658	5.9494	5.8655	3.8031	3.8423	2.7485
1.73E-02	1.00E-03	9.2826	6.5648	5.9495	5.8654	3.8019	3.8428	2.7490

Results page

```
 no. of spectra            23
 no. of resonance values  253
 no. of resonant nuclei    12

Chi-squared = 139.13

   sigma = 0.00066563369         RMS weighted residual = 0.00061361259

       stoich            value   relative    log    standard
       coeff                     std devn    beta   deviation

 Beta  1  1 refined  1.0243E+003  0.0913    3.0104   0.0397  (  GR  )
 Beta  2  1 refined  1.3892E+005  0.2373    5.1428   0.1031  (  R2G  )

 Individual chemical shifts

                    R                          G
 ============================================================
        +        value    error          value    error
CH-1    +                                4.4747   0.0005
CH-7    +                                3.8524   0.0005
CH-7'   +                                3.5255   0.0005
CH-4    +                                3.4384   0.0005
CH-5    +                                3.1460   0.0005
NH-Pyrr +       9.2497   0.0033
CH-A    +       6.5579   0.0010
CH-C    +       5.9489   0.0010
CH-B    +       5.8633   0.0010
CH-Ar   +       3.7930   0.0010
CH-Pyrr +       3.8473   0.0012
CH'-Et  +       2.7534   0.0010
        +
                   1,1                        2,1
 ============================================================
        +        value    error          value    error
CH-1    +       4.3643   0.0055          4.3139   0.0010
CH-7    +       3.6397   0.0101          3.5581   0.0011
CH-7'   +       3.3132   0.0102          3.2288   0.0010
CH-4    +       2.5734   0.0410          2.2418   0.0025
CH-5    +       3.0656   0.0040          3.0278   0.0009
NH-Pyrr +       9.9819   0.0303          9.4781   0.0458
CH-A    +       6.6435   0.0044          6.6360   0.0083
CH-C    +       5.9659   0.0011          5.9519   0.0076
CH-B    +       5.9090   0.0021          5.8817   0.0078
CH-Ar   +       3.9274   0.0063          3.8836   0.0075
CH-Pyrr +       3.8064   0.0025          3.7975   0.0096
CH'-Et  +       2.7114   0.0024          2.7028   0.0084

 Correlation coefficients*1000

       1    2
   1
   2  998

 Parameters are numbered as follows
    1 beta 1,1
    2 beta 2,1
```

Titration Plots

Experimental (symbols) and calculated (lines) chemical shifts
(Only the glycoside signals are shown)

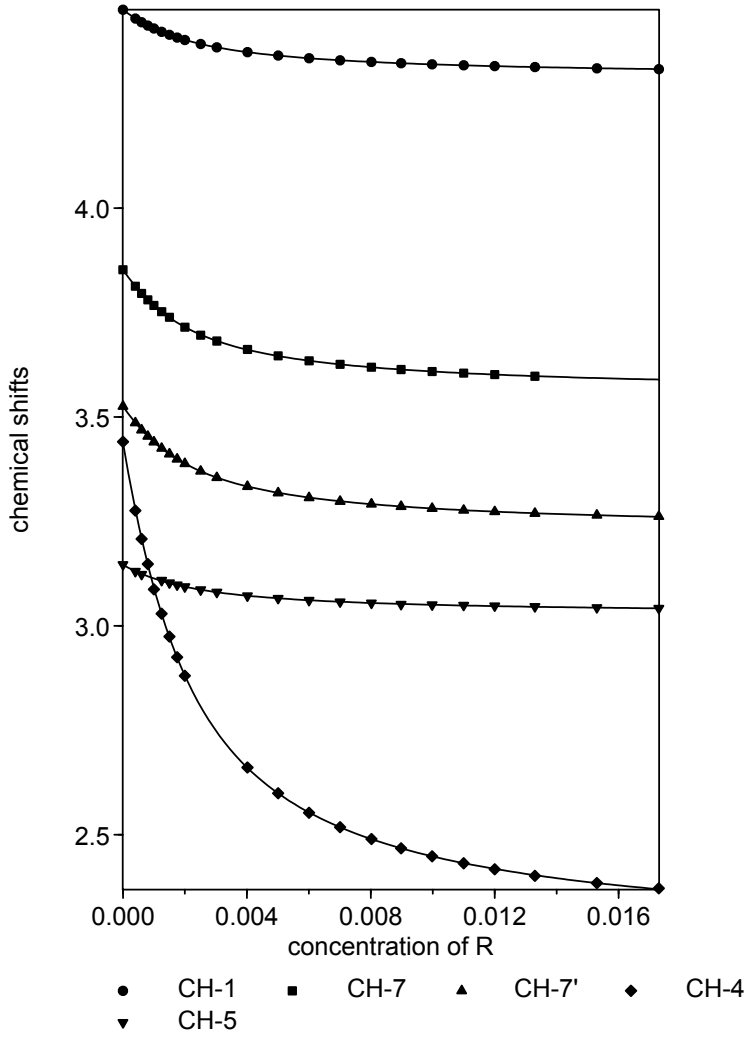

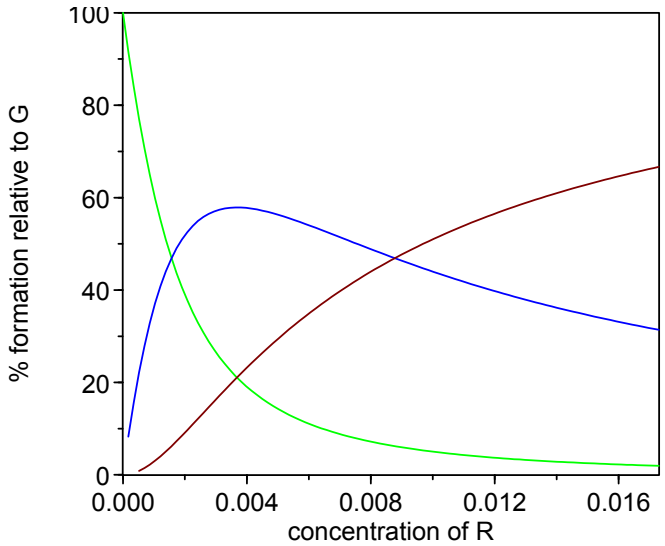

S-34 + OctαMan (CD_3CN, 298 K, 400 MHz)

Titration Data Table

R = ***S*-34** G = **OctαMan** [G] = 1.06 10^{-3} mol L^{-1}

R	G	CH-1 G	CH-6 G	CH-2 G	CH-7 G
0.00E+00	1.06E-03	4.7070	-	3.7153	3.6623
8.49E-04	1.06E-03	4.6559	-	3.6105	3.5870
1.13E-03	1.06E-03	4.6448	3.1965	3.5878	3.5710
1.41E-03	1.06E-03	4.6360	3.1220	3.5708	3.5585
1.70E-03	1.06E-03	4.6291	3.0647	-	-
2.26E-03	1.06E-03	4.6191	2.9813	-	-
2.82E-03	1.06E-03	4.6125	2.9282	-	-
3.39E-03	1.06E-03	4.6078	2.8893	-	-
3.95E-03	1.06E-03	4.6042	2.8608	3.5091	3.5156
4.52E-03	1.06E-03	4.6015	2.8390	3.5043	3.5123
5.10E-03	1.06E-03	4.5992	-	3.5003	3.5097
6.24E-03	1.06E-03	4.5958	-	3.4954	3.5062
7.38E-03	1.06E-03	4.5932	-	3.4917	3.5039
8.32E-03	1.06E-03	4.5914	-	3.4890	3.5027
9.45E-03	1.06E-03	4.5896	-	-	3.5016

R	G	CH-6' G	CH-3 G	CH-4 G	CH-5 G	CH-7' G
0.00E+00	1.06E-03	3.6180	3.5605	3.5077	3.4411	3.3911
8.49E-04	1.06E-03	3.4390	3.4656	3.1116	-	3.3040
1.13E-03	1.06E-03	3.3988	3.4456	3.0273	-	3.2850
1.41E-03	1.06E-03	3.3678	3.4299	2.9623	-	3.2703
1.70E-03	1.06E-03	3.3435	3.4179	2.9111	3.2479	3.2586
2.26E-03	1.06E-03	3.3083	3.4007	-	3.2242	3.2421
2.82E-03	1.06E-03	3.2850	3.3899	-	3.2090	3.2313
3.39E-03	1.06E-03	3.2688	3.3830	-	3.1986	3.2237
3.95E-03	1.06E-03	3.2562	3.3773	-	3.1908	3.2181
4.52E-03	1.06E-03	3.2469	3.3734	-	3.1848	3.2139
5.10E-03	1.06E-03	3.2388	3.3708	2.7091	3.1806	3.2103
6.24E-03	1.06E-03	3.2272	3.3670	2.6914	3.1743	3.2056
7.38E-03	1.06E-03	3.2207	3.3648	2.6800	3.1703	3.2020
8.32E-03	1.06E-03	3.2154	3.3634	2.6740	3.1677	3.1997
9.45E-03	1.06E-03	-	3.3627	2.6685	3.1660	3.1977

R	G	NH-Pyrr R	CH-A R	CH-C R	CH-B R
0.00E+00	1.06E-03	-	-	-	-
8.49E-04	1.06E-03	9.8612	6.6133	5.9541	5.8963
1.13E-03	1.06E-03	9.8110	6.6092	5.9533	5.8933
1.41E-03	1.06E-03	9.7645	6.6054	5.9526	5.8907
1.70E-03	1.06E-03	9.7220	6.6019	5.9520	5.8882
2.26E-03	1.06E-03	9.6515	6.5961	5.9509	5.8841
2.82E-03	1.06E-03	9.5978	6.5915	5.9501	5.8811
3.39E-03	1.06E-03	9.5548	6.5878	5.9494	5.8786
3.95E-03	1.06E-03	9.5209	6.5849	5.9489	5.8767
4.52E-03	1.06E-03	9.4920	6.5823	5.9486	5.8751
5.10E-03	1.06E-03	9.4690	6.5803	5.9483	5.8738
6.24E-03	1.06E-03	9.4381	6.5773	5.9479	5.8721
7.38E-03	1.06E-03	9.4163	6.5749	5.9476	5.8707
8.32E-03	1.06E-03	9.4019	6.5734	5.9473	5.8698
9.45E-03	1.06E-03	9.3904	6.5719	5.9472	5.8693

R	G	CH-Pyrr R	CH-Ar R	CH'-Pyrr R	CH'-Ar R	CH-Et R
0.00E+00	1.06E-03	-	-	-	-	-
8.49E-04	1.06E-03	3.8886	3.8360	3.5349	3.4906	2.7285
1.13E-03	1.06E-03	3.8816	3.8369	3.5365	3.4891	2.7295
1.41E-03	1.06E-03	3.8753	3.8377	3.5380	3.4879	2.7305
1.70E-03	1.06E-03	3.8693	3.8388	3.5395	3.4869	2.7315
2.26E-03	1.06E-03	3.8594	3.8402	3.5419	3.4851	2.7331
2.82E-03	1.06E-03	3.8520	3.8415	3.5438	3.4838	2.7342
3.39E-03	1.06E-03	3.8458	3.8426	3.5453	3.4828	2.7353
3.95E-03	1.06E-03	3.8411	3.8432	3.5465	3.4819	2.7362
4.52E-03	1.06E-03	3.8369	3.8440	3.5475	3.4813	2.7370
5.10E-03	1.06E-03	3.8335	3.8446	3.5483	3.4807	2.7376
6.24E-03	1.06E-03	3.8286	3.8453	3.5495	3.4799	2.7387
7.38E-03	1.06E-03	3.8249	3.8464	3.5503	3.4794	2.7394
8.32E-03	1.06E-03	3.8225	3.8467	3.5507	3.4789	2.7400
9.45E-03	1.06E-03	3.8204	3.8473	3.5514	3.4788	2.7408

Results page

```
no. of spectra            15
 no. of resonance values  236
 no. of resonant nuclei    18

Chi-squared = 227.59

   sigma = 0.00061008771         RMS weighted residual = 0.00053281020

       stoich            value   relative    log    standard
       coeff                     std devn    beta   deviation

 Beta  1  1 refined  2.2180E+003  0.0403    3.3460   0.0175  (  RG  )
 Beta  2  1 refined  1.5892E+005  0.3685    5.2012   0.1600  (  R2G  )

 Individual chemical shifts

        +
                     R                          G
 ============================================================
        +        value    error          value    error
CH-1    +                                 4.7068   0.0006
CH-6    +                                 3.7091   0.0036
CH-2    +                                 3.7151   0.0006
CH-7    +                                 3.6621   0.0006
CH-6'   +                                 3.6181   0.0006
CH-3    +                                 3.5601   0.0006
CH-4    +                                 3.5066   0.0006
CH-5    +                                 3.4412   0.0006
CH-7'   +                                 3.3908   0.0006
NH-Pyrr +       9.2875   0.0050
CH-A    +       6.5547   0.0036
CH-C    +       5.9466   0.0031
CH-B    +       5.8636   0.0031
CH-Pyrr +       3.7960   0.0037
CH-Ar   +       3.8546   0.0033
CH'-Pyr +       3.5565   0.0031
CH'-Ar  +       3.4767   0.0031
CH-Et   +       2.7496   0.0035
        +
                   1,1                        2,1
 ============================================================
        +        value    error          value    error
CH-1    +       4.5951   0.0017          4.5693   0.0046
CH-6    +       2.7803   0.0133          2.6007   0.0344
CH-2    +       3.4842   0.0031          3.4703   0.0028
CH-7    +       3.4962   0.0022          3.4952   0.0023
CH-6'   +       3.2216   0.0056          3.1484   0.0124
CH-3    +       3.3517   0.0025          3.3619   0.0041
CH-4    +       2.6347   0.0107          2.6450   0.0098
CH-5    +       3.1602   0.0036          3.1476   0.0020
CH-7'   +       3.1994   0.0027          3.1759   0.0037
NH-Pyrr +      10.3169   0.0113          9.6624   0.0782
CH-A    +       6.6550   0.0024          6.6836   0.0457
CH-C    +       5.9605   0.0009          5.9419   0.0287
CH-B    +       5.9223   0.0011          5.8822   0.0287
CH-Pyrr +       3.9564   0.0031          3.9615   0.0479
CH-Ar   +       3.8239   0.0013          3.7894   0.0363
CH'-Pyr +       3.5185   0.0011          3.5247   0.0287
CH'-Ar  +       3.5016   0.0010          3.4802   0.0285
CH-Et   +       2.7154   0.0015          2.6673   0.0412

 Correlation coefficients*1000


      1    2
  1
  2  980
```

Titration Plots

Experimental (symbols) and calculated (lines) chemical shifts
(Only the glycoside signals are shown)

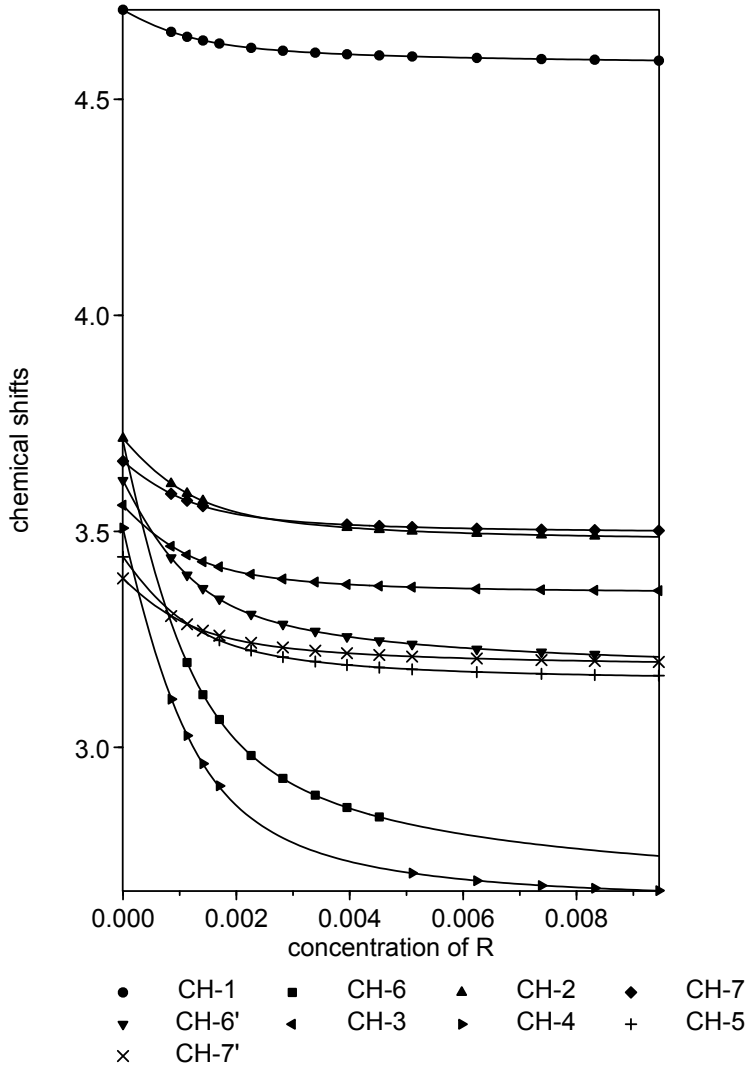

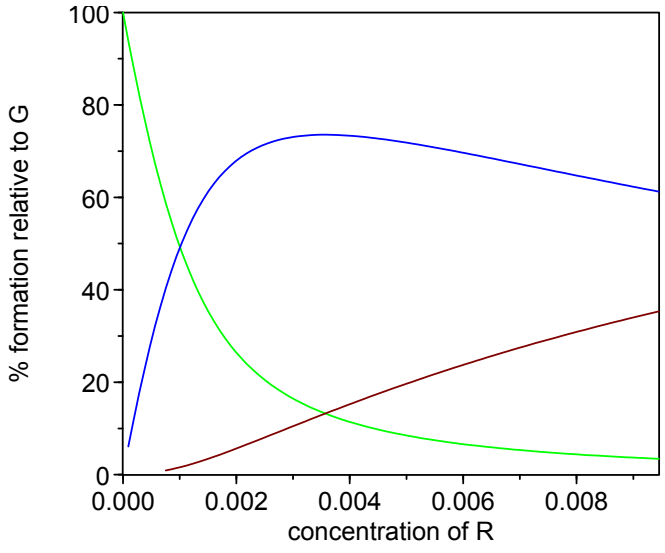

S-34 + OctβMan (CD_3CN, 298 K, 400 MHz)

Titration Data Table

R = ***S*-34** G = **OctβMan** [G] = 1.16 10^{-3} mol L^{-1}

R	G	CH-1 G	CH-7 G	CH-2 G	CH-3 G
0.00E+00	1.16E-03	4.4752	3.8285	3.7780	-
4.01E-04	1.16E-03	4.4330	3.7914	3.7393	-
6.02E-04	1.16E-03	4.4156	3.7762	3.7235	-
7.98E-04	1.16E-03	4.4005	3.7629	3.7095	-
1.00E-03	1.16E-03	4.3866	3.7507	3.6967	-
1.25E-03	1.16E-03	4.3724	3.7381	3.6838	-
1.50E-03	1.16E-03	4.3603	3.7275	3.6726	-
1.75E-03	1.16E-03	4.3500	3.7184	3.6631	3.4062
2.00E-03	1.16E-03	4.3414	3.7107	3.6554	3.3796
2.50E-03	1.16E-03	4.3281	3.6993	3.6432	-
2.99E-03	1.16E-03	4.3184	3.6907	3.6337	3.3215
4.00E-03	1.16E-03	4.3048	3.6790	3.6226	3.2846
5.02E-03	1.16E-03	4.2961	3.6712	3.6139	3.2603
6.02E-03	1.16E-03	4.2901	3.6661	3.6080	3.2438
6.98E-03	1.16E-03	4.2858	3.6624	3.6050	3.2322
7.98E-03	1.16E-03	4.2826	3.6598	3.6004	3.2228
8.99E-03	1.16E-03	4.2796	3.6570	-	3.2147
1.00E-02	1.16E-03	4.2770	3.6546	-	3.2072
1.10E-02	1.16E-03	4.2748	3.6530	-	3.2019
1.20E-02	1.16E-03	4.2733	3.6522	-	3.1978
1.37E-02	1.16E-03	4.2709	3.6501	-	3.1900
1.57E-02	1.16E-03	4.2682	3.6483	-	3.1851
1.77E-02	1.16E-03	4.2663	3.6466	-	3.1760

R	G	CH-7' G	CH-4 G	CH-6' G	CH-5 G
0.00E+00	1.16E-03	3.5018	3.4415	3.3466	3.1471
4.01E-04	1.16E-03	3.4571	3.2370	3.3040	3.0743
6.02E-04	1.16E-03	3.4387	3.1553	3.2821	3.0440
7.98E-04	1.16E-03	3.4226	3.0857	3.2636	3.0196
1.00E-03	1.16E-03	3.4078	3.0226	3.2475	-
1.25E-03	1.16E-03	3.3926	-	3.2294	-
1.50E-03	1.16E-03	3.3799	2.8941	3.2141	2.9509
1.75E-03	1.16E-03	3.3689	-	3.2013	2.9352
2.00E-03	1.16E-03	3.3599	-	3.1908	2.9209
2.50E-03	1.16E-03	3.3458	-	3.1742	2.8982
2.99E-03	1.16E-03	3.3354	-	3.1624	2.8826
4.00E-03	1.16E-03	3.3213	2.6423	3.1468	-
5.02E-03	1.16E-03	3.3125	2.6050	3.1369	-
6.02E-03	1.16E-03	3.3063	2.5808	3.1300	-
6.98E-03	1.16E-03	3.3023	2.5638	3.1255	-
7.98E-03	1.16E-03	3.2989	2.5508	3.1222	-
8.99E-03	1.16E-03	3.2963	2.5411	3.1194	-
1.00E-02	1.16E-03	3.2939	2.5327	3.1166	-
1.10E-02	1.16E-03	3.2919	2.5259	3.1148	-
1.20E-02	1.16E-03	3.2912	2.5215	3.1133	-
1.37E-02	1.16E-03	3.2900	2.5144	3.1113	-
1.57E-02	1.16E-03	3.2884	2.5094	3.1096	-
1.77E-02	1.16E-03	3.2863	2.5061	3.1083	-

R	G	NH-Pyrr R	CH-A R	CH-C R	CH-B R
0.00E+00	1.16E-03	-	-	-	-
4.01E-04	1.16E-03	9.8007	6.6251	5.9550	5.8953
6.02E-04	1.16E-03	9.7692	6.6218	5.9548	5.8934
7.98E-04	1.16E-03	9.7391	6.6188	5.9543	5.8918
1.00E-03	1.16E-03	9.7101	6.6156	5.9538	5.8900
1.25E-03	1.16E-03	9.6773	6.6120	5.9533	5.8878
1.50E-03	1.16E-03	9.6459	6.6087	5.9528	5.8862
1.75E-03	1.16E-03	9.6160	6.6057	5.9525	5.8847
2.00E-03	1.16E-03	9.5894	6.6030	5.9520	5.8826
2.50E-03	1.16E-03	9.5458	6.5982	5.9514	5.8804
2.99E-03	1.16E-03	9.5095	6.5942	5.9510	5.8784
4.00E-03	1.16E-03	9.4580	6.5884	5.9503	5.8752
5.02E-03	1.16E-03	9.4223	6.5840	5.9496	5.8734
6.02E-03	1.16E-03	9.3969	6.5809	5.9491	5.8714
6.98E-03	1.16E-03	9.3797	6.5786	5.9491	5.8709
7.98E-03	1.16E-03	9.3653	6.5767	5.9490	5.8699
8.99E-03	1.16E-03	9.3542	6.5753	5.9489	5.8694
1.00E-02	1.16E-03	9.3439	6.5735	5.9485	5.8686
1.10E-02	1.16E-03	9.3368	6.5722	5.9485	5.8681
1.20E-02	1.16E-03	9.3314	6.5714	5.9485	5.8680
1.37E-02	1.16E-03	9.3246	6.5699	5.9483	5.8677
1.57E-02	1.16E-03	9.3212	6.5685	5.9485	5.8671
1.77E-02	1.16E-03	9.3200	6.5675	5.9486	5.8673

R	G	CH-Pyrr R	CH-Ar R	CH'-Pyrr R	CH'-Ar R
0.00E+00	1.16E-03	-	-	-	-
4.01E-04	1.16E-03	3.8737	3.8267	3.5376	3.4735
6.02E-04	1.16E-03	3.8695	3.8272	3.5382	3.4722
7.98E-04	1.16E-03	3.8654	3.8277	3.5386	3.4712
1.00E-03	1.16E-03	3.8612	3.8286	3.5391	3.4705
1.25E-03	1.16E-03	3.8574	3.8294	3.5397	3.4692
1.50E-03	1.16E-03	3.8528	3.8303	3.5402	3.4682
1.75E-03	1.16E-03	3.8488	3.8311	3.5408	3.4676
2.00E-03	1.16E-03	3.8453	3.8319	3.5414	3.4669
2.50E-03	1.16E-03	3.8392	3.8336	3.5423	3.4658
2.99E-03	1.16E-03	3.8346	3.8346	3.5431	3.4648
4.00E-03	1.16E-03	3.8272	3.8365	3.5443	3.4637
5.02E-03	1.16E-03	3.8218	3.8378	3.5449	3.4627
6.02E-03	1.16E-03	3.8180	3.8388	3.5454	3.4619
6.98E-03	1.16E-03	3.8152	3.8396	3.5458	3.4615
7.98E-03	1.16E-03	3.8129	3.8405	3.5461	3.4611
8.99E-03	1.16E-03	3.8112	3.8429	3.5463	3.4609
1.00E-02	1.16E-03	3.8093	-	3.5463	3.4603
1.10E-02	1.16E-03	3.8079	-	3.5463	3.4602
1.20E-02	1.16E-03	3.8069	-	3.5467	3.4601
1.37E-02	1.16E-03	3.8053	3.8417	3.5466	3.4599
1.57E-02	1.16E-03	3.8039	3.8432	3.5467	3.4600
1.77E-02	1.16E-03	3.8029	3.8437	3.5468	3.4599

Results page

```
 no. of spectra            23
 no. of resonance values  321
 no. of resonant nuclei    16


 Chi-squared = 207.77

   sigma = 0.00094513996         RMS weighted residual = 0.00086841688

       stoich            value   relative    log    standard
       coeff                     std devn    beta   deviation

 Beta  1   1 refined  1.6972E+003  0.0284    3.2297   0.0123  (  RG  )
 Beta  2   1 refined  1.2411E+005  0.2051    5.0938   0.0891  (  R2G  )

 Individual chemical shifts

        +
                    R                        G
 ============================================================
        +        value    error          value    error
CH-1    +                                4.4740   0.0007
CH-7    +                                3.8277   0.0006
CH-2    +                                3.7771   0.0007
CH-3    +                                3.7287   0.0049
CH-7'   +                                3.5013   0.0006
CH-4    +                                3.4365   0.0008
CH-6'   +                                3.3510   0.0007
CH-5    +                                3.1456   0.0008
NH-Pyrr +       9.3101   0.0081
CH-A    +       6.5579   0.0020
CH-C    +       5.9488   0.0019
CH-B    +       5.8668   0.0020
CH-Ar   +       3.7940   0.0019
CH-Pyrr +       3.8491   0.0022
CH'-Ar  +       3.5469   0.0019
CH'-Pyr +       3.4603   0.0019
        +
                   1,1                      2,1
 ============================================================
        +        value    error          value    error
CH-1    +       4.2814   0.0023          4.2475   0.0024
CH-7    +       3.6576   0.0020          3.6315   0.0019
CH-2    +       3.6000   0.0021          3.5707   0.0041
CH-3    +       3.2266   0.0071          3.1186   0.0057
CH-7'   +       3.2941   0.0023          3.2721   0.0016
CH-4    +       2.5104   0.0089          2.4696   0.0024
CH-6'   +       3.1172   0.0026          3.0905   0.0018
CH-5    +       2.8114   0.0040          2.8354   0.0205
NH-Pyrr +      10.1257   0.0041          9.0644   0.1523
CH-A    +       6.6666   0.0016          6.6533   0.0201
CH-C    +       5.9595   0.0009          5.9385   0.0185
CH-B    +       5.9141   0.0009          5.8516   0.0202
CH-Ar   +       3.9237   0.0016          3.8692   0.0182
CH-Pyrr +       3.8126   0.0012          3.7882   0.0214
CH'-Ar  +       3.5310   0.0009          3.5528   0.0184
CH'-Pyr +       3.4816   0.0009          3.4457   0.0190

 Correlation coefficients*1000

       1    2
   1
   2  962

 Parameters are numbered as follows
    1 beta 1,1
    2 beta 2,1
```

Titration Plots

Experimental (symbols) and calculated (lines) chemical shifts
(Only the glycoside signals are shown)

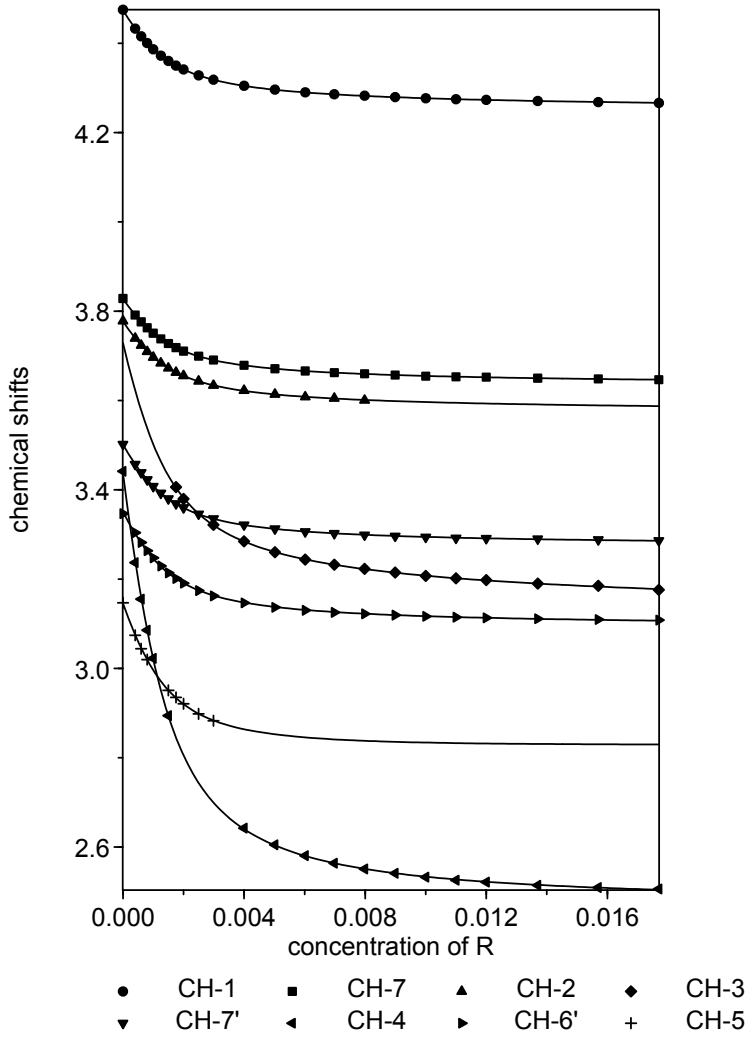

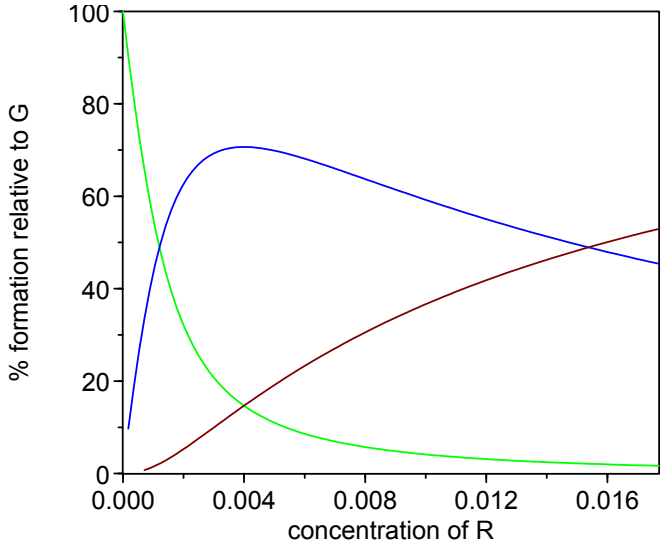

Bibliography

[1.] D. Shental-Bechor, Y. Levy, *Current Opinion in Structural Biology* **2009,** *19,* 524-533.

[2.] B. Ernst, W. Hart, P. Sinay, *Carbohydrates in Chemistry and Biology*, Wiley-VCH, Weinheim, Germany **2000**.

[3.] P. M. Rudd, T. Elliott, P. Cresswell, I. A. Wilson, R. A. Dwek, *Science* **2001,** *291,* 2370-2376.

[4.] Y. van Kooyk, G. A. Rabinovich, *Nature Immunology* **2008,** *9,* 593-601.

[5.] R. A. Ezekowitz, *Journal of Infectious Diseases* **2003,** *187,* S335-S339.

[6.] E. van Liempt, C. M. C. Bank, P. Mehta, J. J. Garcia-Vallejo, Z. S. Kawar, R. Geyer, R. A. Alvarez, R. D. Cummings, Y. van Kooyk, I. van Die, *Febs Letters* **2006,** *580,* 6123-6131.

[7.] T. L. Chang, M. E. Klotman, *Aids Reviews* **2004,** *6,* 161-168.

[8.] E. I. Buzas, B. Gyorgy, M. Pasztoi, I. Jelinek, A. Falus, H. J. Gabius, *Autoimmunity* **2006,** *39,* 691-704.

[9.] J. Balzarini, *Nature Reviews Microbiology* **2007,** *5,* 583-597.

[10.] C. N. Scanlan, J. Offer, N. Zitzmann, R. A. Dwek, *Nature* **2007,** *446,* 1038-1045.

[11.] O. Balzarini, *Lancet Infectious Diseases* **2005,** *5,* 726-731.

[12.] R. Wyatt, J. Sodroski, *Science* **1998,** *280,* 1884-1888.

[13.] R. Wyatt, P. D. Kwong, E. Desjardins, R. W. Sweet, J. Robinson, W. A. Hendrickson, J. G. Sodroski, *Nature* **1998,** *393,* 705-711.

[14.] M. Zhang, B. Gaschen, W. Blay, B. Foley, N. Haigwood, C. Kuiken, B. Korber, *Glycobiology* **2004,** *14,* 1229-1246.

[15.] T. B. H. Geijtenbeek, R. Torensma, S. J. van Vliet, G. C. F. van Duijnhoven, G. J. Adema, Y. van Kooyk, C. G. Figdor, *Cell* **2000,** *100,* 575-585.

[16.] S. Pohlmann, F. Baribaud, R. W. Doms, *Trends in Immunology* **2001,** *22,* 643-646.

[17.] Y. van Kooyk, T. B. H. Geijtenbeek, *Nature Reviews Immunology* **2003,** *3,* 697-709.

[18.] H. Feinberg, D. A. Mitchell, K. Drickamer, W. I. Weis, *Science* **2001,** *294,* 2163-2166.

[19.] Y. Guo, H. Feinberg, E. Conroy, D. A. Mitchell, R. Alvarez, O. Blixt, M. E. Taylor, W. I. Weis, K. Drickamer, *Nature Structural & Molecular Biology* **2004,** *11,* 591-598.

[20.] K. D. McReynolds, J. Gervay-Hague, *Chemical Reviews* **2007,** *107,* 1533-1552.

[21.] C. N. Scanlan, J. Offer, N. Zitzmann, R. A. Dwek, *Nature* **2007,** *446,* 1038-1045.

[22.] O. Martinez-Avila, K. Hijazi, M. Marradi, C. Clavel, C. Campion, C. Kelly, S. Penades, *Chemistry-A European Journal* **2009,** *15,* 9874-9888.

[23.] C. R. Bertozzi, L. L. Kiessling, *Science* **2001,** *291,* 2357-2364.

[24.] A. P. Davis, T. D. James, P. Verdi, *Functional Synthetic Receptors*, T. Schrader, A. D. Hamilton, Eds. ed. Wiley-VCH, Weinheim, Germany **2005**.

[25.] S. Kubik, *Angewandte Chemie-International Edition* **2009,** *48,* 1722-1725.

[26.] Y. Ferrand, M. P. Crump, A. P. Davis, *Science* **2007,** *318,* 619-622.

[27.] C. Nativi, M. Cacciarini, O. Francesconi, A. Vacca, G. Moneti, A. Ienco, S. Roelens, *Journal of the American Chemical Society* **2007,** *129,* 4377-4385.

[28.] A. Vacca, C. Nativi, M. Cacciarini, R. Pergoli, S. Roelens, *Journal of the American Chemical Society* **2004,** *126,* 16456-16465.

[29.] S. Roelens, A. Vacca, O. Francesconi, C. Venturi, *Chemistry-A European Journal* **2009,** *15,* 8296-8302.

[30.] H. Abe, Y. Aoyagi, M. Inouye, *Organic Letters* **2005,** *7,* 59-61.

[31.] C. Schmuck, M. Schwegmann, *Organic Letters* **2005,** *7,* 3517-3520.

[32.] M. Mazik, W. Radunz, R. Boese, *Journal of Organic Chemistry* **2004,** *69,* 7448-7462.

[33.] R. Welti, F. Diederich, *Helvetica Chimica Acta* **2003,** *86,* 494-503.

[34.] Y. H. Kim, J. I. Hong, *Angewandte Chemie-International Edition* **2002,** *41,* 2947-2950.

[35.] Z. L. Zhong, E. V. Anslyn, *Journal of the American Chemical Society* **2002,** *124,* 9014-9015.

[36.] G. Hennrich, E. V. Anslyn, *Chemistry-A European Journal* **2002,** *8,* 2219-2224.

[37.] S. Hanessian, M. Simard, S. Roelens, *Journal of the American Chemical Society* **1995,** *117,* 7630-7645.

[38.] O. Ermer, A. J. Eling, *Journal of the Chemical Society, Perkin Transactions 2* **1994,** 925-944.

[39.] J. L. Sessler, P. A. Gale, W.-S. Cho, *Anion Receptor Chemistry*, The Royal Society of Chemistry ed. Cambridge **2006**.

[40.] C. E. Loader, H. J. Anderson, *Synthesis* **1978,** 295-297.

[41.] O. Francesconi, A. Ienco, G. Moneti, C. Nativi, S. Roelens, *Angewandte Chemie-International Edition* **2006,** *45,* 6693-6696.

[42.] J. Gawronski, K. Gawronska, J. Grajewski, M. Kwit, A. Plutecka, U. Rychlewskaja, *Chemistry-A European Journal* **2006,** *12,* 1807-1817.

[43.] M. J. MacLachlan, *Pure and Applied Chemistry* **2006,** *78,* 873-888.

[44.] N. Kuhnert, A. Lopez-Periago, G. M. Rossignolo, *Organic & Biomolecular Chemistry* **2005,** *3,* 524-537.

[45.] E. A. Katayev, G. D. Pantos, M. D. Reshetova, V. N. Khrustalev, V. M. Lynch, Y. A. Ustynyuk, J. L. Sessler, *Angewandte Chemie-International Edition* **2005,** *44,* 7386-7390.

[46.] X. J. Liu, Y. Liu, G. Li, R. Warmuth, *Angewandte Chemie-International Edition* **2006,** *45,* 901-904.

[47.] M. Albrecht, *Angewandte Chemie-International Edition* **1999,** *38,* 3463-3465.

[48.] C. Moberg, *Angewandte Chemie-International Edition* **2006,** *45,* 4721-4723.

[49.] A. Ardá, C. Venturi, C. Nativi, O. Francesconi, J. Cañada, J. Jiménez-Barbero, S. Roelens, *European Journal of Organic Chemistry* **2010,** *2010,* 64-71.

[50.] S. Anderson, U. Neidlein, V. Gramlich, F. Diederich, *Angewandte Chemie-International Edition* **1995,** *34,* 1596-1600.

[51.] J. Cuntze, L. Owens, V. Alcazar, P. Seiler, F. Diederich, *Helvetica Chimica Acta* **1995,** *78,* 367-390.

[52.] A. Bahr, A. S. Droz, M. Puntener, U. Neidlein, S. Anderson, P. Seiler, F. Diederich, *Helvetica Chimica Acta* **1998,** *81,* 1931-1963.

[53.] D. K. Smith, F. Diederich, *Chemical Communications* **1998,** 2501-2502.

[54.] D. K. Smith, A. Zingg, F. Diederich, *Helvetica Chimica Acta* **1999,** *82,* 1225-1241.

[55.] A. Bahr, B. Felber, K. Schneider, F. Diederich, *Helvetica Chimica Acta* **2000,** *83,* 1346-1376.

[56.] A. S. Droz, U. Neidlein, S. Anderson, P. Seiler, F. Diederich, *Helvetica Chimica Acta* **2001,** *84,* 2243-2289.

[57.] R. Welti, F. Diederich, *Helvetica Chimica Acta* **2003,** *86,* 494-503.

[58.] R. Welti, Y. Abel, V. Gramlich, F. Diederich, *Helvetica Chimica Acta* **2003,** *86,* 548-562.

[59.] K. M. Bhattarai, L. P. Bonar-Law, A. P. Davis, B. A. Murray, *Journal of the Chemical Society, Chemical Communications* **1992,** 752-754.

[60.] R. Liu, W. C. Still, *Thetrahedron Letters* **1993,** *34,* 2573-2576.

[61.] L. P. Bonar-Law, J. K. M. Sanders, *Journal of the American Chemical Society* **1995,** *117,* 259-271.

[62.] G. Das, A. D. Hamilton, *Thetrahedron Letters* **1997,** *38,* 3675-3678.

[63.] H. J. Kim, Y. H. Kim, J. I. Hong, *Tetrahedron Letters* **2001,** *42,* 5049-5052.

[64.] C. Li, G. T. Wang, H. P. Yi, X. K. Jiang, Z. T. Li, R. X. Wang, *Organic Letters* **2007,** *9,* 1797-1800.

[65.] S. Hanessian, A. Gomtsyan, M. Simard, S. Roelens, *Journal of the American Chemical Society* **1994,** *116,* 4495-4496.

[66.] S. Roelens, P. Dapporto, P. Paoli, *Canadian Journal of Chemistry-Revue Canadienne de Chimie* **2000,** *78,* 723-731.

[67.] *Maestro, A powerful, all-purpose molecular modelling environment, version 8.5*, Schrödinger ed. LLC, New York, NY **2008**.

[68.] D. A. Case, T. E. Cheatham, T. Darden, H. Gohlke, R. Luo, K. M. Merz, A. Onufriev, C. Simmerling, B. Wang, R. J. Woods, *Journal of Computational Chemistry* **2005,** *26,* 1668-1688.

[69.] T. Mizutani, T. Kurahashi, T. Murakami, M. Matsumi, H. Ogoshi, *Journal of the American Chemical Society* **1997,** *119,* 8991-9001.

[70.] B. Aguilera, L. Romero-Ramirez, J. Abad-Rodriguez, G. Corrales, M. Nieto-Sampedro, A. Fernandez-Mayoralas, *Journal of Medicinal Chemistry* **1998,** *41,* 4599-4606.

[71.] A. E. Zemlyakov, V. V. Tsikalov, O. V. Kalyuzhin, V. O. Kur'yanov, V. Y. Chirva, *Russian Journal of Bioorganic Chemistry* **2003,** *29,* 286-292.

[72.] V. Adasch, B. Hoffmann, W. Milius, G. Platz, G. Voss, *Carbohydrate Research* **1998,** *314,* 177-187.

[73.] R. Sayre, *Journal of the American Chemical Society* **1955,** *77,* 6689-6690.

[74.] P. Langer, J. Anders, *European Journal of Organic Chemistry* **2002,** 686-691.

[75.] K. V. Kilway, J. S. Siegel, *Thetrahedron* **2001,** *57,* 3615-3627.

[76.] R. F. Nystrom, *Journal of the American Chemical Society* **1955,** *77,* 2544-2545.

[77.] L. H. Amudsen, L. S. Nelson, *Journal of the American Chemical Society* **1951,** *73,* 242-244.

[78.] R. M. Silverstein, E. E. Ryskiewics, C. Willard, *Org.Synth.Coll.Vol.IV* **1963,** 831-833.

[79.] P. Barker, P. Gendler, H. Rapoport, *Journal of Organic Chemistry* **1978,** *43,* 4849-4853.

[80.] A. J. Lampkins, O. Abdul-Rahim, R. K. Castellano, *Journal of Organic Chemistry* **2006,** *71,* 5815-5818.

[81.] W. S. Saari, J. E. Schwering, P. A. Lyle, E. L. Engelhardt, A. C. Sartorelli, S. Rockwell, *Journal of Medicinal Chemistry* **1991,** *34,* 3132-3138.

[82.] C. Frassineti, S. Ghelli, P. Gans, A. Sabatini, M. S. Moruzzi, A. Vacca, *Analytical Biochemistry* **1995,** *231,* 374-382.